AFCRC-TR-56-209

GEOPHYSICAL RESEARCH PAPERS
No. 50

RADAR-SYNOPTIC ANALYSIS OF HURRICANE EDNA, 1954

EDWIN KESSLER, III
DAVID ATLAS

JULY 1956

GEOPHYSICS RESEARCH DIRECTORATE
AIR FORCE CAMBRIDGE RESEARCH CENTER
AIR RESEARCH AND DEVELOPMENT COMMAND

AFCRC-TR-56-209

GEOPHYSICAL RESEARCH PAPERS
No. 50

RADAR-SYNOPTIC ANALYSIS OF HURRICANE EDNA, 1954

EDWIN KESSLER, III
DAVID ATLAS

JULY 1956

GEOPHYSICS RESEARCH DIRECTORATE
AIR FORCE CAMBRIDGE RESEARCH CENTER
BEDFORD MASSACHUSETTS

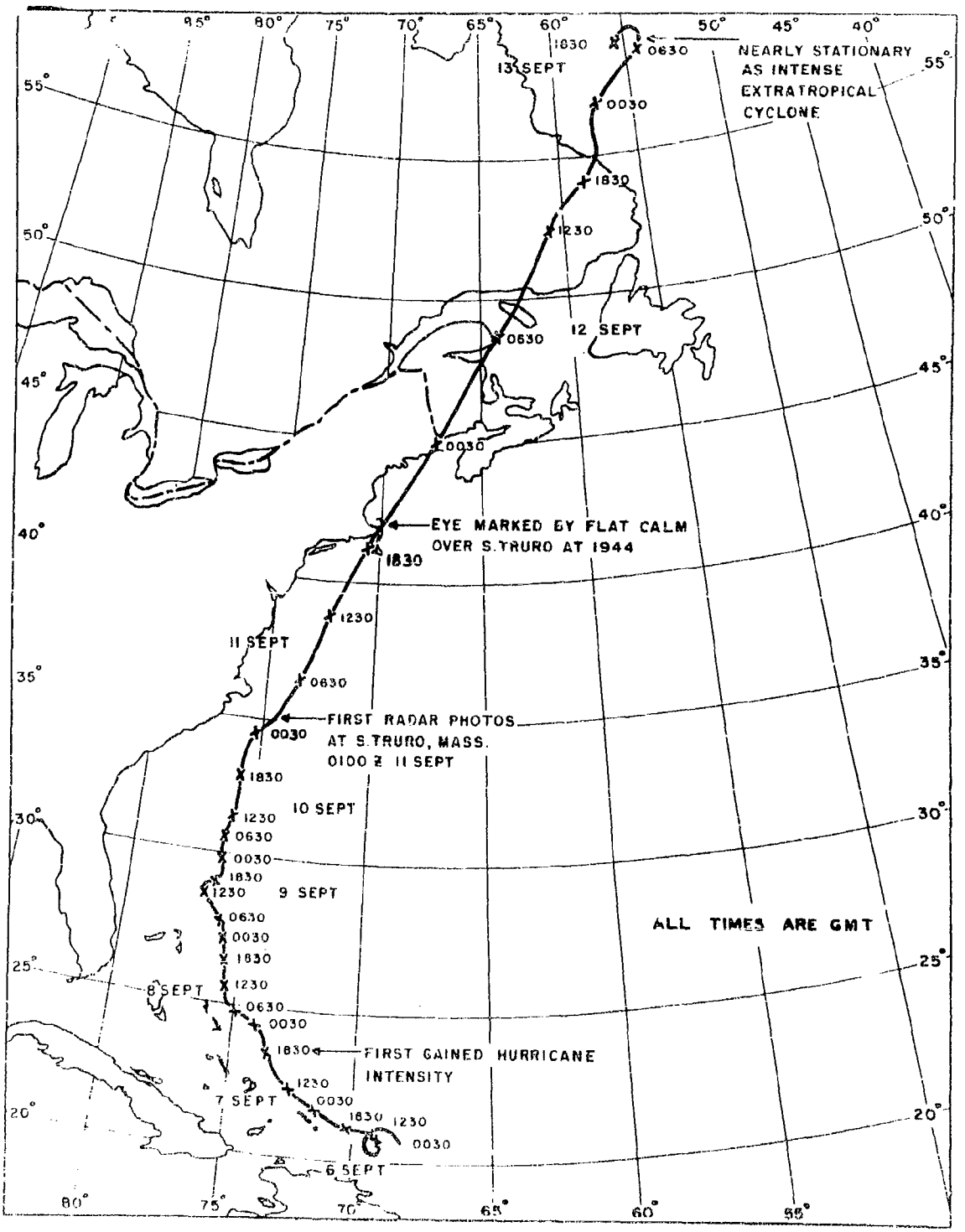

Track of Hurricane Edna, 1954

CONTENTS

ABSTRACT

The eye of Hurricane Edna crossed Cape Cod during the afternoon of 11 September 1954. Unique photographic records were made at several radar sites and include time lapse Range Height (RHI) and PPI movies and stills. These, with regular and special ground based weather observations and the data of aircraft reconnaissance, have contributed knowledge of various features of the storm.

The precipitation of Edna evidences a banded structure roughly concentric with the eye; as is the case with most northward moving hurricanes in middle latitudes, precipitation is mainly confined to the northern semicircle. The major outer bands are relatively broad and far apart and are composed of discrete showers, most of which are revealed by radar to initiate and grow substantially below the melting layer. These showers are often beneath a deck of middle or high clouds, but their histories appear largely independent of the upper cloud masses. Nearer the eye the bands are closer together, narrower and more continuous along their lengths. However, there is radar and rainfall evidence for the presence of a finer structure also within the continuous inner bands.

No consistent relation with vertical wind shear is found for the band orientation. However, the most prominent ones lie approximately parallel to the surface winds or isobars, or about midway between their directions if they differ considerably. Differences between convective and stratiform type bands are attributed primarily to variations of the stability of the air involved. Modification of the stability of the air with continued convergence is illustrated by the relatively convective nature of the upwind ends of the bands and their more uniform character downwind.

The upper portions of the bands as revealed by radar suggest upper level divergence. A weakened radar return from upper masses immediately ahead of the bands is indicative of downdrafts in these localities which compensate the active low level convergence and updraft of the band regions.

The motion of the showers in the northern outskirts of this storm is about 40° to the left of the direction of the storm's motion; while the upper clouds move from the same direction as the storm. Within fifty miles of the eye, the motion of many radar elements is in nearly the same direction as the surface winds and hence nearly along the bands.

The speed profile of radar weather elements is similar in shape to that of the surface winds, showing the decrease of velocity near the eye which is characteristic of mature hurricanes. However, comparison of the velocities of radar echoes in this storm and the known surface winds

indicates that in the lowest 7,000 feet, winds increase in speed with increasing height outside the ring of maximum surface winds. Nearer the eye the winds decrease with height. This pattern of vertical wind shear finds considerable support in recent observational work of Simpson. It is suggested that further research may enable the intensity of a hurricane to be determined by radar on a quantitative basis.

The radar "bright band" appears at the melting level in all the more uniform spiral bands, indicating that these bands are the results of convergence and precipitation release through deep layers of the atmosphere. The conventional "bright band" with normal decrease in echo intensity below the melting zone is qualitatively associated with the lighter rainfall, while the lack of such a decrease in echo intensity is associated with continued growth in and below the melting layer. The latter feature is characteristic of the more intense spiral bands. These data, when supplemented by drop samples, indicate that the drop size distributions observed are the results of a combination of growth by accretion of cloud and aggregation of raindrops below the melting level, coupled with continuous creation of drizzle size drops.

Characteristics of the drop size distribution of the hurricane rain at all observed intensities are in fair agreement with those to be expected on the basis of Marshall and Palmer's empirical relation. Also, there is a reasonably good correlation between radar reflectivity and rain intensity. This suggests the possible use of long wave radar to monitor the intensity of hurricane rains.

Discrete precipitation echoes move about the "eye" in the same sense as the surface winds. However, the eye may best be fixed in practice approximately at the center of spiralling of the bands, which generally differs considerably from the centers of curvature. On the RHI scope Edna's eye is seen as an open "V" in the radar echo which leans toward the northeast; a cirrostratus shield over the eye at 35,000 feet is connected to the northeastern portion of the wall cloud by a thin column. A second eye with pressure minimum and complete wind circulation is present for a short time, as are "false" radar eyes.

The path of Edna is found to be much more regular than originally reported; oscillations of the path are no larger than the eye diameter and may be less. Analysis of position reports from various sources indicates that when an aircraft is within radar range, errors of position may be reduced to a minimum if reports are based on cooperative estimates of both aircraft and radar observers.

Land stations west of Edna's eye experienced highest winds during the storm after the times of lowest pressure. The unusual sudden increase of winds to high values has been tentatively associated with widespread air accelerations accompanying initial conditions of extreme imbalance between the winds and the pressure gradient.

The reader with limited time for study is referred to Sections 8, 9 and especially the summary of Section 10.

HURRICANE EDNA - 1954

1. Introduction

The first indications of the formation of Hurricane Edna came on the night of 5 September in the extreme southwestern Atlantic between Puerto Rico and the Bahama Islands (Malkin and Holzworth, 1954). Subsequently, this storm was the second to ravage the east coast of the United States within eleven days. Its appearance on the scene long before vivid impressions of the earlier storm, Carol, had begun to subside resulted in a high level of preparedness among the populace and keen response to Weather Bureau advisories. Carol accelerated suddenly from the Cape Hatteras region, where it had remained nearly stationary for several days, and arrived while New England was not yet fully braced for the blow. With power lines down and men and standby equipment not fully organized, much radar equipment which could have been used to study the storm was inoperative. In the case of Edna, however, preparations were made well in advance to track the storm, with the fortunate result that great quantities of unique radar data were collected.

The frontispiece illustrates the path of Edna from the time of first detection until it became nearly stationary between Labrador and Greenland, in the manner of many intense storms of high latitudes. Radar photographic data gathered at South Truro, Massachusetts, directly over which the eye passed, are the basis for the bulk of the information contained in this report. Photographs of the radar scopes were taken from this site between 1959 EST 10 September and 1520 EST 11 September and the positions of Edna at these times are indicated on the frontispiece.

The wealth of radar and other data has led the authors to examine many features of this hurricane which had been investigated by more conventional means in other storms. The authors have attempted primarily to describe the hurricane features in terms of the observational data and relatively little space is devoted to theoretical aspects. Since the radar data are of high quality and similar records are not likely to be obtained often, the results of the studies are presented here in considerable detail. The inner and outer bands, the eye, the path of the storm, the wind field, radar tracking and rainfall mechanisms are all discussed with the aim of providing insight into all of the storm features for which there is radar information. (In most cases, other sources have also been utilized.) It is hoped that the information contained herein represents an extension of our knowledge of hurricane structure and will provide a useful reference for future observational and theoretical studies, as well as a key to radar scope interpretation during hurricane conditions.

2. Data Used in This Study

The basis of this study has been the ordinary and special weather data which were collected during Edna's lifetime, especially during the nineteen hours immediately preceding the passage of the hurricane eye over Cape Cod. The basic standard to which all else is referred is the routine synoptic data, i.e. surface observations and radiosonde reports. Special radiosonde reports from Hanscom Field and surface observations at South Truro and Chatham, Massachusetts, have been of great value. Other data gathered at Hanscom Field (which is located partly in Bedford and partly in Lexington, Massachusetts) include the records of three adjacent recording rain gauges (weighing, tipping bucket and Hudson-Jardi). The very complete Blue Hill Observatory records of Edna have also been studied. Figure 2.1 illustrates the location of many of the places to which we shall refer in this report.

The radar data were collected at South Truro and Hanscom Field, Massachusetts, and at Montauk Point, New York. At South Truro, an FPS-3 radar with PPI, and FPS-4 and FPS-6 height finding radars were available. At Bedford, a TPQ-6 cloud base and top radar and 10 cm search radar were used; at Montauk the equipment was an FPS-3 system. The characteristics of these radars are listed in Table 1. Figure 2.2 is a key to the FPS-4 photographs.

Two 35 mm time lapse PPI movies have been available, one from Bedford and one from Montauk. RHI time lapse series and stills were taken at South Truro of the FPS-4 and FPS-6 scopes. In addition, 4 x 5 pictures of the FPS-3 PPI scope at South Truro at average intervals of about five minutes have been available. The South Truro data comprise the best photographic records; the pictures are sharp and contrasty. The Bedford and Montauk pictures are of great value because they have been the only time lapse PPI data available which may be run through a projector for motion studies. Generally, the quality of the latter pictures is not up to the standards necessary for extensive reproduction here.

A further valuable source of data has been the instrumental and visual observations of the crew of the WB-29 which conducted reconnaissance of the storm on 11 September 1954 between 0600 and 2100 EST.

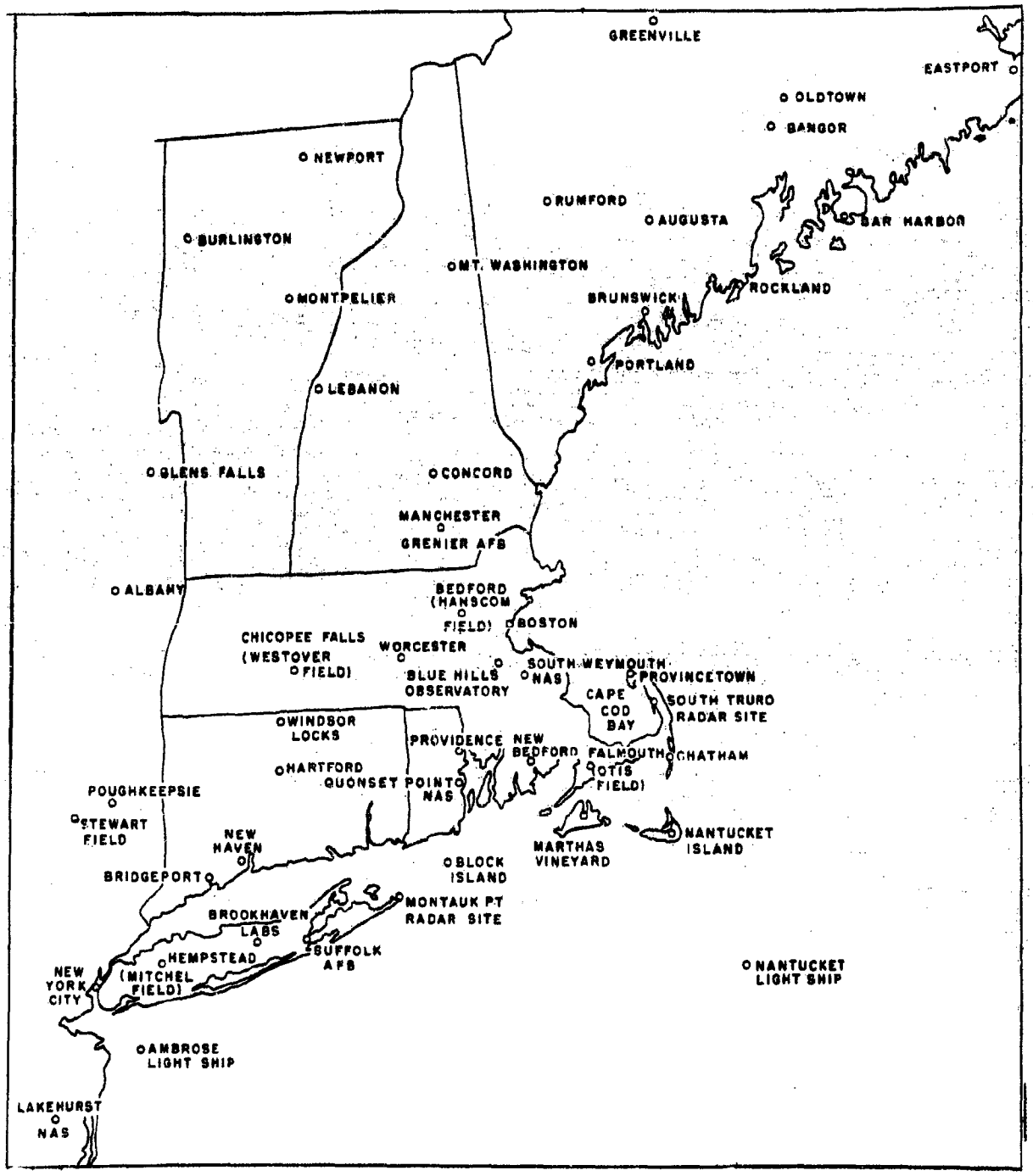

Fig. 2.1. Location of places contributing data to this report.

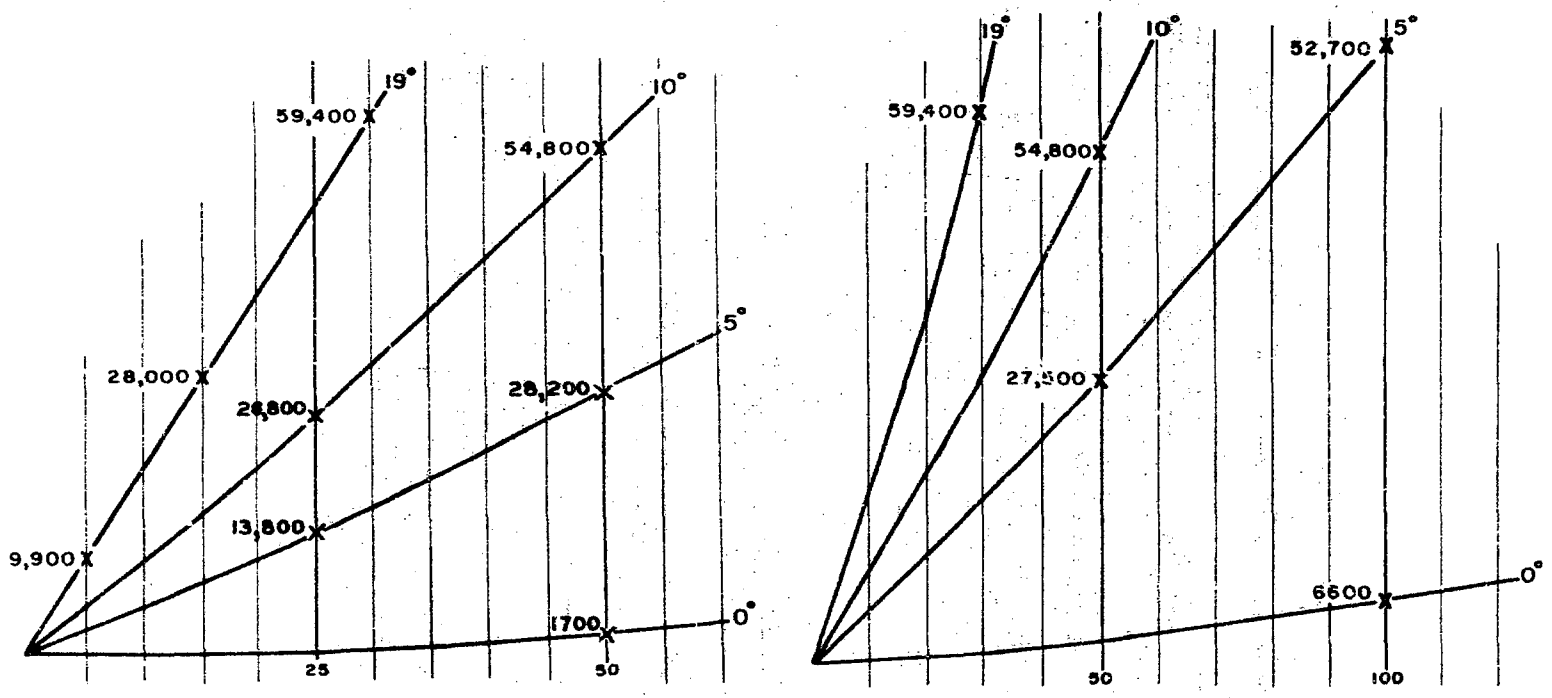

Fig. 2.2. Key to FPS-4 photographs, taken with 5 and 10 nautical mile range markers. Numbers at the marked intersections are elevations in feet. Note the non-linearity of the 100 mile presentation at great range and elevations.

Table 1. Characteristics of the radars contributing data to this study.

Radar	Wave-length (cm)	Pulse length (μsec)	Beamwidth (horiz)	Beamwidth (vert)	Peak Power (Kw)	PRF (sec^{-1})	Notes
TPQ-6	.86	1.0	0.29°	0.29°	25	492	Vertically pointing
FPS-4	3	2	2.05°	0.755°	200	539	RHI only
Special radar of Project Lincoln	10	1.1	1.7°	1.7°	500	1200	PPI, MTI* only
FPS-6	10	2	3.4°	0.9°	4000	270	RHI only
FPS-3	23	3	1.3°	3° to 18°	700 on each of 2 xmitters	400	PPI only MTI available

* MTI signifies "moving target indication."

3. Forerunners of Edna - High Clouds and Warm Showers on the Northeast Fringe

3.1 Radar Data

The radar photographic record at South Truro was begun at 1959 EST, 10 September, with photography of the FPS-4 (3 cm) RHI scope. First photos show a tenuous echo, presumably high cloud and undoubtedly composed of ice crystals,* with radar base at about 22,000 feet and about 8,000 feet thick (Fig. 3.1). Subsequent records show that, although breaks are present, this cloud sheet is widely distributed over the area and the base slopes downward and the cloud thickens to the southwest, i.e. toward the eye of the storm. This observation is consistent with the presence of a nearly saturated layer with base at 400 mb on the Nantucket sounding of 2200 EST, Fig. 3.2. Time lapse pictures represented by the first three of Fig. 3.1 demonstrate that the feature there marked by an arrow moves with a component from 220° of approximately 52 knots. This is in very good agreement with the winds reported by the Nantucket 2200 EST upper-air observation. It is noteworthy that

* Ordinary water clouds are generally not detectable by the FPS-4 and FPS-6 radars.

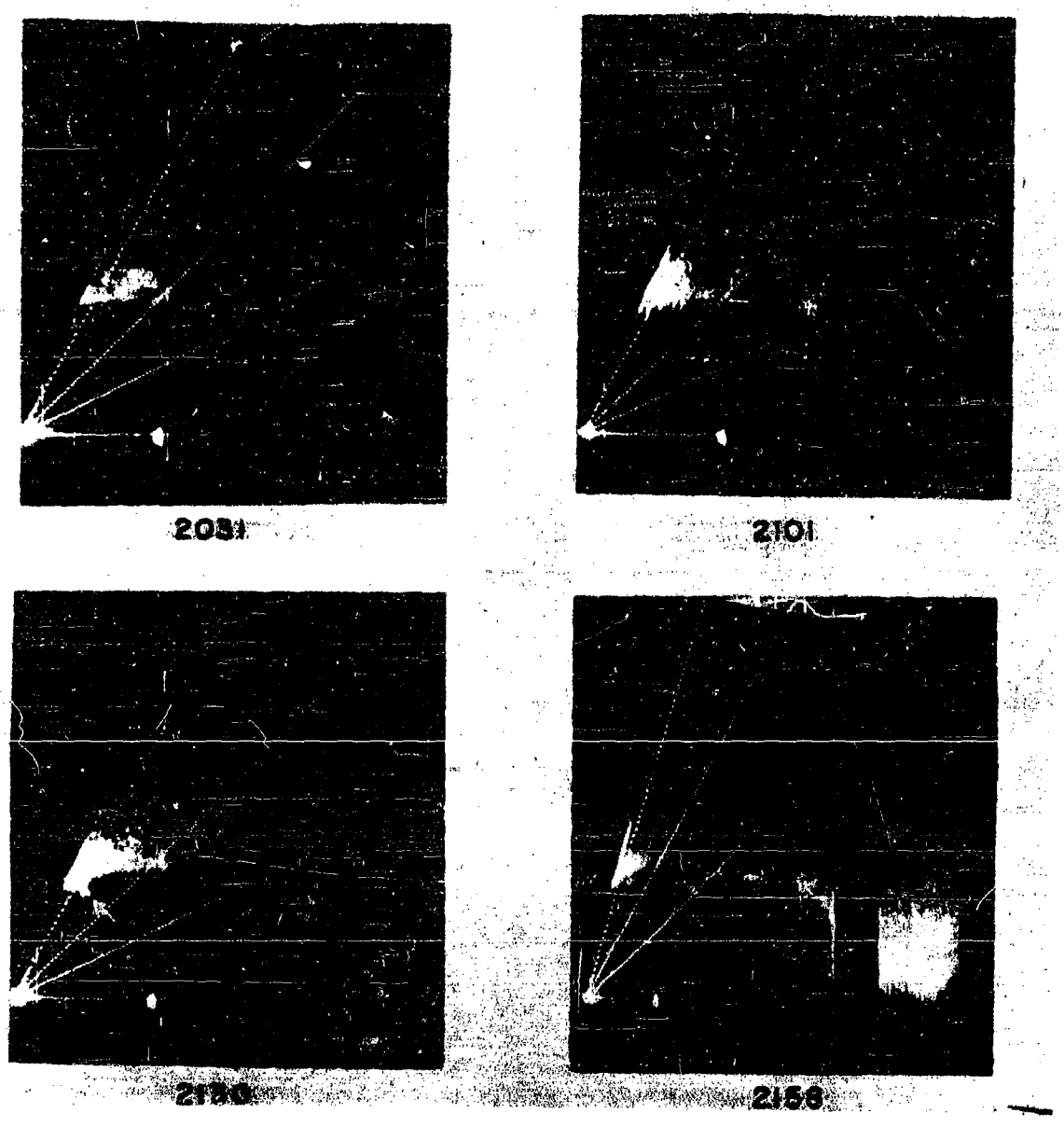

Fig. 3.1. Cloud deck with base at about 22,000 feet as seen by FPS-4 radar at So. Truro, 10 Sept. 1954. Range marks are at intervals of 5 nautical miles in the first 3 pictures, 10 in the last. Azimuth is 220°, and the indicated times are EST. Edna's eye is about 475 miles SSW of the radar. Note the feature marked by an arrow, which moves with a component of about 52 knots from 220°. At 2101, the jagged base of the upper cloud indicates evaporation. In the last picture note the gap in the upper cloud deck immediately ahead of the rain band at 95 miles. Keys to these photographs are presented as Fig. 2.2.

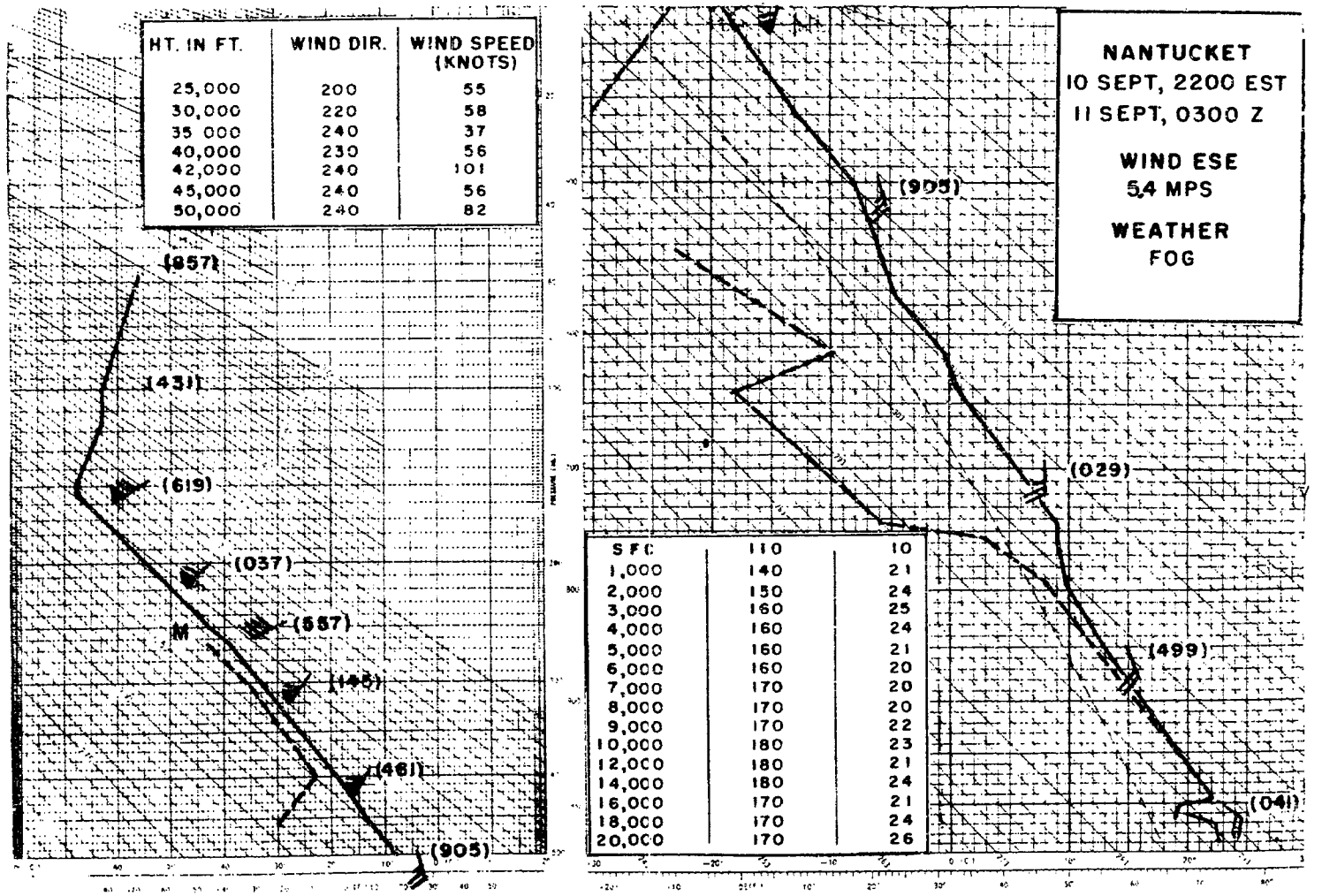

Fig. 3.2. Nantucket radiosonde report, 2200E, 10 Sept., plotted on a pseudo-adiabatic diagram. The full lines of the sounding are the plots of temperature, the dashed lines are dewpoints. The tables list the reported wind speeds in knots and directions in degrees at the heights in feet indicated. The sloping solid lines of the diagram are dry adiabats, and the single light dashed line is a moist adiabat. Numbers in parentheses are the heights in feet of the mandatory pressure levels (thousands and units figures omitted).

study of the early portions of the FPS-3 time lapse record obtained at Montauk Point likewise indicates a rapid movement from the SW or SSW of faint and very diffuse echoing masses which are believed to be dense upper clouds and appear because of the wide vertical beam of the FPS-3. Their motion from the SW occurs while discrete intense echoes, observable at the same time, move more slowly from the SE.

At about 2200 EST 10 September 1954, the 23 cm (FPS-3) PPI presentation at South Truro shows nothing significant north of the first major rain band of the hurricane, seen at about 100-140 miles to the southwest in Fig. 3.3, although the 3 cm RHI data demonstrates that the whole area is blanketed by upper clouds. Shortly thereafter, however, as shown by Fig. 3.3, sharply defined cells are observed to form along a nearly east west line passing near Nantucket (180°, 41 miles). By 2300 EST they are well organized and a conspicuous part of the PPI picture. The horizontal motions of nine of these cells have been studied, using PPI photographs at five minute intervals, and the results are given in Table 2 below.

Table 2. Statistics concerning warm showers

Cell #	Speed (knots)	Direction (°)	Time of Start (EST)	Time Tracked (min)	Initial Bearing from S. Truro	
					Range (naut. miles)	Azimuth (°)
1	25	320	2227	18	75	245
2	17	340	2227	39	30	210
3	22	320	2233	43	55	235
4	30	355	2336	65	50	260
5	22	345	2336	45	45	070
6	23	340	2341	100	75	030
7	15	000	2341	40	75	075
8	22	340	2355	46	30	345
9	19	345	2355	56	100	065
Average	22	340		50		

The average velocity is 22 knots toward 340°. This is in excellent agreement with the reported Nantucket winds between 3,000 and 9,000 feet (Fig. 3.2). The average tracking time of the cells chosen for study is fifty minutes. For several reasons, this is only a rough measure of the lifetime of the average cell. In some cases, tracking becomes impossible because a cell changes its shape or position discontinuously, making it impossible to know that the same feature is in fact

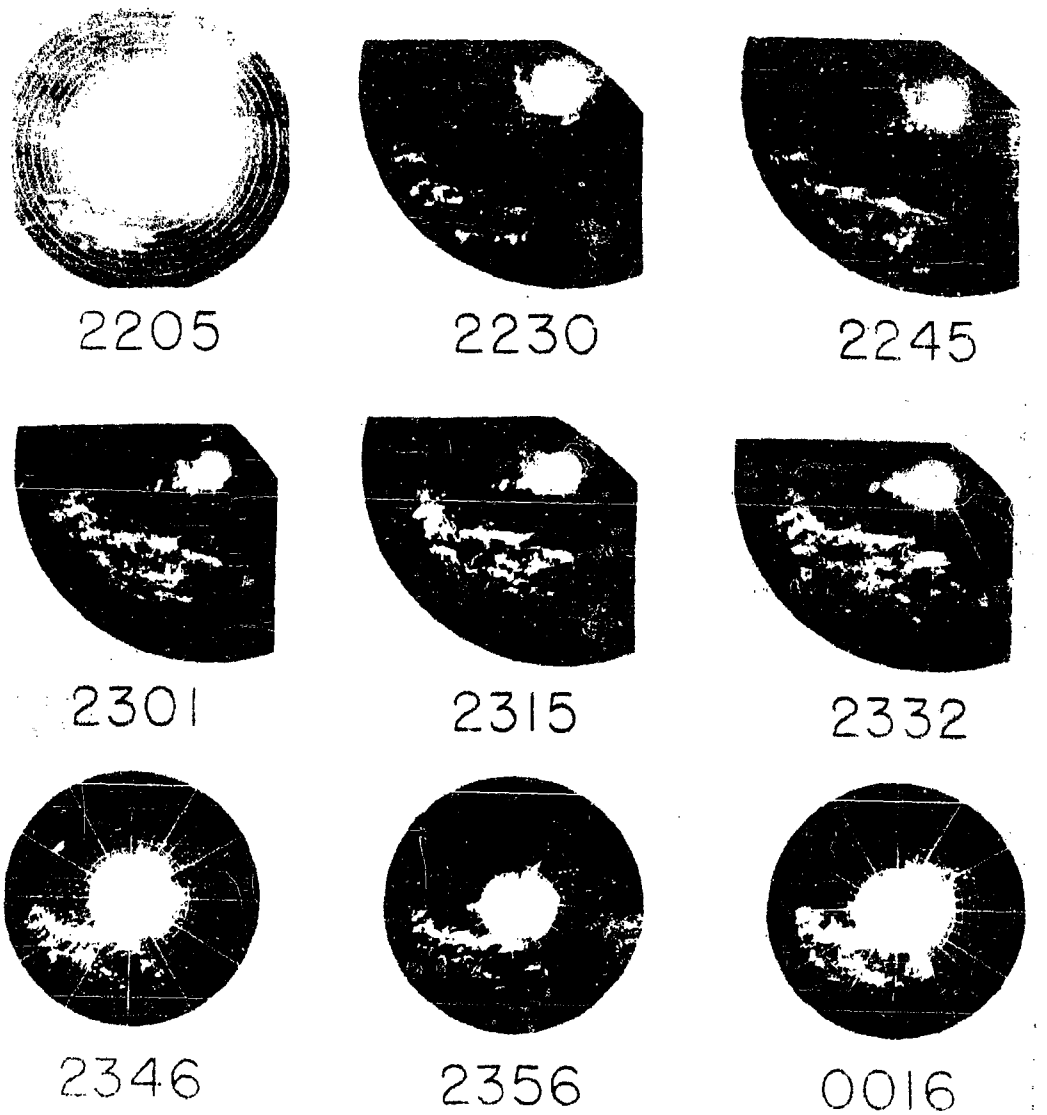

Fig. 3.3. Development of warm showers 400 miles ahead of the eye of Hurricane Edna, 10-11 September 1954. Times are EST. Note the rapid development of showers at 220°, 40 miles, between 2230 and 2300E. Range marks are at intervals of 10 nautical miles.

being followed; in others, because of a discontinuity in the sequence of pictures; in still others, because the cells disappear. The five-minute spacing of the pictures makes it impossible to study accurately cells whose duration is less than about fifteen minutes; on the other hand, those cells selected for tracking and which are observed to appear and disappear may exist up to ten minutes longer than observed. The authors have tried to take account of these factors and have subjectively estimated that the average cell lifetime in these warm showers is between thirty and fifty minutes. The variation of velocity measurements from cell to cell indicates the probable influence of strong intermittent development components.

Fortunately, RHI records are also available at this time. The 3 cm time lapse pictures have been studied in order to determine the altitude of the tops of these showers. The data on eleven discrete echoes are given in Table 3. Because no attempt was made to follow individual cells using the RHI and the azimuth of the beam was kept essentially unchanged at 220°, the echo heights and the growth observed are probably mostly indicative of the physical structure of already established cells and only slightly a measure of their development. However, it is evident that none of the cells exceeded 15,000 ft at first appearance, while five of them possessed maximum tops below the melting level near 14,000 ft (see Fig. 3.2). This is strong evidence that these low level shower echoes developed entirely in the water phase.

Table 3. Showers observed to pass through the beam of the FPS-4 (Azimuth, 220°)

	1	2	3	4	5	6	
	Time of 1st	At first appearance		Time	Maximum	Horiz. Dim.	
Cell #	appearance (EST)	Ht of top (1000 ft)	Ht of midpt. (1000 ft)	visible (minutes)	Ht observed (1000 ft)	(miles)* a	b
1	2154	15	12	merged w/others	-	-	3
2	2219	11	8	14	19	4.5	4
3	2221	13	11	6	13	1.9	2
4	2233	11	8.5	4	11	1.3	1.5
5	2233	10	5	14	16.5	4.5	4
6	2235	11	7	2	11	0.6	2
7	2243	10	5	10	13	3.2	4
8	2243	12	7	15	22	4.8	4
9	2248	12	10	4	12	1.3	1
10	2256	12	9	18	22	5.7	6
11	2300	11	5	25	22	7.9	5

* Column 6a gives the dimension perpendicular to the direction of the beam as computed from the time visible (see text). Column 6b gives the maximum dimension along the beam, as observed directly.

The orientation of the beam is such that the cells progress through it at an angle of about 60°. In fact, the horizontal breadth of a cell normal to the beam direction, neglecting the complicating effects of beam width, is given by d = 22 x t x sine 60°, where 22 knots is the assumed speed of the cells and t is the time visible. The dimensions given in Column 6a of Table 3 are based on this equation. Column 6b indicates the maximum breadth of the cells observed in the direction of the beam. The average of Column a is but 0.2 mile greater than that of Column b, although consideration of beam width effects leads us to expect a considerably larger difference in the absence of systematic departures from cylindrical shape.* This discrepancy arises in part because of the one minute interval between RHI pictures which causes the average duration of cell observations to be somewhat less than the average period "in the beam."

While many more cells are visible on the RHI pictures than are given in Table 3, these are the only ones which can be observed as distinct entities during the intervals when the azimuth was kept unchanged; two or more cells often combine in a way that makes identification difficult.

It may be noticed in Table 3 that the cells which are small in height are also of relatively small horizontal extent, and there is a definite tendency for the broader storms to reach greater maximum heights. Another interesting fact is that the later cells are, on the average, larger than those at the beginning of the period of study. This confirms the PPI observation that the cells increased in size and intensity for at least an hour after they first appeared.

Toward the end of the period of RHI observation, several cells are observed with tops at 22,000 ft; at this and later times, scattered cumulonimbus are also present, as discussed below. The period of RHI observation is less than that on PPI; after 0000 EST the cells are mostly north of the station and are no longer seen by the radar beam directed toward 220°. At 2300 EST, photographs are available at 20° intervals of azimuth completely around the horizon. Figure 3.4 illustrates the three dimensional structure at this time. The main band of convective cells runs just south of the station. Except for one large cumulonimbus, the cells have about the same elevation as those listed in Table 3.

---

* A pulse length of 2 μsec represents a range resolution very close to 1000 ft; a beam width of 2° represents an azimuthal resolution of about 5000 ft at a range of 25 miles. Thus, a cylinder passing through the beam at a range of 25 miles will, in theory, appear about a mile greater in dimension across the beam than along it. The FPS-3 PPI photos show the effect as a widening of the azimuthal dimension of the weather echoes. This is most apparent with the smaller discrete echoes.

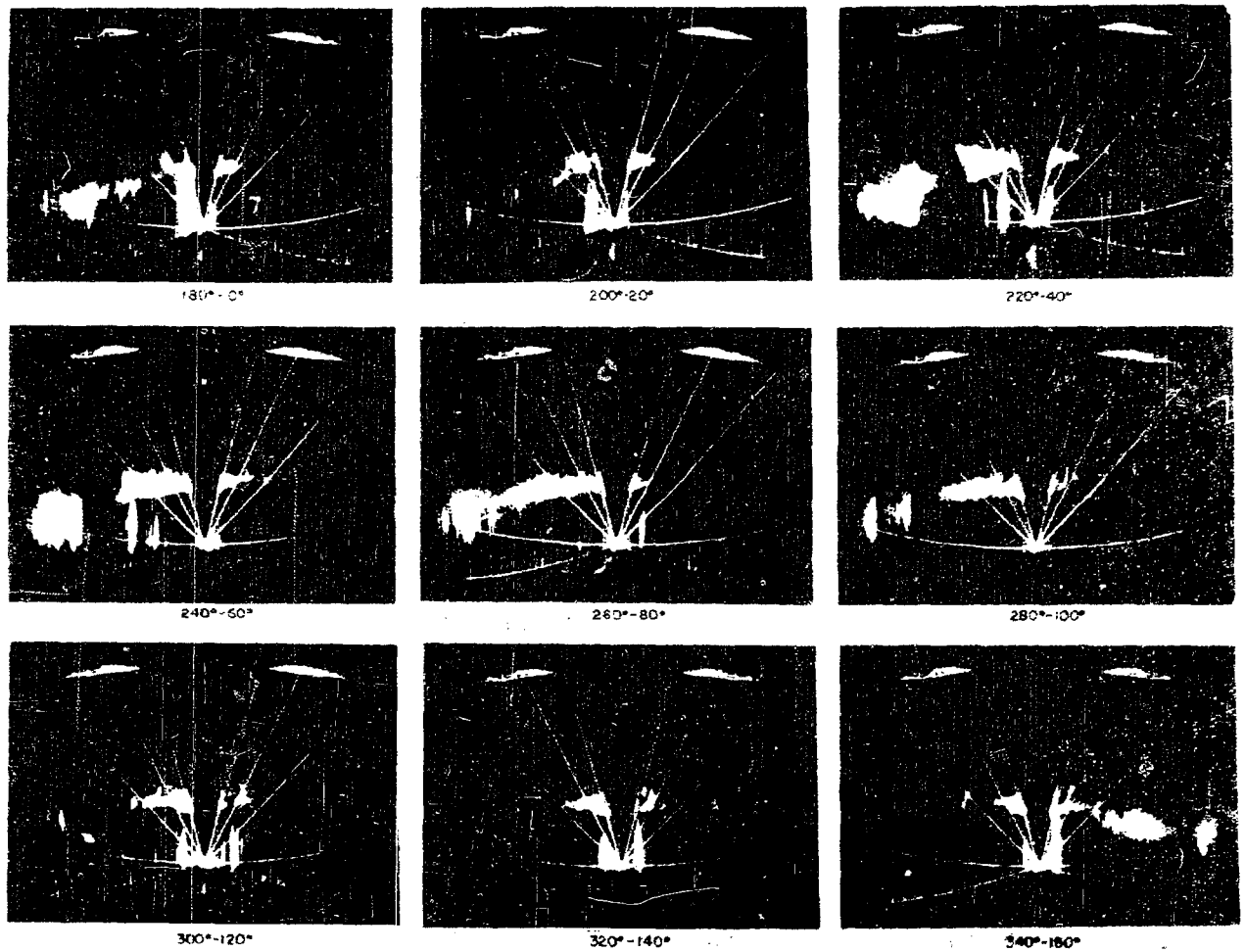

Fig. 3.4. Three dimensional cloud and precipitation structure at about 2303 EST, 10 September, as seen from So. Truro by FPS-4 radar. Range marks are at intervals of 10 nautical miles, and explanation of the angle marks may be had by reference to Fig. 2.2. The hurricane eye is positioned at 207°, 450 miles relative to the radar site at this time. Note the cumulonimbus in the first picture (180°) and the gap in the upper cloud deck which occurs just ahead of the rain band in the third picture (220°). The gap is attributed to downdraft which compensates the updraft characteristic of the rain band. The vertical shower columns are indicative of the absence of important shear in the layer through which the showers are growing.

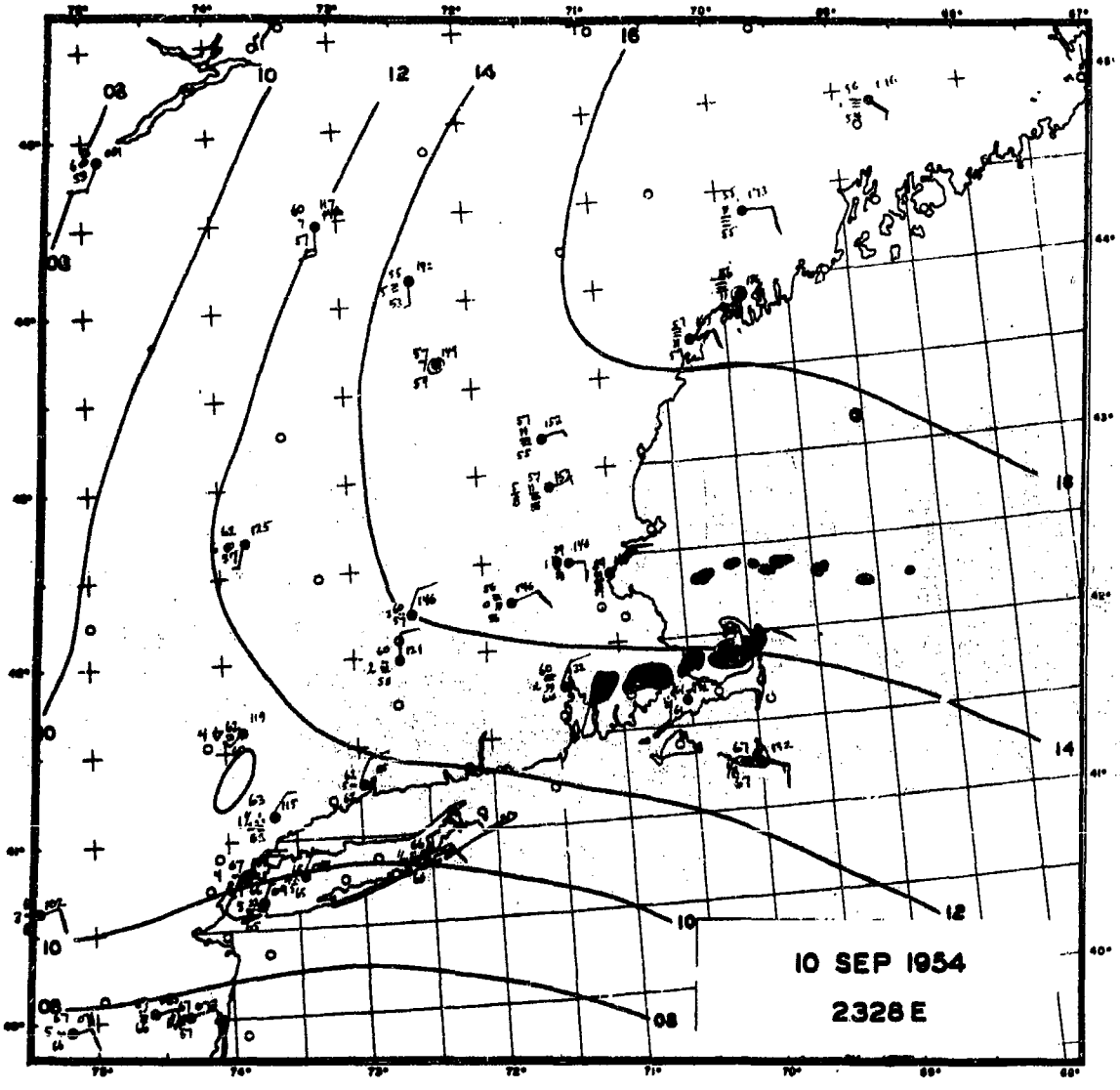

Fig. 3.5. Convective echoes in black as observed by 23 cm radar at So. Truro, and a large scale weather map of New England. The echo positions and shapes have been derived from photographs taken within 10 minutes of the time of the map. The similarity of size among the cells within each line suggests that all cells within a line are initiated at nearly the same time. This is indicated also by study of the PPI sequential photographs. The hurricane eye at this time is located SSW from So. Truro, about 440 nautical miles.

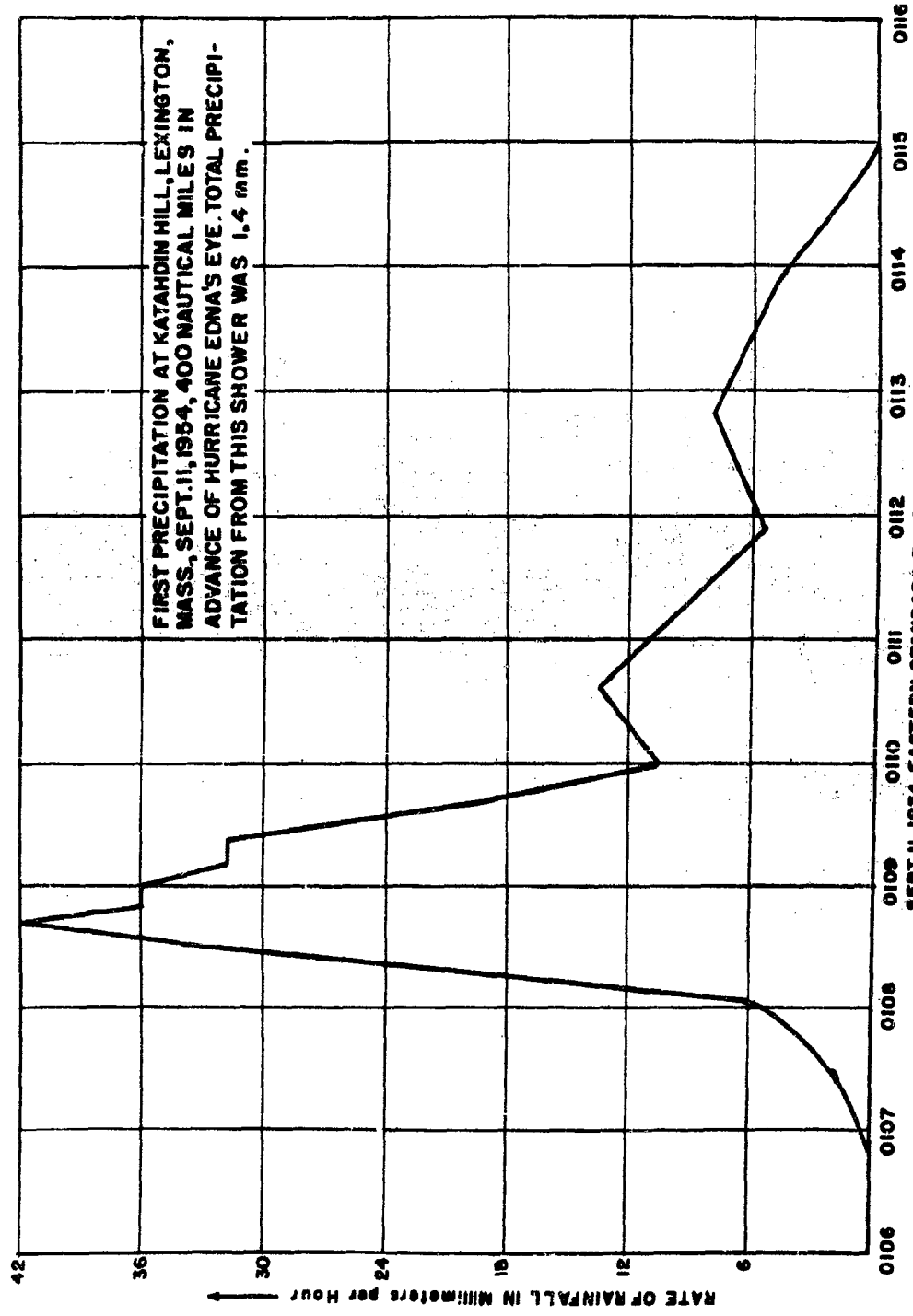

Fig. 3.6. Rainfall rate during a shower associated with the outer convective bands of Hurricane Edna, as measured by a tipping bucket gauge.

It is of interest to note that the passage of the first band of warm showers at South Truro and at Hanscom Field was associated with lightning and thunder. At no other time during the remainder of the storm was electrical activity observed at South Truro. In other hurricanes also, lightning has been observed in the outer regions (Dunn, 1951) and the cellular nature of the outer bands as seen by radar has been noted (Ligda. 1955). Judging from the radar appearance as well as surface weather effects illustrated by Wexler's meteorograms (1949), the outer convective activity is akin to the summer squall lines of temperate latitudes. It is significant that thunderstorm activity is usually observed only in the peripheral area of mature storms and not in association with the more continuous type rain nearer the eye, even when the rain intensity is very great. (Exceptions to the rule are, of course, observed in even casual studies of reports of individual storms.) This is one of the indications of the stability of the continuous inner bands which will be treated later. It should be mentioned that the presence of an overlying ice crystal layer above the warm showers has suggested to some* who have examined the observations that the lightning may be initiated as a discharge between the snow and the warm shower as the top of the shower approaches the upper deck. Alternatively, the heavy riming which occurs in the ice crystal cloud when its base is penetrated by dense supercooled water cloud may provide the charging mechanism responsible for the lightning activity. (There is some suggestion, although by no means conclusive, that the electrical activity occurs at about the time that the tops of the low level showers penetrate the upper ice crystal deck.)

3.2 Synoptic Data

The surface weather map for 0130 EST shows Edna east of Norfolk, Virginia. Northeasterly flow prevails at low levels over New England, and southerly flow aloft is indicated by the Mt. Washington report and by upper wind reports to be discussed. Over the waters southeast of New England, the flow is southeasterly and tropical maritime air is being borne by this flow into New England. Light to moderate continuous rain and some light showers are reported at southern inland stations; the Cape Cod and Maine coastal areas are reporting fog and drizzle. There is practically no suggestion from these synoptic reports of the convective echoes displayed by the radar, which are superimposed in part in Fig. 3.5 on a large scale weather map of New England for 2328E, 10 September.

The wind record at South Truro shows a gradual wind shift from ENE to SE between 2330 EST 10 September and 0030 EST 11 September, which coincides with the passage of the first main line of cells. The 0111 PPI picture (see Fig. 3.9) shows that the center of a detached cellular

---

* Prof. J. S. Marshall of McGill University, for one.

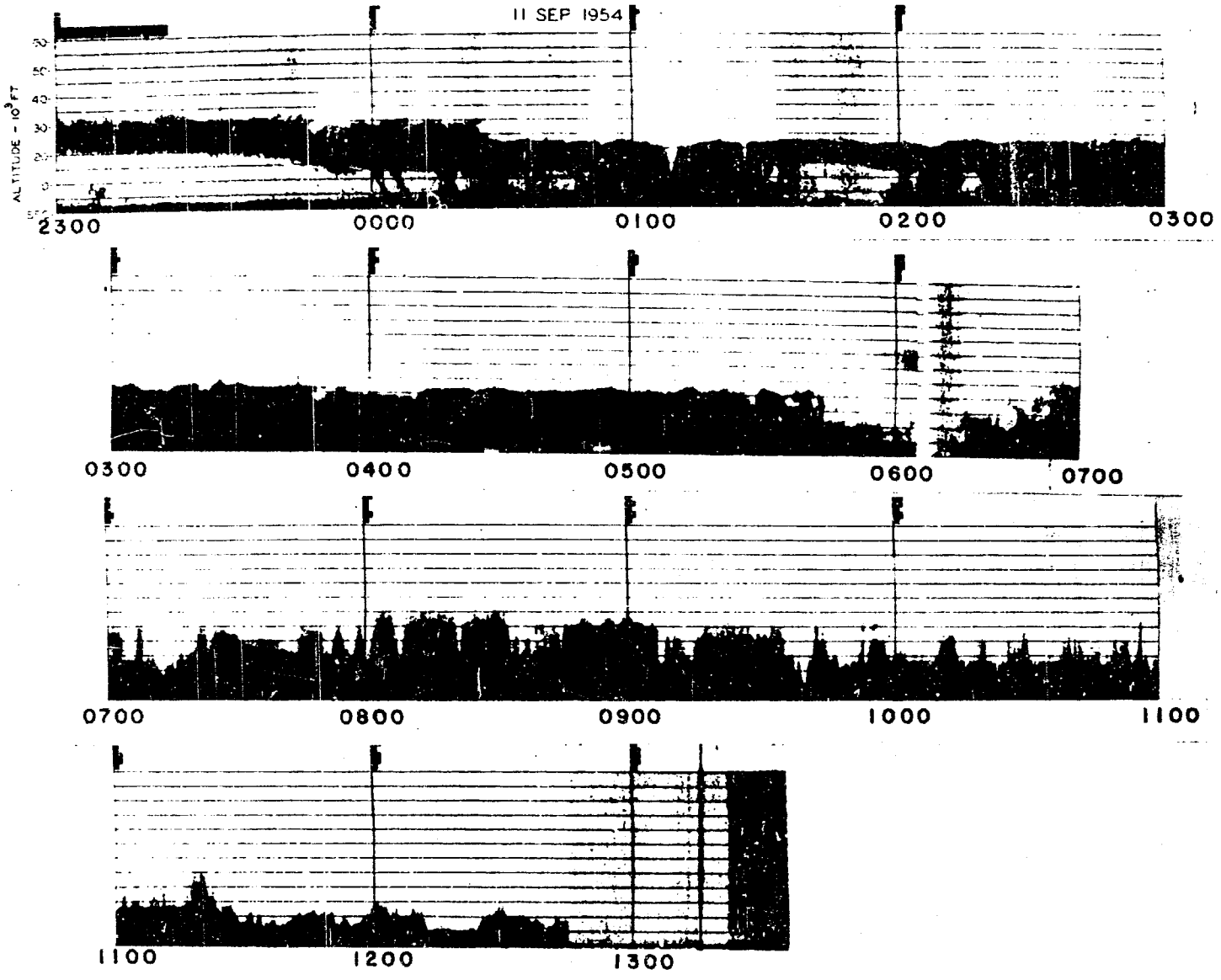

Fig. 3.7. TPQ-6 (vertically pointing beam) time-height record of Hurricane Edna made at Reservoir Hill, Hanscom Field, Mass. Indicated times are EST. The height of the cloud base at 2300E is in excellent agreement with the 22,000 ft. elevation observed with 3 cm radar at So. Truro at this time. Note the "V" in the return at 0110, caused by attenuation in a thundershower, and the symmetrical appearance of the precipitation structures in this area, suggesting low level inflow and outflow aloft. After 0700, the valleys in the return are mostly due to attenuation, the height of the echo being least when the rainfall is heaviest.

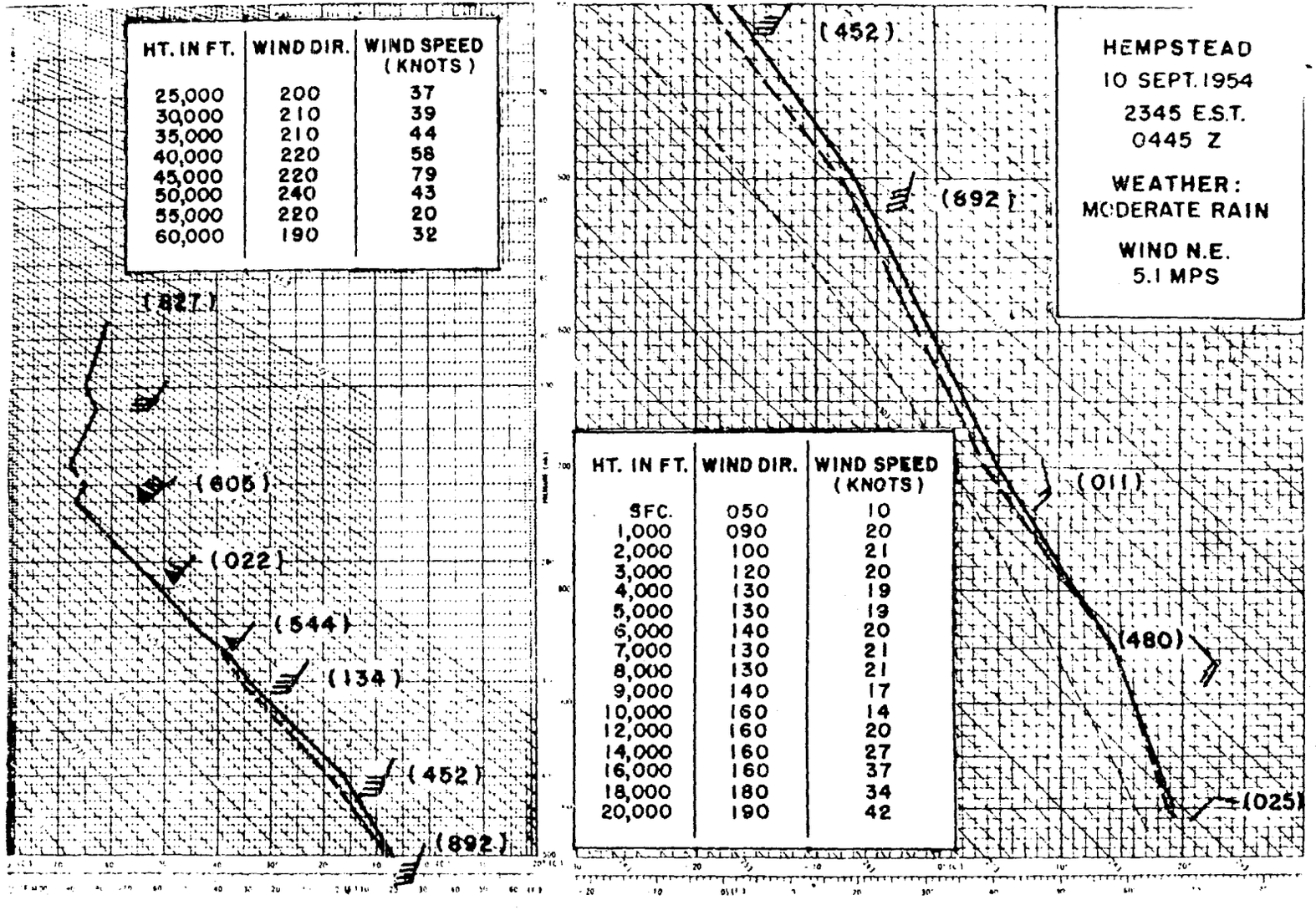

Fig. 3.8. Hempstead radiosonde report, 2345EST, 10 September, plotted as in Fig. 3.2. Edna's eye is located at about 309 nautical miles, 186°, from Hempstead at this time.

mass is just south of the Katahdin Hill site (Hanscom Field, Mass.) located at 63 miles, 302°. A very brief but heavy shower commenced at the latter site at 0107 EST, ended at 0115, and is probably a part of this region of radar return. The tipping bucket record of this shower at Katahdin Hill is presented as Fig. 3.6. Note that the total precipitation is only 1.4 mm. Rain fell at a maximum recorded rate of 42 mm per hour and at 30 mm per hour or more for a minute. As already noted, some thunder was reported to have occurred at Hanscom Field and South Truro during the passage of this shower band, indicating that this intense rain fell from a well developed storm. Indeed, this is indicated by the TPQ-6 record made at Reservoir Hill, one mile NW of Katahdin Hill, which shows this heavy shower in time-height cross section. It is identifiable on the record (Fig. 3.7) as a "V" in the return at 0110 EST. The "V" is caused by attenuation at the time of greatest rain intensity. Perhaps the most interesting feature of this portion of the record is the reversed slope of precipitation columns on either side of the main shower (at 0110) and the generally symmetrical appearance of the precipitation structures in this area. Low level inflow and outflow aloft (at about 15,000 to 20,000 ft) are suggested by the directions of the shear.

The Nantucket raob, released at 2200 EST of 10 September (Fig. 3.2), is also of interest. It indicates that practically saturated conditions exist from the surface to 790 mb. A temperature inversion exists from 1019 to 995 mb and above this the lapse rate is in excess of the moist adiabatic to the base of a dry layer at 790 mb. Between 995 mb and 790 mb the condition is, therefore, one of marked instability. From 790 mb to 640 mb the air is convectively unstable. The wind exhibits strong shear only in the lowest 1000 feet and again between 20,000 and 25,000 where the wind increases in speed from 26 to 55 knots and shifts in direction from 170° to 200°. As already noted, the average drift of the convective echoes toward 340° is in excellent agreement with the winds between 3,000 and 9,000 feet. Reference to Table 2 shows that echoes 1 and 3, which move from the SE, are also at the greatest range to the southwest. Interpolation between the Nantucket sounding and the 2345 Hempstead sounding, Fig. 3.8, indicates that the motions of these two cells are again consistent with the winds between about 3000 and 9000 feet.* The Hempstead and Nantucket wind data lend further support to the idea that effective generation of the echo is occurring well below the melting level, which is between 13,700 and 13,800 feet.

The Hempstead wind report has explained a portion of the variations of observed cell velocities. The Hempstead dew point and temperature-height curves for the same time indicate a neutral or somewhat

---

* Velocities of echoes on the PPI are generally representative of those levels in which the RHI scope shows the echoes to be vertical. See Section 5 for further discussion.

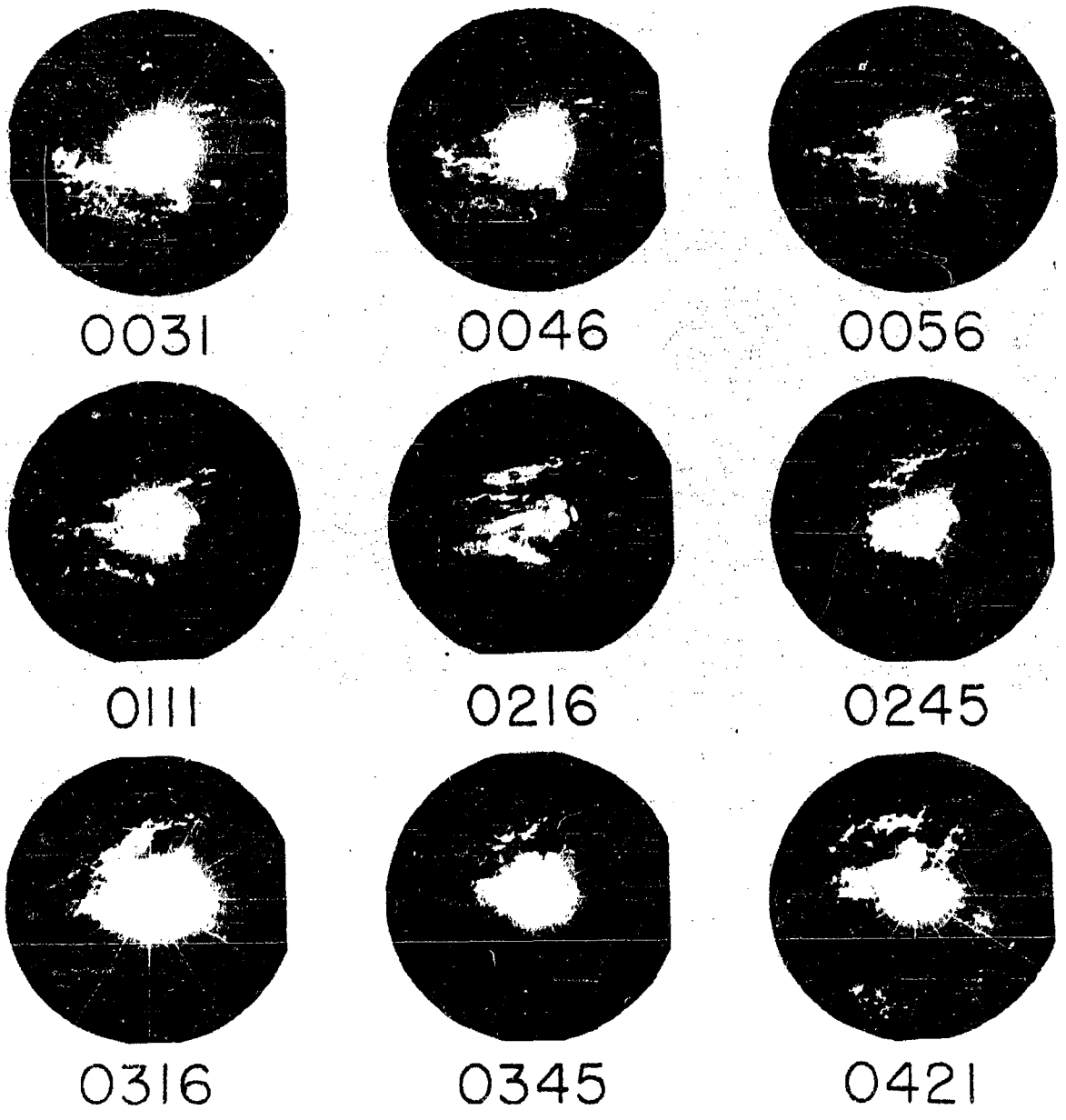

Fig. 3.9. Evolution of the PPI pattern, 11 Sept. 1954, as observed at So. Truro by 23 cm radar, and as Edna moves toward the station. Maximum range of these pictures is 170 nautical miles. Range marks are spaced 10 nautical miles. Note the convective bands just north of the station in the first pictures, which move northward and gradually transform to rain of more stable type. Bands of continuous rain (with some convective lines) are meanwhile moving from the south as well as developing locally over the station. At the time of the last picture, Edna's eye is located at 300 nautical miles, 205 °.

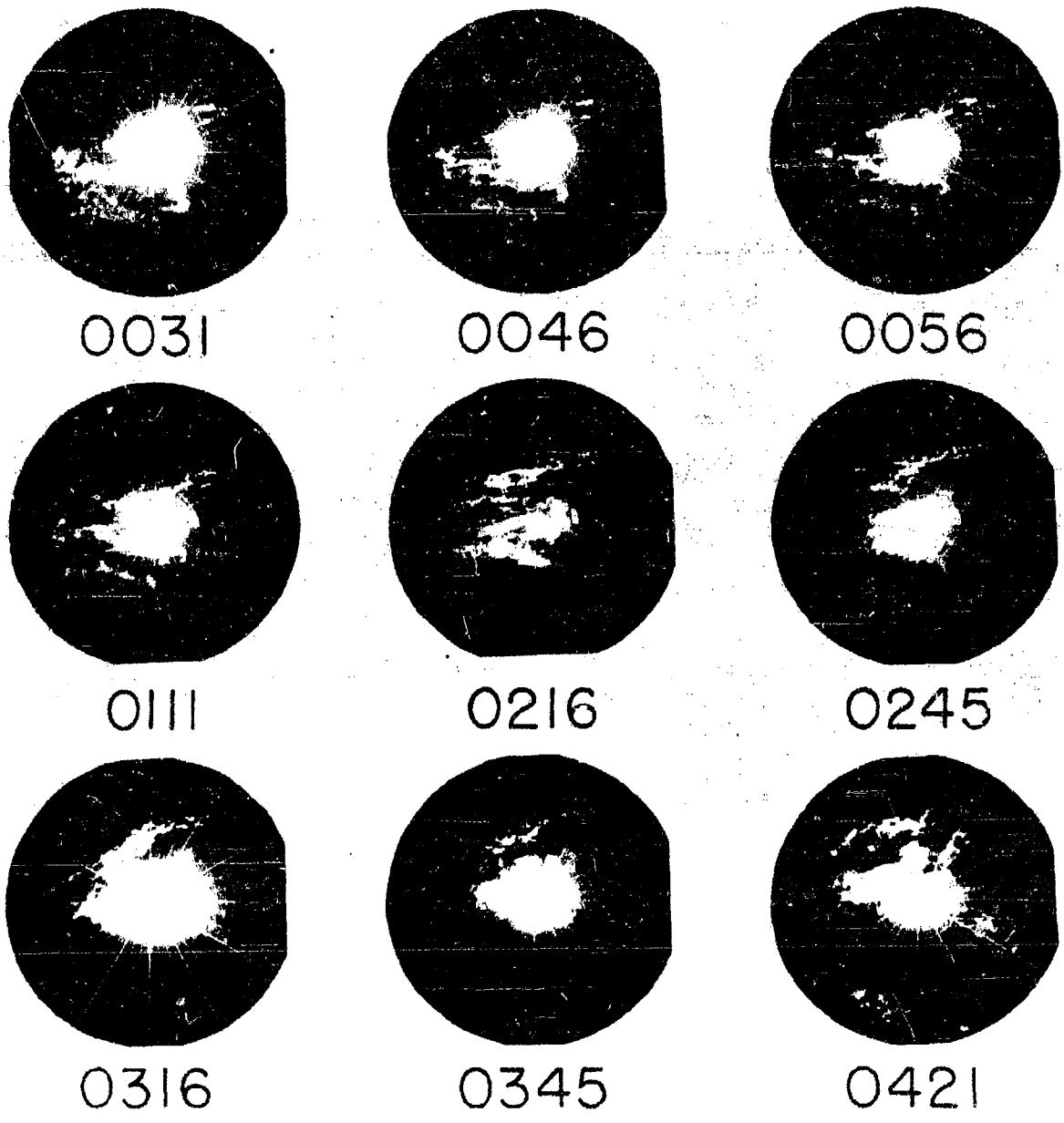

Fig. 3.9. Evolution of the PPI pattern, 11 Sept. 1954, as observed at So. Truro by 23 cm radar, and as Edna moves toward the station. Maximum range of these pictures is 170 nautical miles. Range marks are spaced 10 nautical miles. Note the convective bands just north of the station in the first pictures, which move northward and gradually transform to rain of more stable type. Bands of continuous rain (with some convective lines) are meanwhile moving from the south as well as developing locally over the station. At the time of the last picture, Edna's eye is located at 300 nautical miles, 207°.

stable temperature stratification and this is a reasonable accompaniment of the more uniform type of echo observed toward that site (Fig. 3.3).

It is difficult to understand, simply on the basis of the Nantucket and Hempstead wind reports, why the cells should form in lines or bands. If the lines are directly related to the vertical wind shear, as proposed by Kuettner (1955), the relationship must be delicate indeed. In Fig. 3.5 the convective bands are seen to be nearly parallel to the surface winds or isobars and this relationship seems to hold approximately for the major banded structures throughout the storm. The PPI records (Fig. 3.3) near the time of initial formation and the similarity among the sizes of cells within a line indicate that their initiation is nearly simultaneous, and that growth proceeds more or less uniformly along the lines. In view of the above, it appears more reasonable to ascribe the line to unknown dynamics of the horizontal flow rather than to its variations in the vertical.

A last item of interest is the indication of Table 1 that several convective cells were limited at the same height of 22,000 feet. This observation may be an indication of a barrier to further growth near that level. The Nantucket sounding indicates that this may be strong wind shear between 20,000 and 25,000 feet. RHI pictures after 2320 EST, however, show significant penetration of the upper shear layer and formation of large cumulonimbi reaching to at least 35,000 feet. Such growth may have been occasioned by the natural seeding of the supercooled water in the convective cloud tops by particles from the upper ice crystal deck. This process would cause a sudden increase of cloud top temperature through release of the latent heat of fusion, and provide an accelerating impulse for continued growth. It should be noticed further that the layer of strong shear also separates the dry zone of the middle troposphere from the moist, nearly neutral layer at 400 mb and above, which has been mentioned earlier. The formation of the convective cells at very low levels and the failure of many of them to penetrate through the dry shear layer show that these cells are basically a low level phenomenon, only remotely connected to events in the upper troposphere.

The PPI photographs give us some idea of the evolution of the bands of convective cells after they had moved northward, and were not extensively observed by RHI. Figure 3.9 illustrates the progressive change to stable type rain which occurred. The cells gradually lose their sharp outlines, and by 0421 EST when the band is located about 100 miles to the north, the conversion to more or less stable type rain is virtually complete, except at the eastern end of the band. It is apparent also from the figure that the banded structures as well as individual cells lose definition, and there is a tendency for merger of initially discrete bands. This conversion may be attributed to continued low level convergence which operates to establish a neutral lapse rate. When this occurs, the precipitation must be more nearly uniform and due

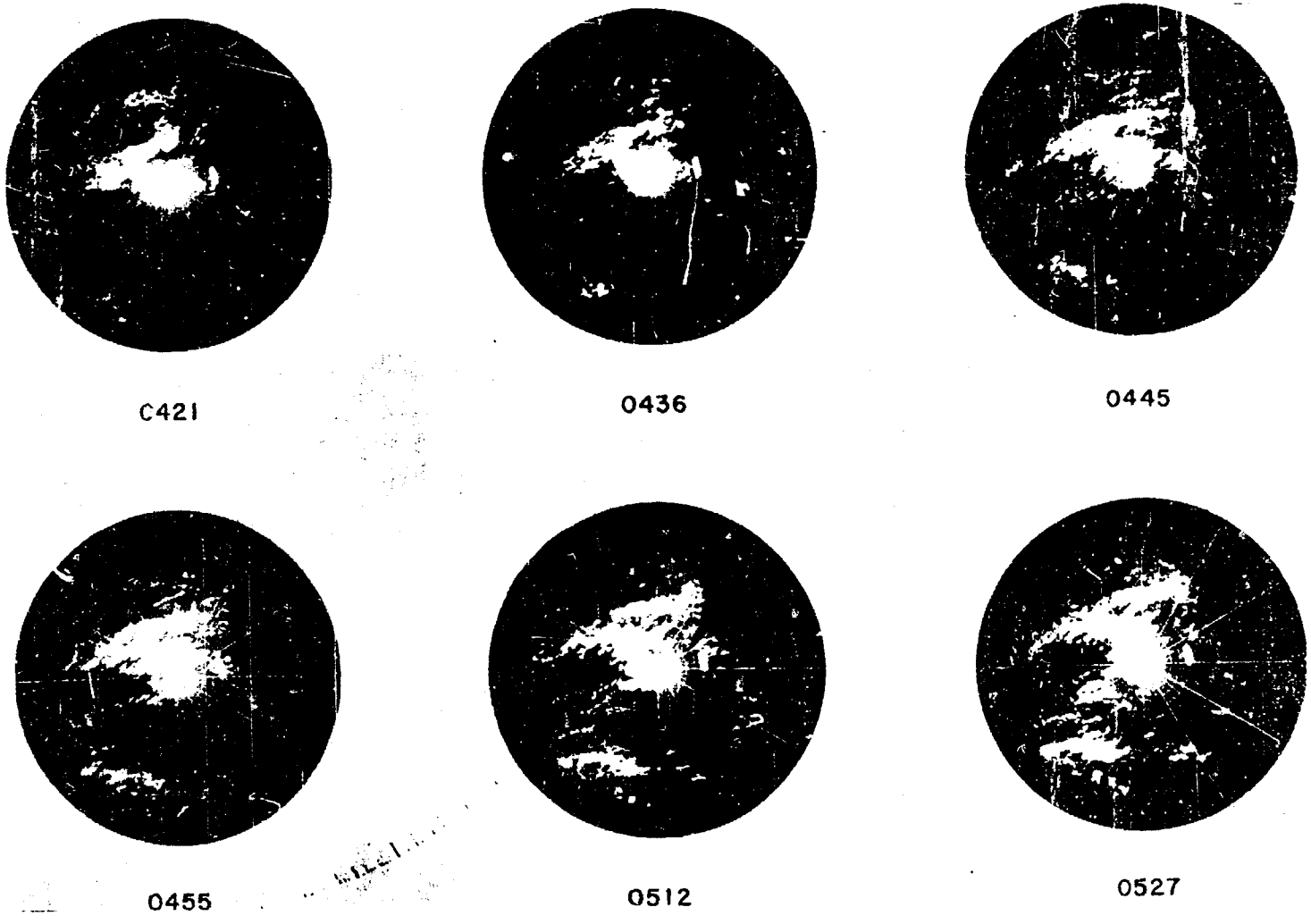

Fig. 4.1. Rapid development southwest of So. Truro as Hurricane Edna moves toward the radar site. Range marks are at intervals of ten nautical miles. The first picture of this sequence is the same as the last of Fig. 3.9. In the lower row of photographs, discrete echoes (convective cells) and continuous fuzzy echo (stratiform type rain) are visible together in the area centered at 240°, 75 miles. This is due to the wide vertical beam of the FPS-3 radar, which scans the low level convective elements and higher ice crystal clouds simultaneously. Both types grow in the general updraft which arises during the period illustrated. To the extreme south, elements associated with strong winds of the hurricane circulation move NNW.

almost entirely to the large scale convergence accompanying the hurricane.

It is believed that the air passing Nantucket at 2200 EST was previously even drier above the low level inversion, but convectively unstable. The air may have attained such a state by the operation of subsidence and radiative processes in the middle troposphere, and heat and moisture transfer from the ocean surface, over a period of days. As large scale convergence begins, the lowest layers are rendered saturated and unstable first, because of the great moisture values near the ocean surface. Convective overturning and continued large scale convergence then operate to increase the moisture content of the upper layers. Virga falling from the upper cloud deck (Fig. 3.1) to the drier air beneath may also serve to decrease the stability of the middle layers by evaporative cooling. Transport of heat upward by the low level convergence and the convective overturning, however, must ultimately stabilize the air. The 2200 EST sounding apparently catches this process in the middle of its act. That showers of this type occurred in the Cape Cod area in advance of the storm, but not at Hempstead (radar photographs taken at Montauk Point indicate little convective activity ahead of the storm over Long Island), appears to be related simply to the different air mass types present at the two locations. In a sense then, this occurrence may be viewed as a synoptic accident, though the flow pattern about a storm in middle and high latitudes must be instrumental in drawing air of characteristically different properties into specific regions.

4. Banded Structures Observed in Hurricane Edna

The radar photographs of "Edna," like those of other hurricanes, indicate that the precipitation area is comprised mainly of banded structures. However, it is found that stability, moisture, vertical wind shear and other meteorological parameters vary irregularly over the rainy region. It is difficult, therefore, to relate banded structures to these parameters. Variations in the internal structure of the bands also occur, as is shown below; it appears that many of the patterns are similar mainly with respect to their bandedness, and otherwise bear little resemblance. This section deals primarily with the observations in the hope that others may be stimulated to seek appropriate hydro- and thermodynamic explanations.

4.1 Outer Bands

The characteristics of the outermost hurricane bands are reviewed only briefly here, in view of the treatment in the preceding section on warm showers. First evidences of these structures are observed near Nantucket at 2200 EST. Approximately 20 dots about one mile in diameter appear nearly simultaneously in a region 50 miles long and 10 miles wide. Like most of the bands to be discussed later in this

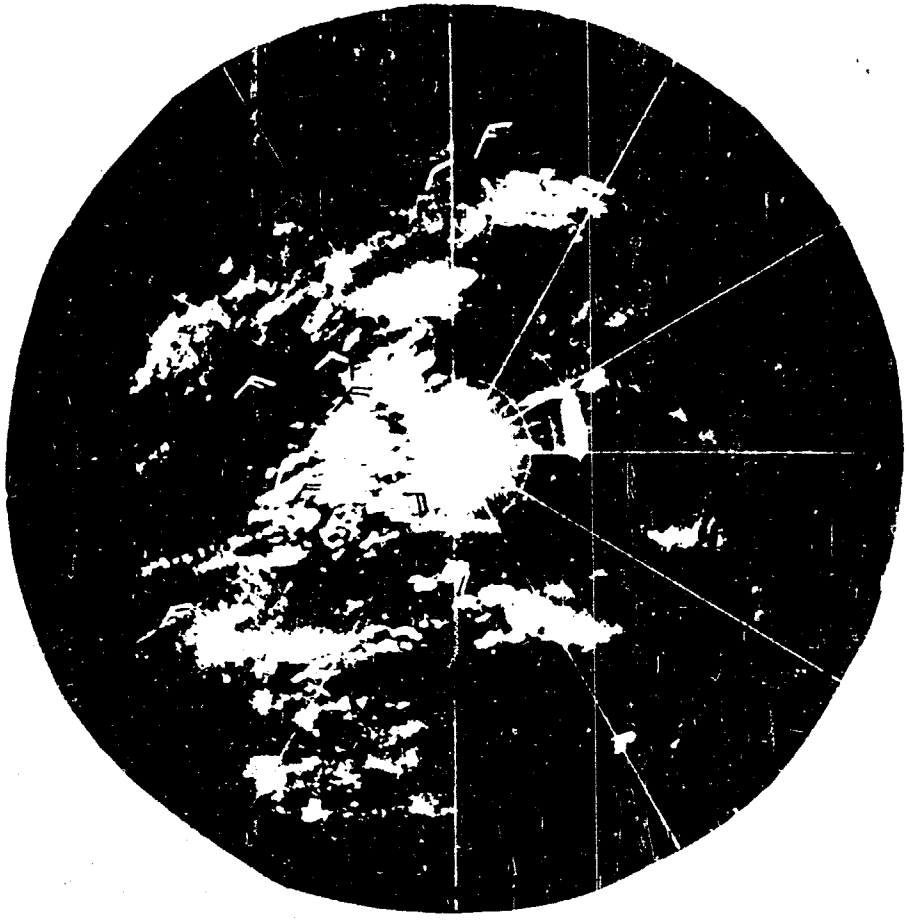

Fig. 4.2. So. Truro FPS-3 presentation at 0601 EST, 11 Sept. 1954. Edna's eye is 260 nautical miles SSW of the radar. Plotted winds are derived from original reporting forms of the New England airways stations. Convective elements which originate in the lowest levels coexist in many areas with continuous return which is associated with precipitation originating in an altostratus layer. (The outline of Cape Cod may be seen within the 20 mile range circle.)

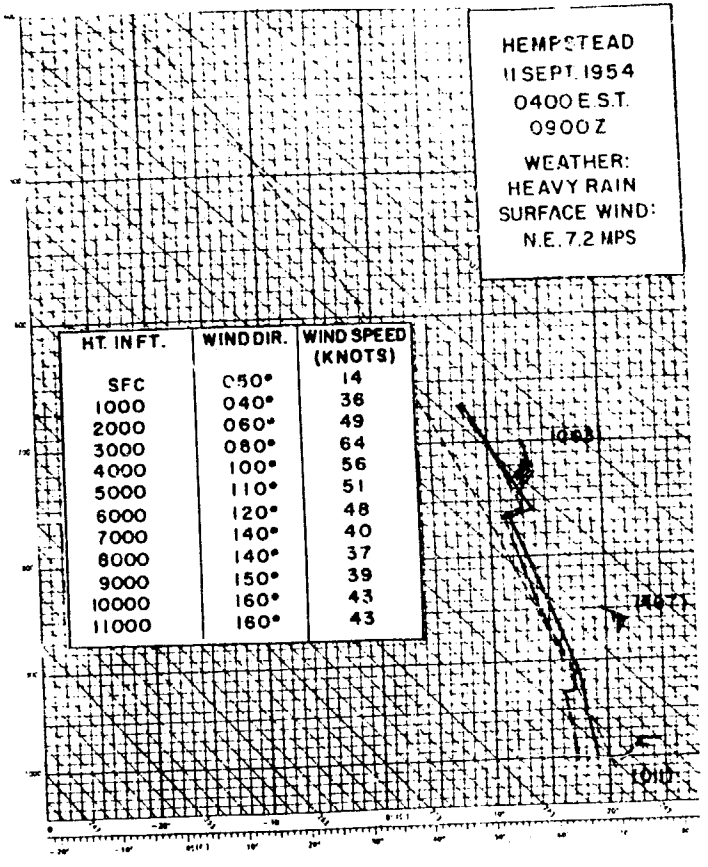

Fig. 4.3. Hempstead ascent of 0400 EST, 11 Sept. 1954. Note the strong veering of the wind in the lowest layers and the wind speed maximum at 3,000 ft. The sharp inversion is reminiscent of Simpson's findings of significant stratification in rain areas of Hurricane Dolly, 1953.

section, their orientation approximates that of the surface isobars or surface winds. Within twenty minutes many of these grow to a diameter of five miles. At nearly the same time, a second line of showers appears to form over Cape Cod proper, but is masked by general scope saturation at close ranges. As noted in Section 3, the average motion of individual cells in the bands is 22 knots from 160°, in excellent accord with the Nantucket winds between 3,000 and 9,000 feet. The cells form in a convectively unstable layer in which there is only very slight wind shear. As large scale rising motion and horizontal convergence and smaller scale overturning continue, the air is rendered less unstable and the cells gradually merge and form a nearly continuous precipitation area. Some low level convergence is indicated by the South Truro observations, the wind being light southerly from 1430 to 1830, light NE from 1900 to 2330, and SE after passage of the main band. Boston, at the western extremity of the band, and Nantucket, near the band when it is first observed to form, report no such wind shifts. The wind at Boston is NE to NNE from 2400 of the tenth to 0330E of the eleventh, while that at Nantucket is SE or SSE at these times and also earlier, from 2200E of the tenth when the band first appears.

It appears, therefore, that the initial trigger for the main band of warm convective showers is a line of convergence parallel to the surface winds or isobars. While the individual showers move with the winds from 3,000 to 9,000 feet, they remain in this line. Further, the absence of noticeable tendency for new development ahead of the band suggests that the line of convergence progresses with the showers. The duration of precipitation for a period over four hours also indicates that the line of convergence is a persistent feature. There is a suggestion that a convergent region developed or spread with an eastward component, for new convective cells are seen in Fig. 3.9 to be initiated east of the main precipitation area.

The reader is referred to the figures of the preceding section on warm showers for illustrations of these bands and the wind field accompanying them.

The second banded structure developed swiftly, as portrayed in Fig. 4.1. Almost perfectly straight rows of echoes about one mile in diameter appear oriented along 260° - 80°. At times, the orientations appear to vary slightly. Individual rows are often staggered, their ends lying parallel to one another and at a separation of about eight miles, although this distance varies between five and twelve miles. Surface winds at this time are generally ENE to NE in the area of these bands; therefore, the surface winds blow from a direction counterclockwise to the eastern ends of the bands. This is illustrated by Fig. 4.2.

Figure 4.3 is the Hempstead raob for 0400 EST, 11 September, approximately one-half hour before the first of these bands was observed from South Truro and fifty miles WSW from the point of their appearance.

Portions of the Montauk Point radar record (not reproduced here) show that stable type precipitation is present in the Hempstead area at the time of the sounding with these fine bands somewhat to the east. Subsequently, these fine lines appear still further to the east, and this tendency for filling in the space between two major precipitation belts is also evident in Fig. 4.1. The sounding indicates stable (nearly neutral) conditions from the surface to 750 mb and slightly unstable stratification above the marked inversion at 750 mb to 700 mb, the highest point reached by this ascent in heavy rain. The wind veers with increasing height from NE to SSE and has a maximum speed at 3000'. RHI pictures indicate that two precipitation types comprise the echo patterns shown in Figs. 4.1 and 4.2. The cellular lines are undoubtedly low level, while the more continuous fuzzy echo in which the cells seem embedded has its origin in the middle troposphere. Such overlapping of two distinctly different types of precipitation echoes is due to the wide vertical beam of the FPS-3 radar. (See pictures 11-14 of Figs. 10.1 and 10.3.)

It may be hypothesized that the air is originally somewhat more unstable than is indicated by the Hempstead sounding (Fig. 4.3). Particles comprising the upper deck grow as large scale convergence proceeds; this explains the increasing echo received from the upper layer and the lowering of its base. Simultaneously, the low level warm showers are initiated. These serve as an additional mechanism leading to saturation of the middle troposphere and a more rapid descent of the upper mass. Finally, the air is stabilized as in the case of the warm showers previously discussed, and a nearly uniform precipitation pattern is observed. Except for the smaller size and closer spacing of the cells, it does appear that much of the precipitation observed here is quite similar to the warm showers observed earlier. While RHI pictures (Figs. 10.1 and 10.3) suggest that advection of the precipitation from the SE may play some role in the apparent lowering of the upper echo masses seen at 220°, the PPI pictures indicate that area-wise, development rather than advection is the primary factor. Of particular interest is the suggestion that the outbreak of precipitation in the space between the bands in this case spreads eastward approximately parallel to the surface isobars. The velocity of spread can only be estimated, but 100 to 150 knots seems to agree with the observations. A similar, but less spectacular, development to the east was noted in the outermost band. Attempts should be made to corroborate these observations in other storms, since they may provide a clue to the hurricane dynamics. Figure 4.4 illustrates the three dimensional structure of precipitation and heavy cloud as seen by the FPS-6 radar from South Truro shortly after the last PPI photo of Fig. 4.1. The lowering of upper echo masses described in the text above is complete to the south; however, the onset of precipitation from aloft is indicated at 120°.

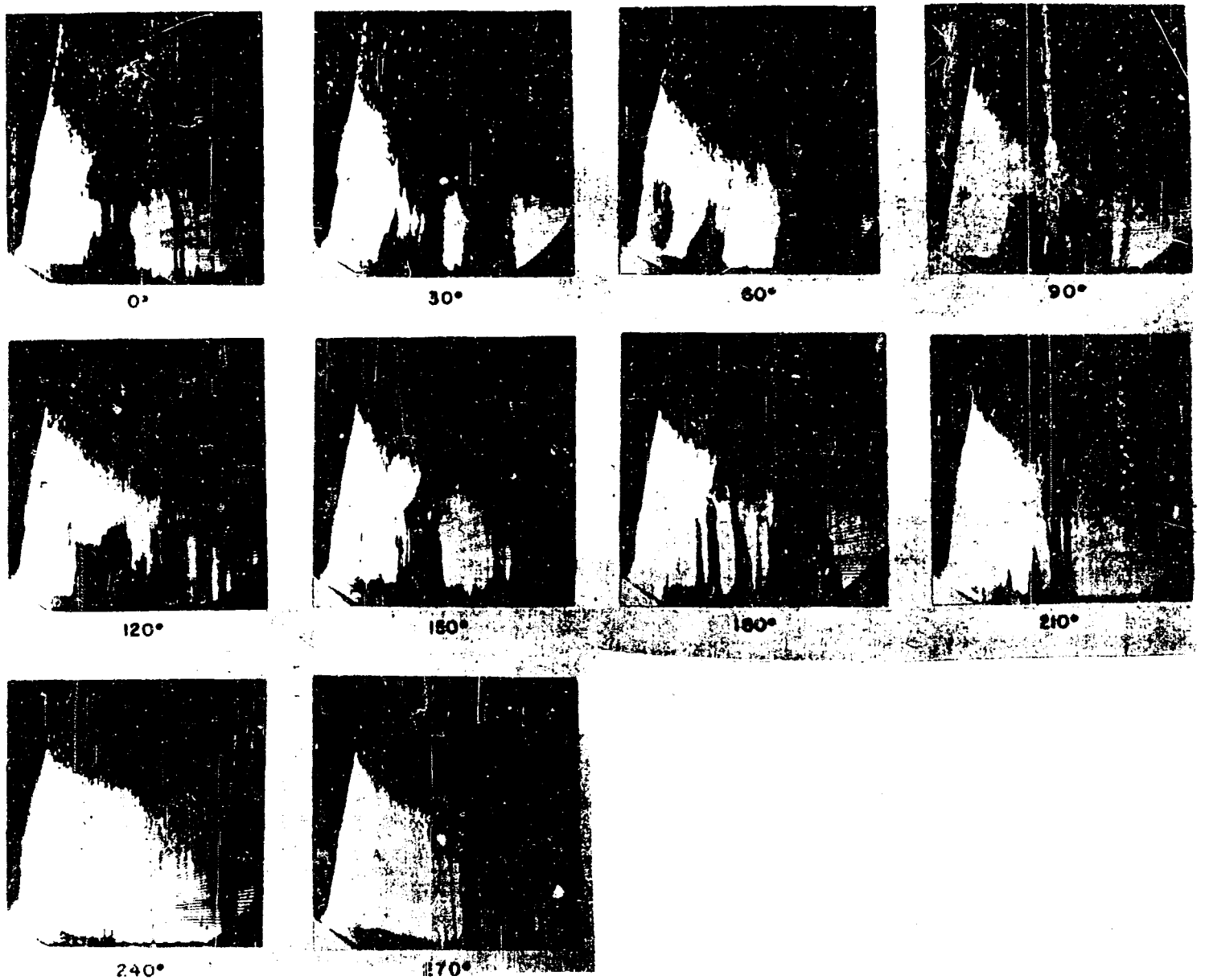

Fig. 4.4. Three dimensional structure of precipitation and heavy cloud as observed with FPS-6 radar at So. Truro. All the photos are within a few minutes of 0530 EST, when the eye of Edna was 270 na miles SSW of the radar. Note the upper echo layer at 90° and 120°, previously manifest also to the south and southwest, but now extending to the ground in those directions. Effects of vertical wind shear appear in the pictures at 30°, 60°, 90°, and 210°.

4.2 Inner Bands

More or less homogeneous bands are most prevalent within about 150 miles of the eye. Figure 4.5 illustrates such a structure about 70 miles NNE of Edna's eye. Examination of PPI time-lapse film indicates that the motions of a few small precipitation areas in this location relative to the eye (not deduced from these pictures, however, but from others at different times) are toward 310° at about 60-65 knots (see Section 5). However, Fig. 4.5 shows that the band area moves toward the NNE at 50 or 60 knots. The South Truro PPI photographs in this case are not spaced closely enough in time to allow positive identification of the same elements in successive pictures. However, careful examination of the original films suggests the following explanation of this apparent discrepancy. First, the band area is undergoing constant development along its eastern end, giving the impression that its motion has an eastward component. Also, development along the northern edge of the precipitation region gives an exaggerated first impression of the speed of northward motion. Thus, the development components account for part of the discrepancy. Secondly, it is believed that the motion toward 310° in this location is probably representative of imbedded convective cells, the generation of which is similar to that of the warm showers discussed earlier. The elements within the more or less homogeneous bands under discussion here are of a different origin, and should not be expected to move in the same direction as the convective cells. This is amplified below.

Figure 4.6 contains selections from the RHI record associated with Fig. 4.5. Note the striking appearance and persistence of the bright band first seen between 80 and 90 na. mi. on the 1010 photo. In the last frames, especially, convective cells also appear. These appear similar in their generation to the warm showers and should move with the winds below the melting level; here toward 310°. Therefore, it is not surprising that the motions reported in Section 5 should reflect those of the more convective elements, since these are usually easier to follow, and the quality of the film used in deriving most of the velocities allows little choice. On the other hand, the rain associated with the bright band is generated aloft and moves with the upper winds. Indeed, careful scrutiny of the original South Truro film suggests that such discrete, though ill defined, elements as exist in the nearly homogeneous area move toward 350°. While we shall discuss the significance of these bright band observations in greater detail below, it may be noted here that the persistence of the bright band implies that: (1) some of the bands on the PPI scope already exist aloft in the earlier stages of snow formation; (2) vertical velocities at the 0°C level in these regions cannot exceed a value of about 1 m/sec which would prevent dry snow from falling out of the upper layers.

The raobs so far presented in this report strongly indicate a turning of the winds with height in the manner suggested above (see

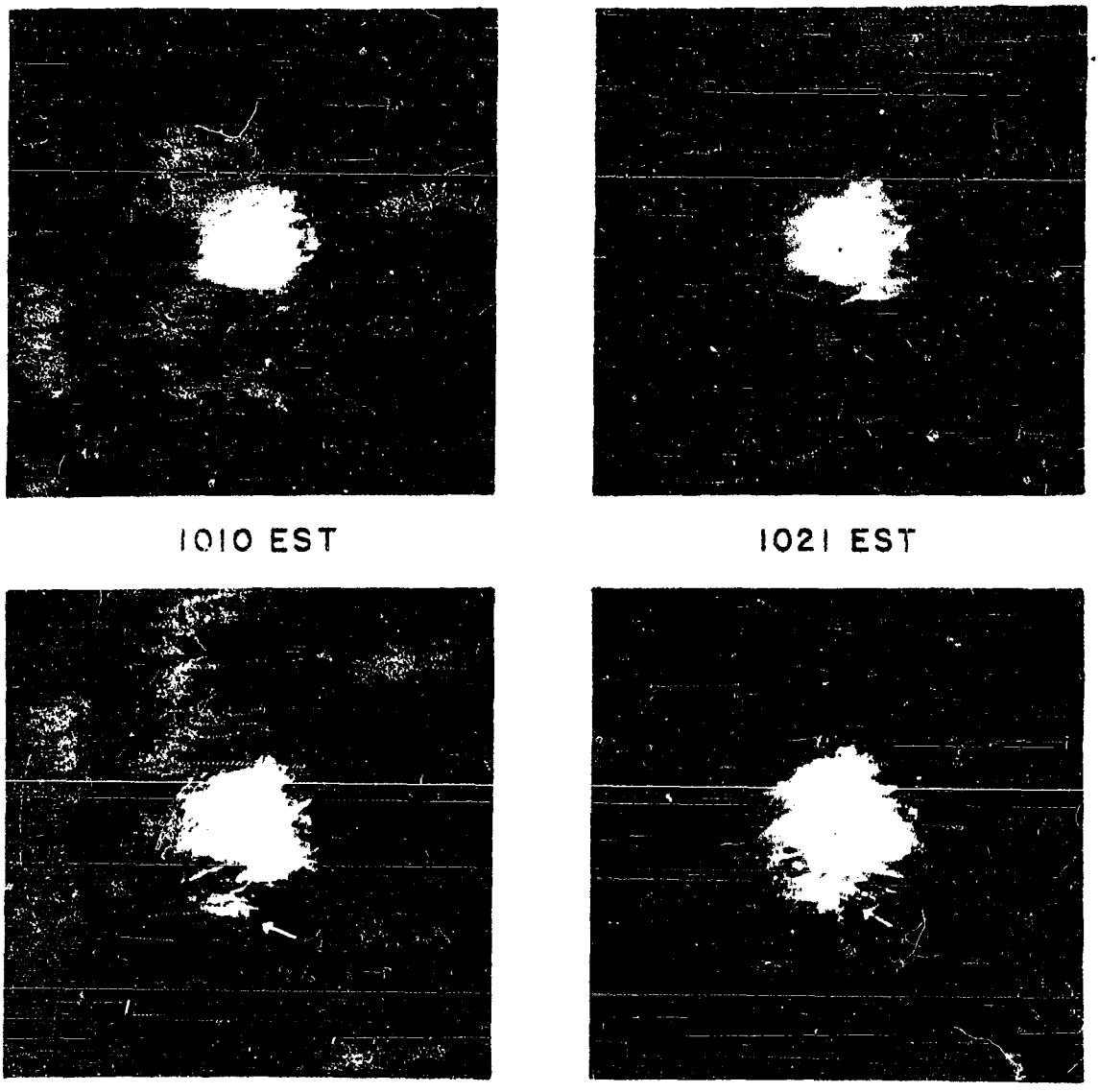

Fig. 4.5. EPS-3 presentation at So. Truro, 11 Sept. 1954. Maximum range is 170 nautical miles. Bands are mostly continuous now with few "hard" or convective cells. Arrow marks region characterized by the "bright band" in Fig. 4.6. The wall cloud north of the eye area appears in the 1040E. picture at 200°, 110 nautical miles.

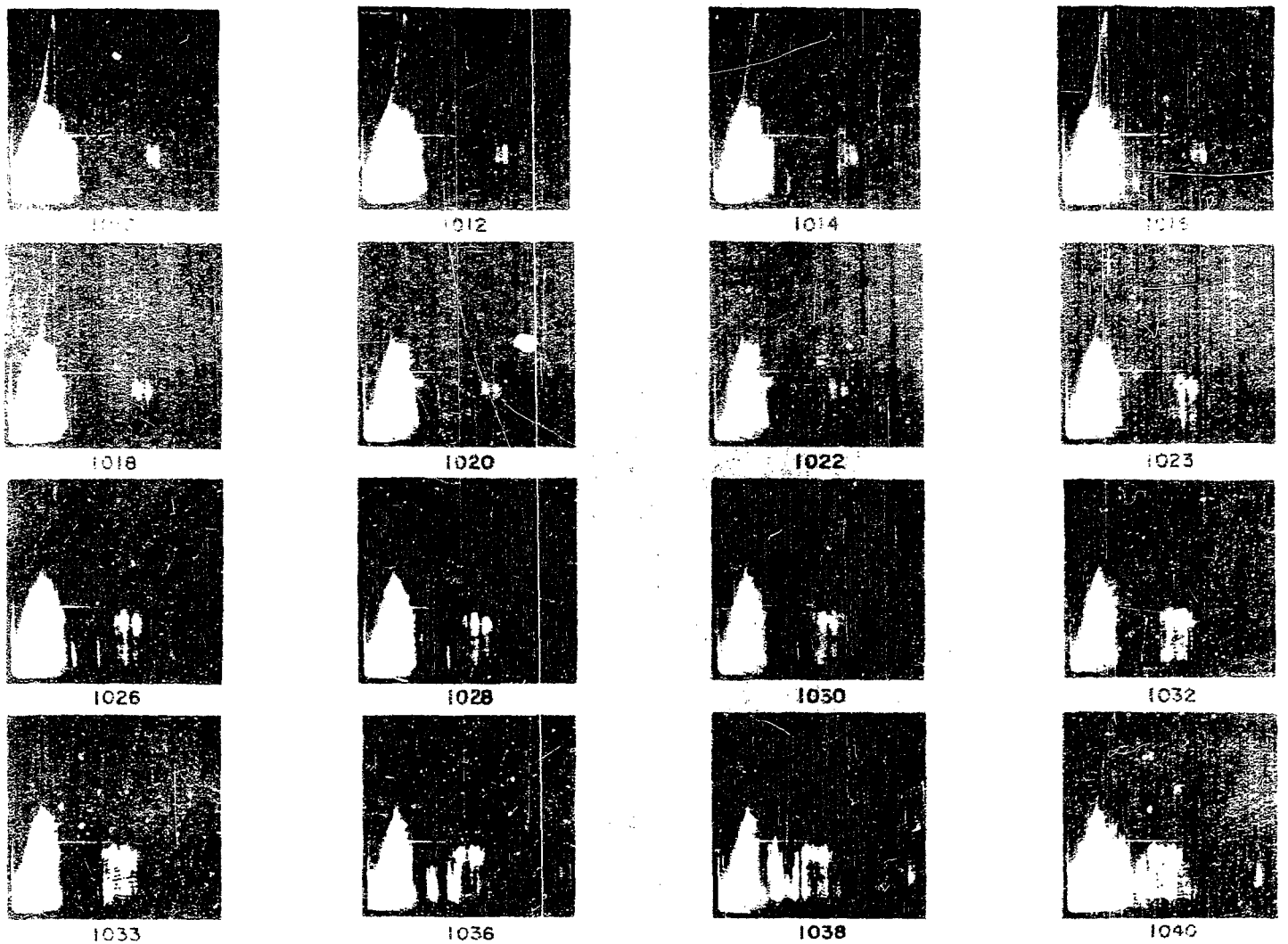

FIG. 4.6. EPSCAT RHI photos looking toward 200° from So. Truro at indicated EST's. Range marks are at intervals of 10 nautical miles and the horizontal line on each photo is at about 17,500 ft. The bright band rain which is seen to steadily approach the radar is associated with the area marked by an arrow in Fig. 4.5.

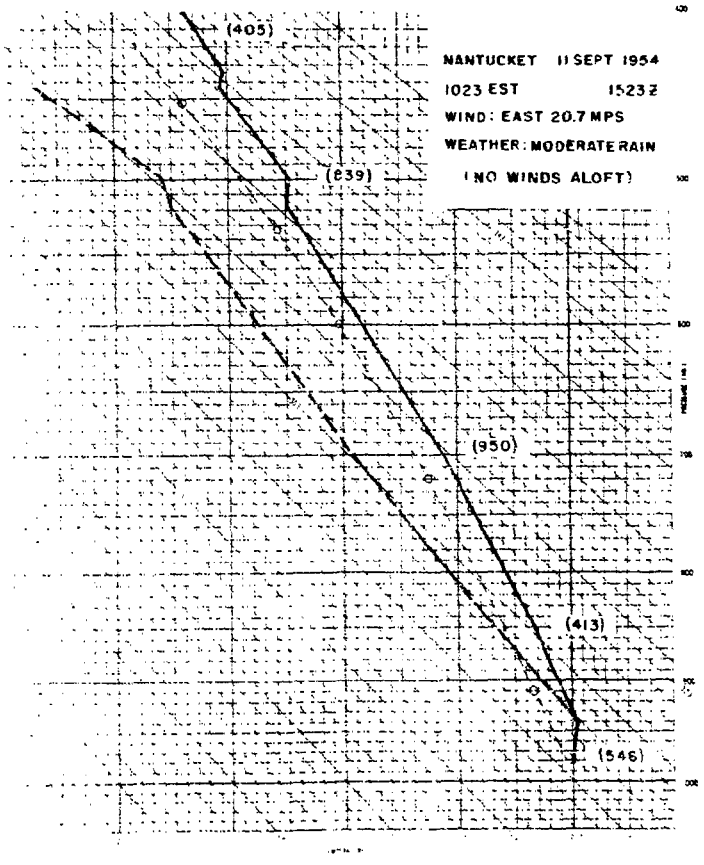

Fig. 4.7. Sounding made with GMD-1A equipment at Bedford, Mass. Temperature and dewpoint curves are indicated by the heavy solid and dashed lines; the light dashed line is a moist adiabat. The low humidities reported aloft are almost certainly in error.

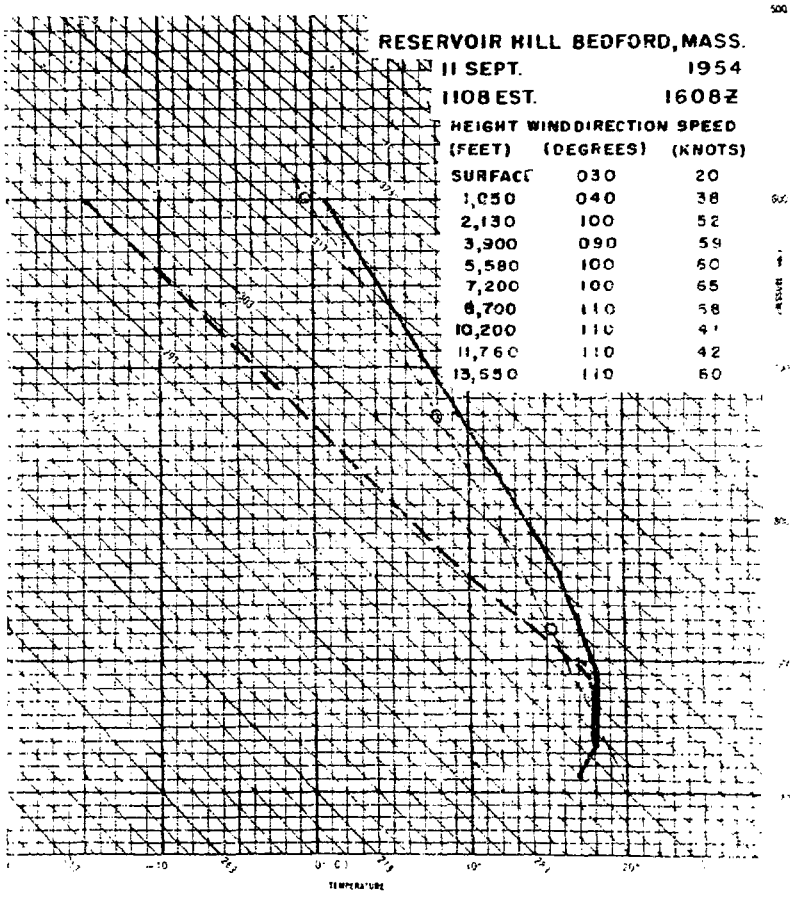

Fig. 4.8. Nantucket sounding on the morning of Hurricane Edna. As in Fig. 4.7., the low humidities reported aloft are probably erroneous, and may arise from an active washing of the humidity element by rain.

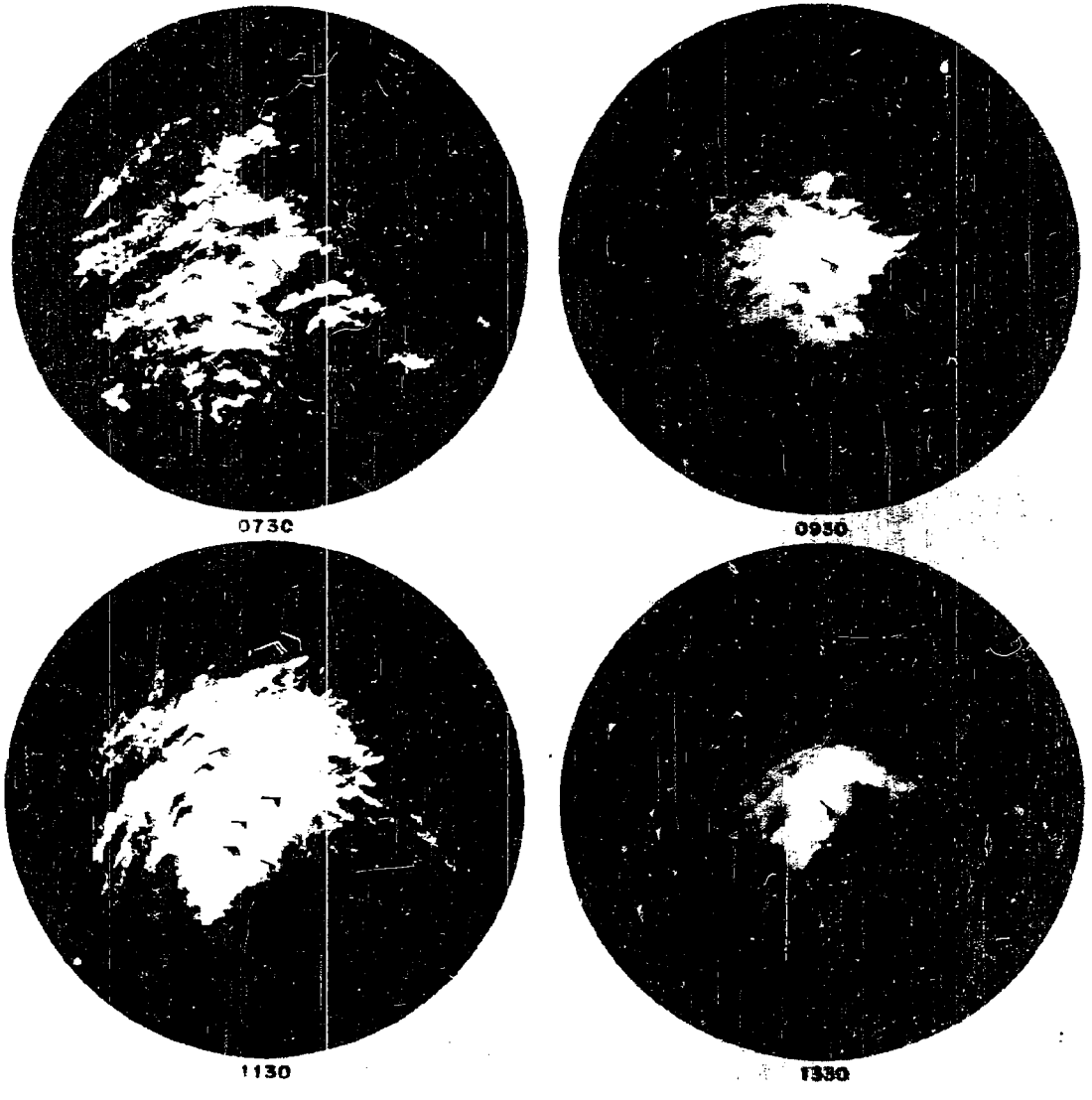

Fig. 4.9. Relationship between banded structures observed by FPS-3 radar from So. Truro and surface winds, as reported by airways stations. The date is 11 Sept. 1954, and indicated times are EST. Range marks are at intervals of 10 nautical miles. The arrows in the lower pictures indicate the WB29 aircraft, which is in or very close to the eye. Each half barb on the wind arrows represents 5 statute miles per hour, and a pennant 50. The 1330 picture is at much reduced gain and range. Note the better agreement between winds and band orientation of the continuous bands in the 1130 photo than with the more convective bands in the 0730 photo.

Figs 3.2 and 3.8) The veering of the wind with height may be associated in many cases with outflow aloft from the hurricane vortex and increased wind components away from the eye at the upper levels. This is a necessary adjunct to the large scale low level convergence and rising motion accompanying the widespread precipitation. These outward components in the vicinity of the eye are shown by Jordan (1952) to be most pronounced in the sector immediately ahead of the storm, in accord with what we have found here for Edna. In future radar hurricane studies, careful programing of observations may lead to a more accurate description of the wind distribution with height in the precipitation area near the eye, where all types of more conventional observational techniques suffer seriously from adverse weather conditions.

Raobs taken at about the same time as the photographs of Figs 4.5 and 4.6 are given in Figs. 4.7 and 4.8. Note that the Bedford sounding about 50 miles north of the downwind end of the precipitation region indicated by the 1040 EST PPI picture shows very little change of wind direction with height above a thin surface layer. The sounding terminates near the melting level, probably because of balloon icing. The humidity measurements are obviously in error at upper levels. The wind direction of 110°, between 8,000 and 14,000 feet, is within 20° of the direction of radar weather elements in this location relative to the eye, as reported in Section 5. In view of the above analysis, we must assume that the wind veers at levels higher than those reached by this ascent. The Nantucket sounding of 1023 EST (Fig. 4.8) taken at the upwind end of the region indicated in the 1028 picture confirms the almost neutral stratification for saturated conditions given by the Bedford sounding. The same error in humidity measurements is present and this may be due to a washing of the lithium chloride from the humidity element by rain. (The occurrence of these errors has been noted by Jordan and Jordan (1954) and has been commented on briefly by Middleton (1941).)

4.3 Banded Structures in General

Figures 4.9 and 4.10 are intended primarily to illustrate the relationships between the band directions and those of the surface winds and isobars. The isobars and wind and band directions are most nearly parallel at the upwind ends of the bands, if some intense convective echoes in the eastern semicircle of the storm be excluded from consideration. Parallelism is poor in the northern outskirts of the storm, illustrated by the northern half of the 0730 picture, where light winds make a large angle with bands and isobars. Downwind along the bands, both bands and winds tend to spiral in toward the eye, with the winds showing the greater incurvature. The bands are therefore oriented between wind and isobar directions at their downwind ends. (The wind and pressure fields of Edna are discussed in Section 9.) It is of interest that the N-S elongation of the hurricane circulation, as given by the changing distribution of surface winds and isobars as Edna approaches Cape Cod, is in some measure reflected by the changing band orientation depicted in Fig. 4.10. The N-S band elongation shown at 1433E, Fig. 4.10, may be related to a similar extension of the surface isobars which

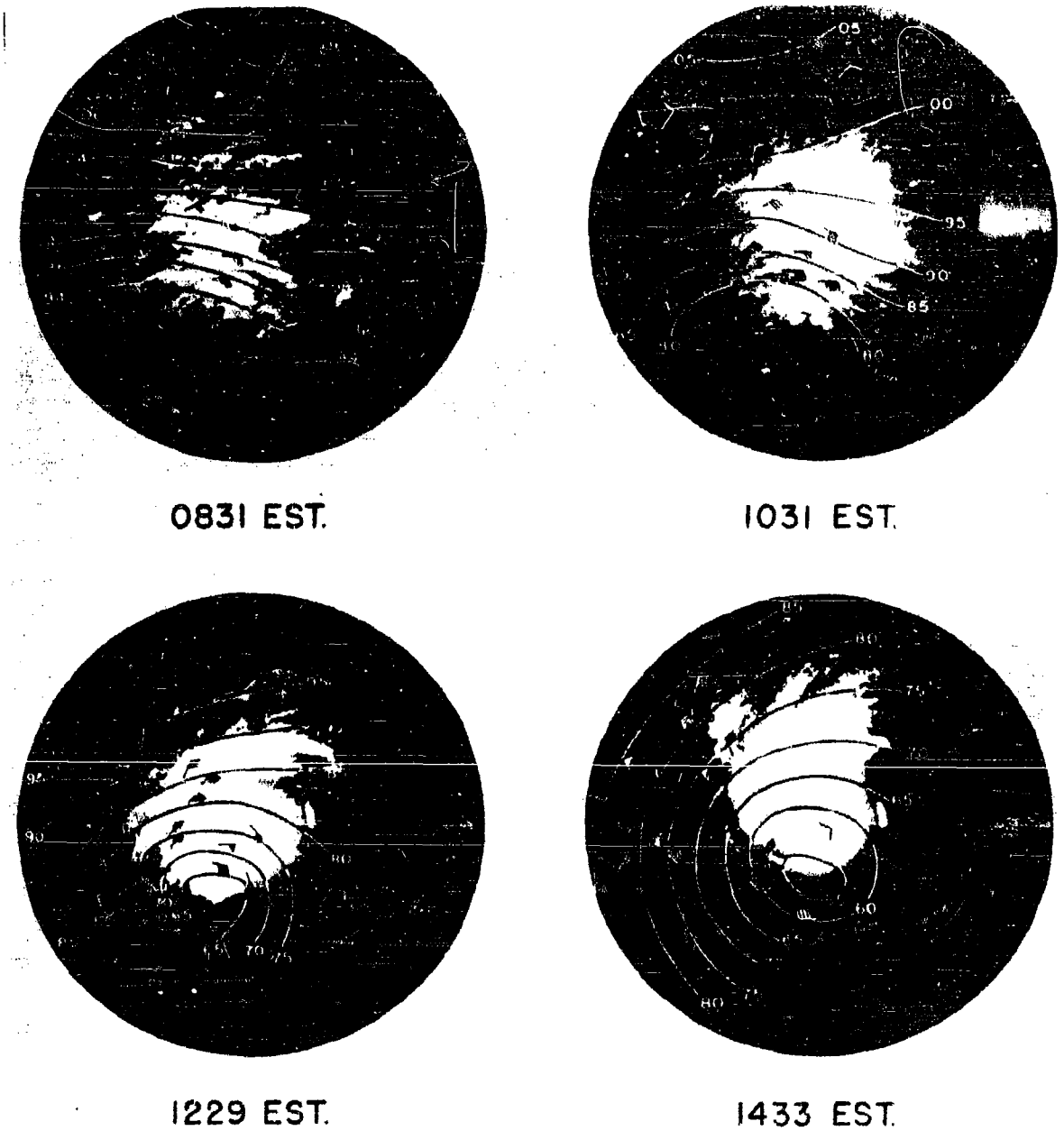

Fig. 4.10. Relationships of winds, isobars, and banded radar structures as observed from So. Texas. For further explanation, see Fig. 4.9. Note the changed size of the 965 mb isobar between 1229 and 1433. Between these times the central pressure changed only a millibar or two. For discussion of the cross isobar wind components illustrated at 1433, see Section 9. Maximum range of the first three pictures is 170 na. miles, that of the last is 109

commenced about an hour earlier, and is shown to better advantage by the 1330E synoptic chart, Fig. 10.1. Sharp edged and small echoes of convective origin frequently have their long axes at a large angle to the surface wind direction and, as suggested above, these are most commonly observed in the northeastern quadrant of the hurricane. It appears to be generally true that both winds and bands spiral inward toward the hurricane eye, with the winds displaying somewhat greater incurvature.

It is also of interest to examine in Figs. 4.9 and 4.10 and elsewhere, the detailed structure of the bands. It will be remembered that the outermost bands are lines of convective cells. Nearer the eye rain falls generally, but evidence of cellular structure appear within the long banded concentrations of heavy rain. Within 200 miles of the eye, cellular structures no longer predominate, although they still occur; most of the rain is contained in relatively diffuse bands ranging in width from 5 to 30 miles. It is noticeable too that the bands at great ranges from the radar appear wider than those which are close. This is believed due to an actual widening of the major bands with increasing height, associated in turn with high level divergence. This is consistent with the theory that the major bands are loci of intensified low level convergence and high level divergence, other evidence for which has been obtained by Simpson (1954). Incidentally, only little direct evidence concerning intensified low level convergence in the vicinity of bands has been obtained in this study from the reported surface winds, since the distances between reporting stations are large compared to the band widths.

One of the interesting features of the nearly homogeneous banded structures is a small scale graininess and filamentary structure. These structures are apparent only in some of the photographs. Their detectability is a function of the radar settings as well as their actual physical presence. These small scale structures, a typical dimension of which may be taken as 1/2 mile (although the filaments at times appear several miles long) can be associated with short period fluctuations of the precipitation rate at the ground, as revealed by the rate of rainfall record taken at Katahdin Hill, Figs. 4.11 and 4.12. The second of these figures is particularly interesting because it illustrates the records of two independent gauges, which were situated ten feet apart when the records were made. (See Section 7 for further discussion of rain gauge details.) The general similarity of the traces during the heavy showers (and at other times as well) is evidence that the fluctuations are real. The fluctuations, which have periods as short as 1/2 minute throughout the time of heavy rain, are suggestive of an intermediate scale of cell or turbulent structure within the bands which agrees qualitatively with the graininess observations. A period of 1/2 minute at the ground corresponds to a length of 1/2 mile with an upper wind of 60 knots; these figures are in reasonable accord with the synoptic observations and the observed speeds of weather radar elements (Section 5). We thus come to picture some of the rain bands within 150

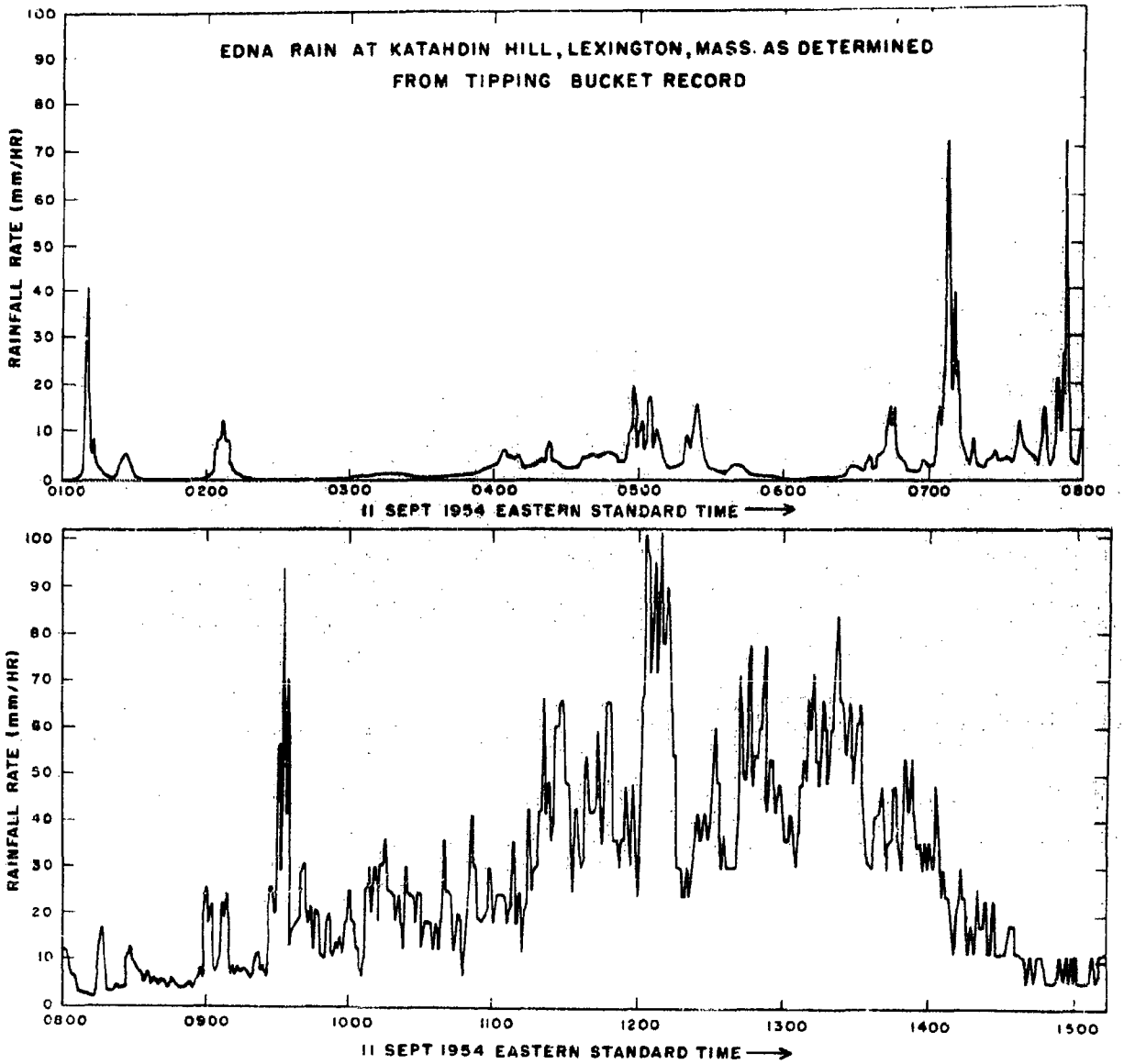

Fig. 4.11. Edna rate-of-rainfall record, determined from a Friez tipping bucket gauge located at Katahdin Hill, Mass. (Hanscom Field). The rate of rainfall is given by the time interval between successive tips, which are individually registered by an Esterline Angus recorder. The intensities reproduced here have been computed from each tip prior to 1000 EST; at later times only the total number of tips each minute are considered, thus the average rate during each minute.

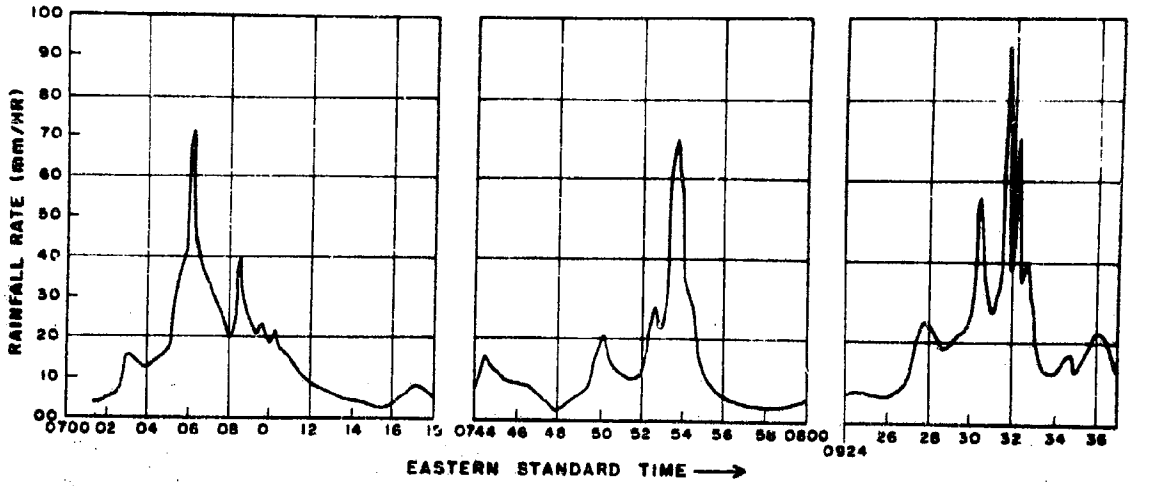

MICROSTRUCTURE OF EDNA SHOWERS AS RECORDED AT KATAHDIN HILL, LEXINGTON, MASS BY TIPPING BUCKET RAIN GAUGE. 11 SEPTEMBER 1954

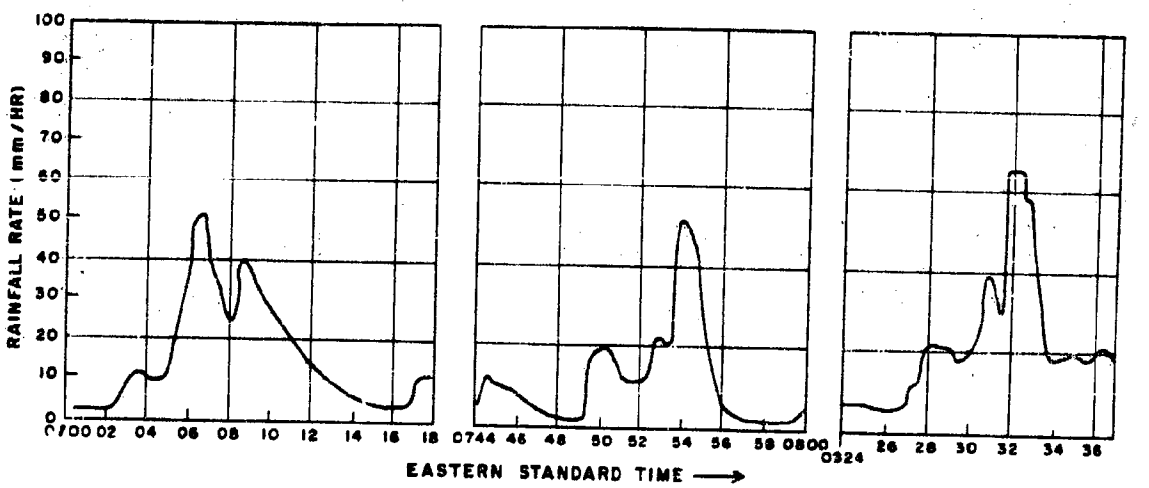

MICROSTRUCTURE OF EDNA SHOWERS AS RECORDED AT KATAHDIN HILL, LEXINGTON, MASS. BY HUDSON-JARDI RAIN GAUGE. 11 SEPTEMBER 1954

Fig. 4.12. Comparison of records of Tipping Bucket and Hudson-Jardi type rain guages, 11 Sept. 1954, Katahdin Hill, Mass. The two gauges are situated about 10 feet apart. The collector of the tipping bucket gauge is round and 19 in. in diameter; that of the Hudson-Jardi is square and 6 feet on a side. The records of the gauges are made on the same sheet of paper. The H-J record is a continuous line; that of the T-B is a succession of tick marks, each of which denote 1/10 mm or rain. In the last shower shown above, the H-J registers its maximum recordable rate for a brief period.

miles of the eye as consisting of ensembles of small cells or filaments. The width and breadth of a band are both large compared to a typical cell dimension, although some filamentary structures extend for considerable lengths along the bands.

The relatively uniform and very light, but gradually increasing, precipitation at Katahdin Hill between the hours of 0200E and 0500E is suggestive of a descent of particles which are first created in the main rain area of the hurricane and carried ahead of it by strong upper winds. Ice crystals, descending from such an advected upper cloud and melting, may grow by accretion in the lower clouds. An ice particle with a fall velocity of 2 ft/sec, carried forward at a speed of 60 knots, would travel about 100 miles while falling 10,000 feet. (These figures are applicable, of course, only above the melting level; other mechanisms are probably also of importance in determining the nature of the first rain. See Section 6.) It must be recognized that the high ice crystal clouds in advance of the storm need not arise by ejection from the main precipitation area, but can also form as a result of ascending currents at their high levels; the operation of the two processes cannot usually be distinguished by means of radar alone.

In the region of heaviest rain, the background precipitation rate of one to two inches per hour implies the presence of updrafts in the middle troposphere of one to two meters per second (see Section 6). Thus, many smaller particles could conceivably be carried to high levels and be swept ahead of the storm by the diverging flow aloft. As noted above, the centers of the bands very probably mark precipitation and updraft maxima; in the areas between them the falling precipitation is attributed in part to particles carried away from the band tops by divergence and in part to condensation within the weaker updrafts surrounding the main bands. In many cases the area immediately ahead of a rain band, as shown by radar, is associated with a diminution of cloud and precipitation. This is attributed to a downdraft and region of low level divergence which compensates the intense convergence of the band. These phenomena are illustrated in Figs. 3.1, 3.4, 10.1 and 10.3.

Yet another example of fine structure is indicated by Fig. 4.13. Here we have the "band within a band" structure at its best. One is reminded of Simpson's visual observation (1954) of the fine structure of spiral rain bands which "revealed a series of billow type striations of small clouds oriented about 45° to the line of the spiral band." It appears, however, that those in the attached figure cover a larger area than could be adequately surveyed visually; furthermore, since they are imbedded in precipitation they cannot be readily observed by visual means alone. It may be noted that the orientation of these internal striations is almost perfectly parallel to the surface isobars (see Fig. 4.10). Their character and orientation suggest that they may represent regions of low level cloudiness in which the raindrops grow and their reflectivity is enhanced.

A final characteristic of the inner rain bands is the presence of comparatively great convective activity at their upwind ends. (Note, for example, Figs. 4.9 and 4 10.) If the air flowing into these bands is initially convectively unstable, then the rising motion will set off convective cells which decay as the air is rendered of neutral stratification by overturning and by the continued large scale ascent. Downwind along the bands, the precipitation would then become more continuous, as is observed.

4.4 Some Further Remarks on the Origin of the Bands

Ligda (1955) has also noted the convective nature of the outer bands and the relatively smooth structure of the inner ones, and has speculated that the inner and outer bands owe their development to different processes. He associates the outer bands with a type of squall line phenomenon. The inner, less convective spirals are attributed by him to the low level growth in spiral stratocumulus roll clouds of widespread continuous rain, which is supposed to have its origin at upper levels. While not denying the importance of such low level clouds, the present authors incline to attribute both band formations to the same dynamic (unknown) mechanism. Since inner hurricane bands are often detected at great distances, e.g. 150 miles, they assuredly exist aloft in many cases* and do not derive their basic structure entirely from low level growth. Indeed, Fig. 4.6, showing the bright band on RHI, offers direct evidence of the existence of a banded orderliness in the snow prior to its fall into the lower levels. Also, in this case there is little or no low level growth, indicating that the corresponding band (Fig. 4.5) must have obtained its form in the upper levels. It is believed that structures such as that of Fig. 4.6 are frequently well defined aloft, but the precipitation is so spread by wind shear between the layer of its generation and the ground that it appears diffuse in most cases on the PPI.

On the other hand, we have shown in Section 3 that the outer convective bands originate in the low levels, but retain banded structure even as they change their character to a more stable type (e.g. Figs. 3.3, 3 4 and 3 9). In view of this kind of evidence, it seems very likely that the banded rains occur because the horizontal distributions of convergence and ascending motion, which give rise to the rain, are themselves banded. Whether the rain at one place is stratiform or convective, light or heavy, depends on the stability of the air masses involved and the intensity of the convergence bands, other factors being equal. The presence or absence of low level growth is dependent on advection into the rainy region of clouds formed elsewhere and on the

---

* Under standard conditions of propagation, closely approximated in hurricanes, the minimum height of a radar signal at a range of 150 statute miles from a ground station is 12,000 feet.

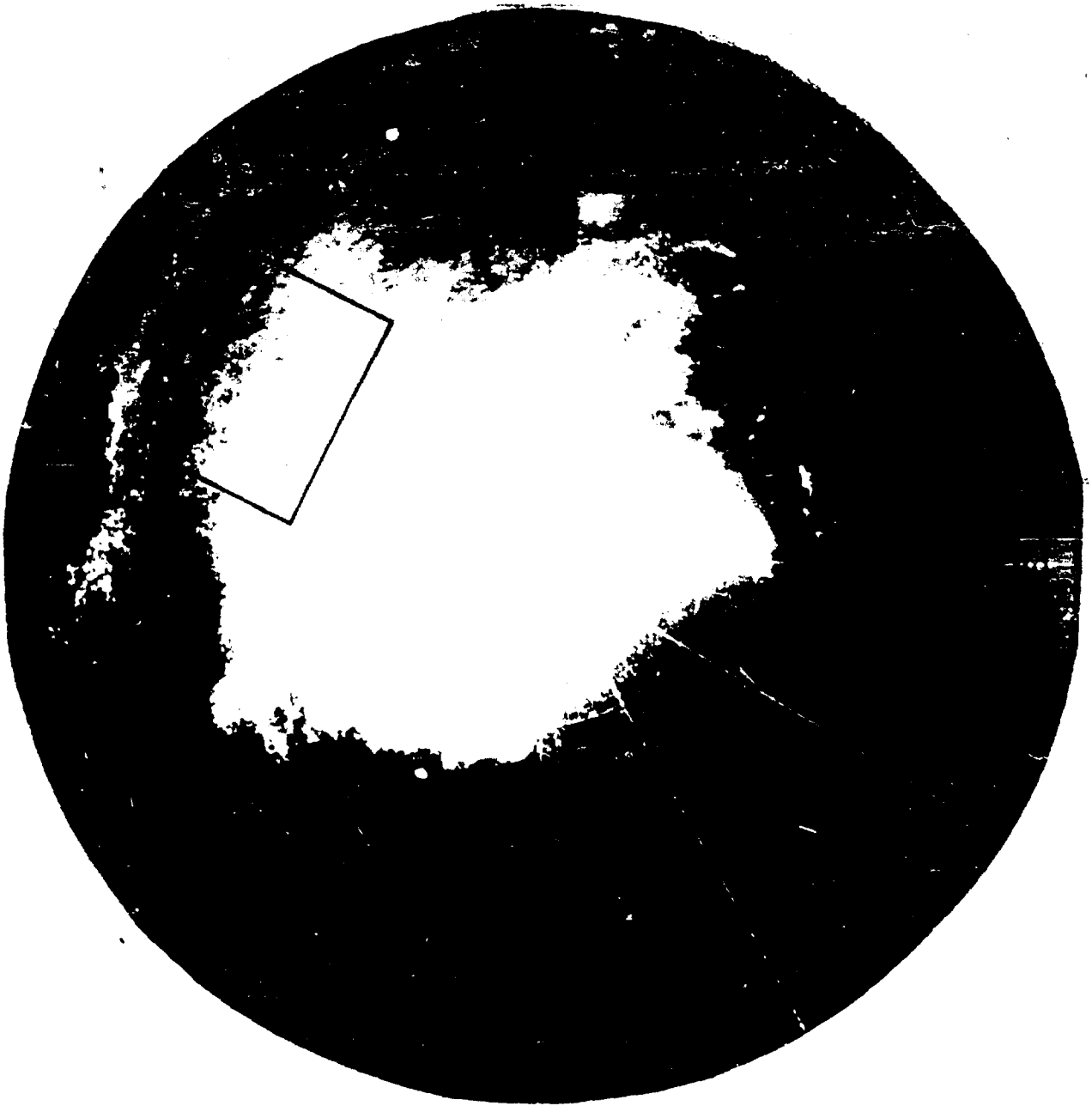

Fig. 4.13. Banded structure of Hurricane Edna, 11 Sept. 1954, 1334 EST, as seen from So. Truro by 23 cm radar. Note the "bands within bands" structure enclosed within the rectangle, and the WB 29 aircraft at 210°, 45 miles. Maximum range depicted in this picture is 100 nautical miles.

presence of low level convergence and updraft. As in the case of the internal striations of Fig. 4.13, we believe that low level stratocumulus rolls sometimes give rise to relatively fine bands and filamentary structures, by providing the pattern of low level growth and enhancement of radar signal described by Ligda.

While the quantitative explanation of the banded structures in hurricanes and in other weather systems is unknown, they may reflect little more than selectively amplified disturbances or the occurrence in a circular vortex of structures akin to cloud streets of the tropics, as suggested by Wexler (1949). In this connection, Abdullah's recent analysis (1954) is also a very interesting approach. Attempts by the present authors to relate the bands to wind maxima and wind shear, as proposed by Kuettner (1955), have not led to consistent results.

Understanding of these varied phenomena will proceed slowly so long as detailed measurements of meteorological elements through large regions of the storm atmosphere are lacking. Careful use of radar, especially systems of high resolution, may prove of considerable aid in such a measurement program.

5. Horizontal Velocities and Vertical Shear

5.1 Horizontal Velocities

The velocities of many individual radar weather elements have been determined, using PPI pictures taken at Hanscom Field and South Truro, Massachusetts, and Montauk, Long Island; and the locations of individual velocity determinations have been related to the known positions of the eye. The Hanscom Field pictures provide data for most of the measurements to the north and west of the eye. The Montauk pictures provide data for most of those to the NNE of the eye, while the South Truro pictures provide many of those at the most easterly compass points. The number of measurements based on data gathered at the three stations is: Montauk - 32, Lexington - 18, South Truro - 34, or a total of 84.

In general, it has been possible to determine speeds and directions of precipitation elements most readily at the upwind ends of the bands. At the downwind ends, the patterns are so diffuse and the lifetimes of discrete elements which are present are so short that it is virtually impossible to determine the speed of movement. Although the hurricane passed east of Montauk, the pictures at that location give little information on the velocities west of the eye because they were taken at the rate of one every 2 1/2 minutes. In this interval the radar weather elements transform so greatly that few can be identified as the same on successive frames. In many cases, a direction of motion, but not speed, can be determined.

Figure 5.1 illustrates the velocities of radar weather elements

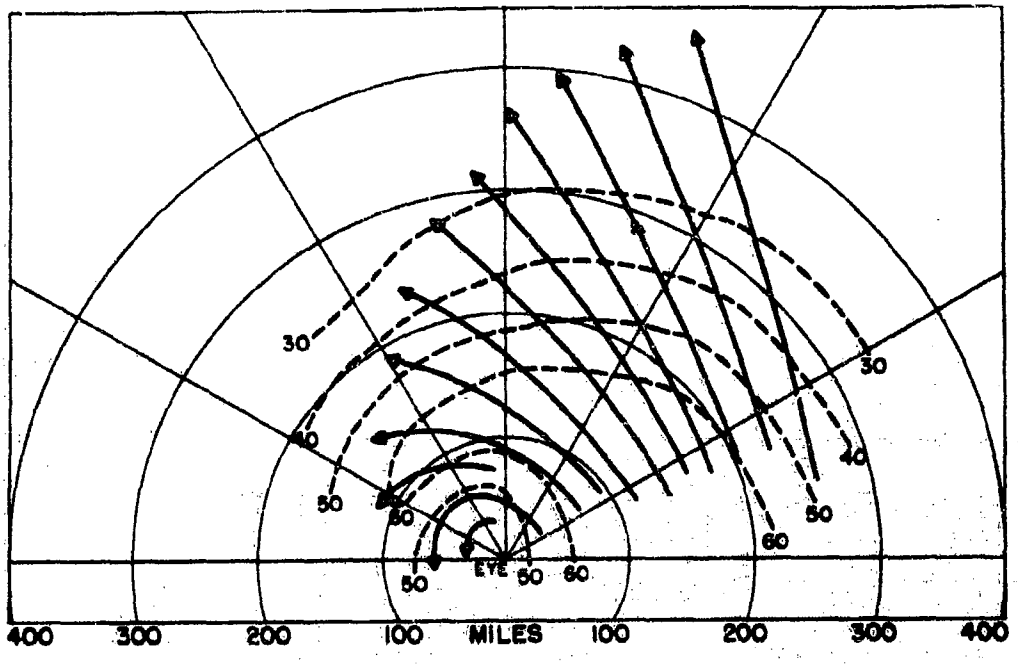

a)

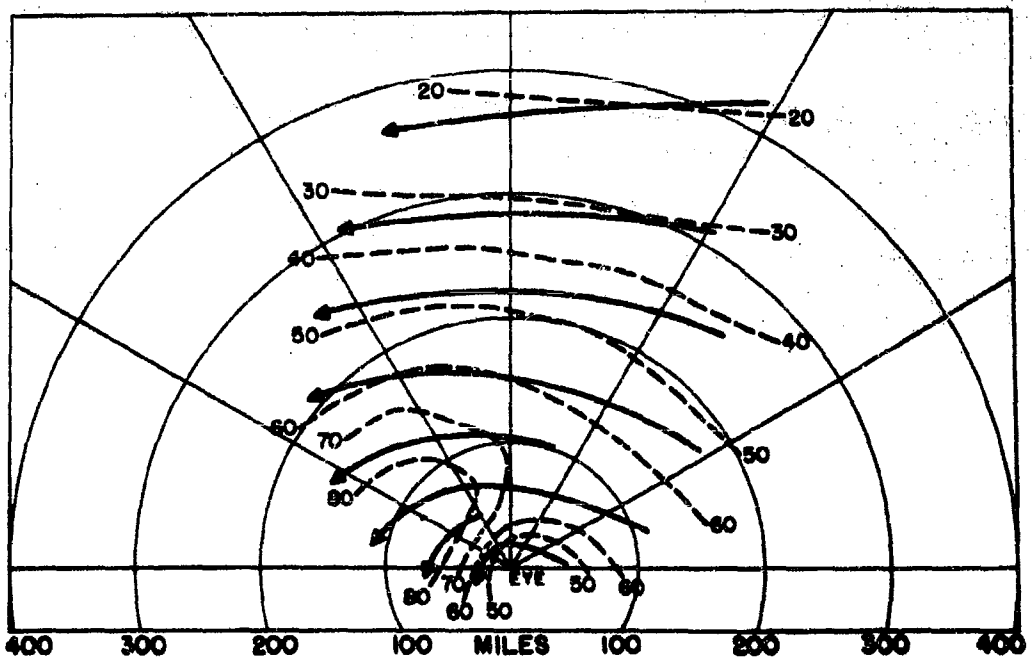

b)

Fig. 5.1. a) Streamlines and isovels (relative to the earth's surface) of radar weather elements positioned with reference to the Eye of Edna. b) Streamlines and isovels of radar weather elements as related to Edna's eye, moving toward 30° at a speed of 30 knots. Both diagrams are based on 84 velocity determinations. The motions are believed representative of convective cells which generate primarily below the melting level.

based on the quantitative measurements, as a function of position relative to the eye of the hurricane. The patterns have been smoothed considerably from the original measurements. As explained in Section 4, the velocities are believed to represent most closely the motions of convective cells whose substantial generation occurs between 3,000 and 9,000 feet, these discrete cells being the most readily observed on the photographs. Figure 5.1(a) depicts the motions as directly observed on the radar scope. When the velocity of the hurricane as a whole is subtracted from the observations as in Fig. 5.1(b), the motions are seen to be nearly tangent to circles moving with the storm and with the eye at their centers. It is noteworthy that the center of rotation of the radar echoes coincides, as nearly as can be determined, with the pressure minimum and center of surface circulation, as revealed by airways reports. This is even clearer from examination of the time-lapse photos when these are projected like a movie than from study of the limited quantitative observations on individual cells. In Typhoon Lorna, 1954, it appears that the surface center of circulation and the pressure minimum were separated by about 35 miles, unlike Edna. In the case of Lorna, the radar center, as deduced from individual echo velocities, is about midway between the surface pressure and wind centers (Hatakeyama et al, 1955).

Figure 5.2 represents the distribution of speed (relative to the earth) as a function of distance from the eye and shown for sectors east and west of 20° azimuth. Although the scatter among the points is great, there is little doubt that the maximum speed of the echoes is to be found at about 125 miles from the eye. Figure 5.2 also shows that the velocities on the easterly side of the storm are somewhat higher at all ranges than those more nearly ahead of the eye; this tendency is the same as that of the surface winds. It is usual for the stronger winds to be in the right semicircle of a hurricane (Dunn, 1951). Comparison of these curves with surface winds enables one to deduce the variation of wind with height in the storm. In Fig. 5.3, there is plotted the average of the curves of Fig. 5.2 and the average winds and gusts reported at Nantucket and South Truro. The exposure at both these sites is ideal and the winds reported should be nearly representative of those over the open sea. The wind records of the two stations are nearly the same when referred to the eye except very near the eye, and the curves for the two stations are therefore presented as one in most of the figure. It may be recalled (frontispiece) that the center of Edna passed directly over South Truro, but west of Nantucket. At the time of closest approach, Nantucket reported her highest winds.

The most probable representative low level wind may be taken between the reported average winds and the gusts. Figure 5.3 therefore indicates that outside of the zone of maximum surface winds, the winds increase with height. Within 40 miles of the eye the winds appear to decrease with height. The scatter of the points of Fig. 5.2 is such that in the zone between 40 and 90 miles, and also within 20 miles of

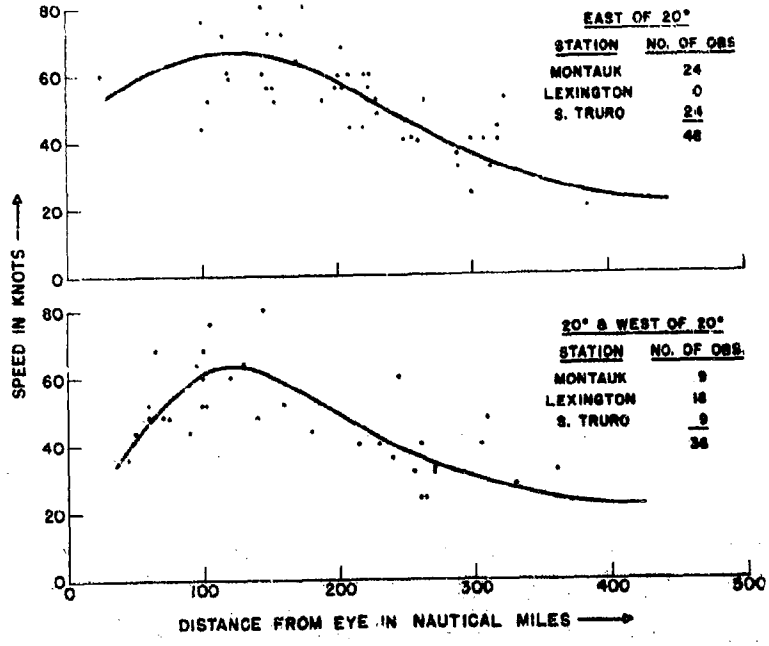

Fig. 5.2. Speed of radar weather elements vs range from Edna's eye, as determined for two azimuthal sectors. The curves are fitted by eye. The speeds are believed representative of convective cells which generate primarily below the melting level.

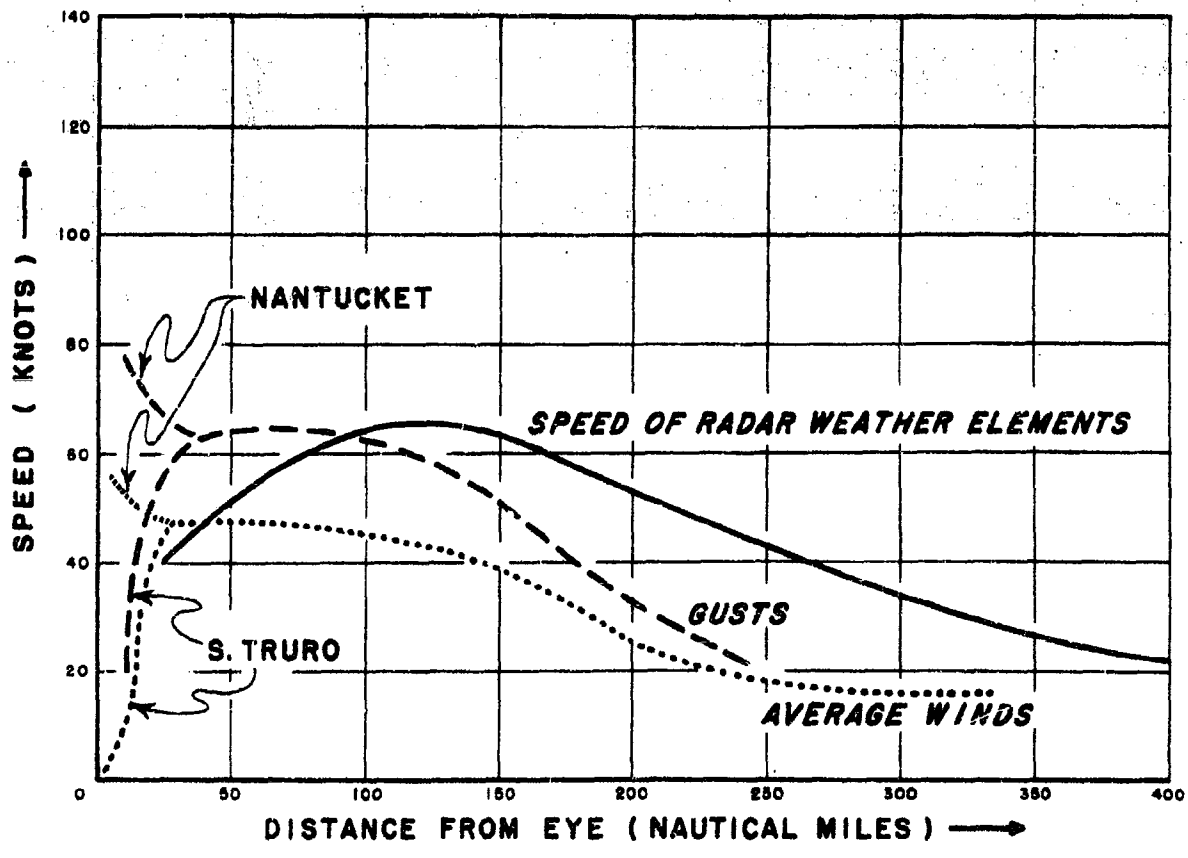

Fig. 5.3. Comparison of speeds of radar elements and surface winds in Hurricane Edna. Wind speeds at So. Truro and Nantucket are nearly the same when referred to the Eye of Edna except within 40 miles of the eye and the curves for the two stations are combined in this figure. The radar weather speeds have been derived from the curves of Fig. 5.2. This illustration indicates that the wind increases with height outside the radius of maximum surface wind speed, and decreases with height only within about 50 miles of the eye.

the eye, the sign of the change of windspeed with height is uncertain. As noted earlier, the radar wind data are probably most representative of the winds around 6,000 feet and these comments should, therefore, be applied to the low levels only.

We may compare the latter results with some work of Simpson (1954). After his reconnaissance of Hurricane Dolly, 1953, Simpson computed the change of pressure gradient force with height in the lowest 7,000 feet and found "that while there was a rapid decay of pressure gradient force with height immediately adjacent to the eye, there was conversely an appreciable increase with height at a radial distance of 60-70 miles from center to either side of the eye, but not along the line of storm movement." (Sixty miles ahead of the storm, the pressure gradient force showed a very small increase with height, while behind in the rain-free sector, it showed a decrease.) It is also of interest that the maximum surface winds in Dolly occurred at radii of about 40 to 60 miles from the eye, thus placing the zone of pressure gradient increase with height in about the same relation to the maximum surface winds that is suggested by this study of Edna.

The absence of warm core structure in the low levels is indicated by Simpson's reconnaissance of Typhoon Marge (1953). Here little or no change of temperature was recorded along a track into the eye at a level of 9,000 feet. Simpson's most recent work (1955) shows the warm core structure only immediately adjacent to the eye of Edna. Indications are, therefore, that this pattern of decreasing winds with increasing height does not obtain in the low levels of a hurricane rain area outside of the radius enclosing the eye and the maximum surface winds.

Figure 5.4 illustrates the fields of divergence and vorticity represented by Fig. 5.1. It is seen that near the eye, especially on the west side, the computations indicate a strongly divergent field. In the outer fringes of the storm, convergence is indicated at the effective generating level (for the discrete echoes), believed to be around 6,000 ft. These results, insofar as they indicate strong divergence, are rather startling and should probably not be taken seriously at present.

Accuracy of the original velocity measurements is not high, and errors are likely to be compounded in the determination of derivatives (a network of points 20 miles apart is used in computing Fig. 5.4). Furthermore, we do not definitely know the level to which the diagrams apply, or even if any one level can be associated with the observed velocities. It will be interesting to compare Fig. 5.4 and the others with the results of future investigations of individual storms.

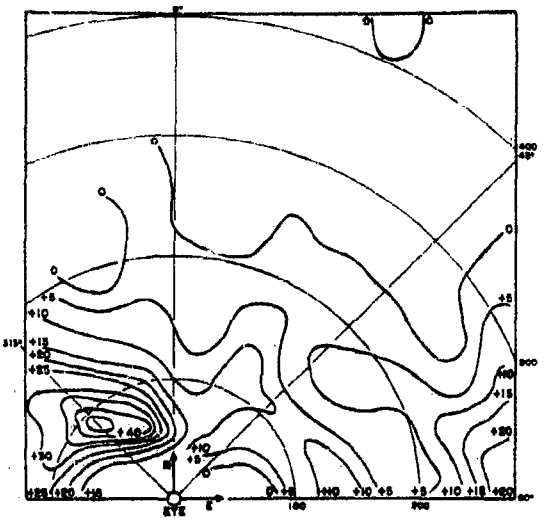

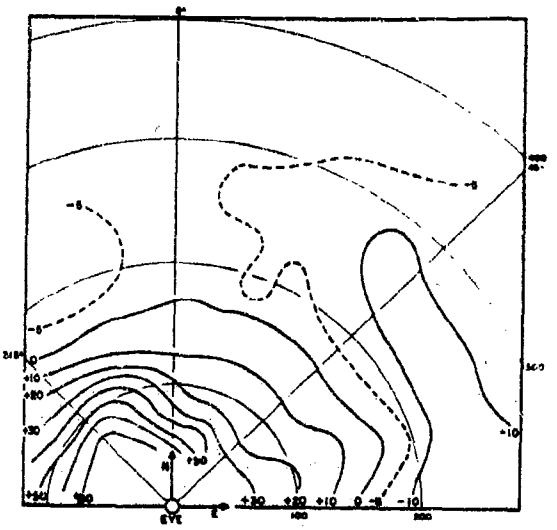

Fig. 5.4. Horizontal divergence and vertical component of vorticity determined from the velocity measurements depicted in Fig. 5.1. The results apply to the generating level for discrete identifiable showers, presumably about 6,000 feet. In the computations, these results appear as differences, the magnitudes of which are about the same as the probable errors inherent in the basic data. The validity of these charts is therefore in considerable doubt at this time.

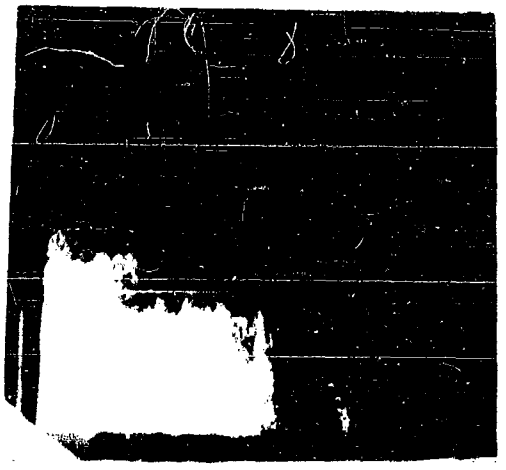

Fig. 5.5. This photograph of the FPS-6 scope was taken at 0945E, 11 Sept. 1954, with the antenna directed toward 200°. It illustrates sloping precipitation streamers, the rain of which is initially generated as snow. The brightest range mark indicates 50 nautical miles. The relatively sharp upper edge of the echo from 20 to 40 miles marks the melting level.

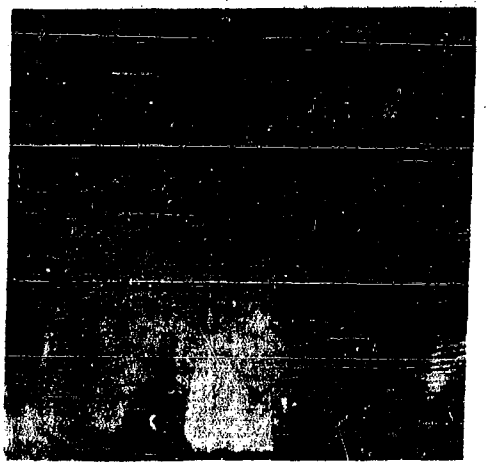

Fig. 5.6. This picture of the FPS-6 scope was taken at 0605E, 11 Sept. 1954, with the antenna pointing toward 60°. Note the relatively great slope of the nearby echo, as compared to those at 50 nautical miles (center of photo). The rather extreme difference illustrated here is probably due in part to real variations. However, the occurrence of similar effects on many other photographs at widely differing azimuths indicates that the observation is due also to the width of the radar beam, which produces a gross averaging of echoes at great ranges.

In order to obtain improved velocity data in the future, it is suggested that: (1) a high quality time lapse PPI film be taken with intervals not to exceed 1/2 minute; (2) particular cells be selected for velocity measurements during the storm and that RHI photographs be made in the directions of these cells. (The slope of the pattern on the RHI scope is indicative of the level at which the velocity measurement is valid. See below.) Of course, optimum velocity measurements on the PPI require a narrow vertical beam radar which does not superimpose the echoes received from a thick layer of precipitation. Such measurements would also be facilitated by constant level PPI presentations.

5.2 Vertical Shear of the Horizontal Wind

The vertical shear of the horizontal wind may be determined from RHI pictures with certain assumptions. If particles of the same size are continuously generated in an element, the slope of the pattern on the RHI scope is given by:

$$\frac{dx}{dz} = \frac{w_g - w_z}{v_z - u_z} \qquad (1)$$

where x and z are horizontal and vertical displacements, respectively; w_g is the velocity of the generator responsible for the release of the precipitation elements (usually assumed to be the same as the wind at its level); w_z is the component of the wind velocity at height z in the direction of motion of the generator; v_z is the particle fall velocity and u_z is the velocity of the updraft through which the particle is falling (Marshall, 1953 and Atlas, 1955). It is of interest that, with continuous generation of particles in an element, the pattern formed moves with the velocity of that generating element. (This is the reason for the assumption made in Section 5.1 that the generating level is that at which the winds given by the soundings are the same as the measured velocities of radar weather elements.)

Two regions of shear are shown in the South Truro RHI pictures. The first is illustrated by Fig. 3.4, where numerous streamers may be noted at heights between 18,000 and 30,000 feet. However, the orientations along different azimuths do not appear consistent and the pictures are not sufficiently detailed to enable accurate measurements of slope to be made.

The second region of noticeable shear is in the lower levels and is illustrated by Fig. 5.5. The average of some dozen observations of this type between 0600E and 1600E, 11 September, indicates that the term $(x-x_o/z-z_g)$ (a space average of dx/dz) for streamers between the melting level and the surface, ranges from about 0.6 to 1.0; with the direction toward which the lower portions of the trails slope indicated

as between 200° and 240°. Scope saturation at close ranges and the great range-height distortion introduced by the long horizontal ranges used, cause the individual measurements to be somewhat uncertain.

As indicated by Eq. (1), the pattern is vertical where $w_z = w_g$; thus a vertical pattern is expected at the generating level. The photographs show, in general, that in the widespread continuous rain the patterns are not vertical at or below the melting level, but somewhat above it. Just how far above is not known, since most of the photographs which show snow at all demonstrate a rather complex structure of nearly vertical streamers which do not lend themselves to accurate slope measurements. The extreme range-height distortion of the Edna RHI pictures also makes precise measurement difficult.

It is interesting to consider the upper wind observations within the storm area in connection with the observed precipitation trails. The Reservoir Hill (Hanscom Field) sounding of 0900E, 11 September, given in Table 4 below, is like most others in the main storm area in that there are no reports from above the melting level. However, the reported low level wind velocities can be associated with the observed low level trail directions if the winds at the generating level are from the southwest and have somewhat greater speeds than those in the low levels. The vector differences of the low level and generating level winds would then be about parallel to the direction of the low level trails. Arguments similar to these apply, in consideration of the other upper wind reports available. It may be noted that the veering of the wind with height deduced here is similar to the result obtained in Section 4 by consideration of the motion of a diffuse band (Fig. 4.5).

Table 4. Winds reported from Reservoir Hill, 0900 EST, 11 September 1954

Height (feet)	Wind Direction (°)	Wind Speed (knots)
sfc	060	13
1500	050	13
3180	130	36
4800	140	39
6260	150	41
7950	150	43
9580	150	46
11100	150	44
12900	150	60

With regard to the warm showers at the fringes of the storm, Fig. 3.4 gives little evidence of shear in the shower columns. This is in accord with the small shear indicated by the Nantucket ascent of 10 September, 2200 EST, in the low levels and with the intense convective nature of the motions within the showers.

An interesting effect may be noted in Fig. 5.6, where the shear appears most pronounced at close ranges. While this may in part reflect real variations of the slope of shower columns, similar observations at different azimuths and times suggest that the variation of slope is largely apparent and due to effects of radar beam width. By way of explanation, we may note that at close ranges the beam is narrow and only small cross sections of the target are averaged to produce the radar picture. At 50 miles, however, the 1° vertical beam of the FPS-6 is nearly a mile wide. A large cross section then intercepts the beam and the radar scope picture at any point reflects the averaging of great portions of the echo. The 3.4° azimuthal beam width of the FPS-6 effects even more important reduction of resolution at great ranges. A sloping column at great range will thus appear more nearly vertical than one near at hand and will show less detailed structure.

The conclusions above, with regard to wind shear, are in reasonable agreement with knowledge derived from other lines of evidence. Also, it is evident that generating theory provides a potentially powerful tool for the study of detailed wind structure in rain areas. However, various aspects of the theory require further study, particularly with regard to the exact mechanisms by which the trails are generated, if it is to be used with confidence in the future. Further studies of this kind can be facilitated by having pictures at various gains. The radar RHI scope should also be adjusted for short ranges so that investigation of nearby showers may be made under conditions of relatively high resolution and minimum range-height distortion.

6. Notes on the Growth Mechanisms of Hurricane Rain

The heavy rainfall rates and very high melting level of Hurricane Edna make the analysis of its rain of special interest. However, data suitable for a comprehensive analysis of the rainfall in terms of the growth mechanisms involved are not available; the following is, therefore, intended only as a brief introduction to what appears to be a fascinating and important subject.

At Katahdin Hill, Lexington, Massachusetts, near the center of the path of maximum Edna rain, drop size samples were collected using the filter paper technique. Some of the results are presented in Table 5. The Hudson-Jardi gage listed in Table 5 operates on a float and expanding orifice principle and has been constructed according to British and American designs. (For one discussion see Rossman, 1949.) The collector of this gage is six feet square and the instrument has a time

Table 5. Analysis of drop samples collected by the filter paper technique at Katahdin Hill during Edna rain - 11 September 1954.

1	2	3	4	5	6	7	8	9	10	11	12
			Precipitation Rate(mm/hr)								
Sample No.	Time (EST)	Exposure Time(sec)	Drop Sample	Hudson Jardi	Tipping Bucket	No. of drops counted	D_o (mm)	D_{max} (mm)	M (gm m^{-3})	ΣND^6 (mm^6 m^{-3})	Character of precipitation echoes
1	0603	10.0	0.084	0.5	--	1366	0.326	0.7	0.017	1.8	No echo-Between bright diffuse areas
2	0810	6.8	3.30	2	2	540	1.84	3.1	0.155	2470	Fine banded structures
3	0505	3.05	7.14	7	8	743	1.21	2.5	0.379	2670	Edge of intense banded area
4	1035	1.9	16.6	11	15	809	2.60	3.8	0.653	27900	Heavy bands
5	0907	1.55	23.1	10	15	864	2.34	3.9	0.936	31600	Fine continuous bands
6	0931 1/4	1.35	28.9	32	29	573	2.18	3.5	1.20	29700	Heavy bands
7	0707 1/3	1.1	36.5	36	37	1050	1.93	2.9	1.69	24800	Edge of intense area 20x20 miles
8	1121	0.9	50.3	29	42	1491	2.60	4.3	2.02	91900	Intense band 25 miles wide
9	1200	0.65	74.4	46	40	1501	2.14	3.8	3.17	77000	Intense echo all around

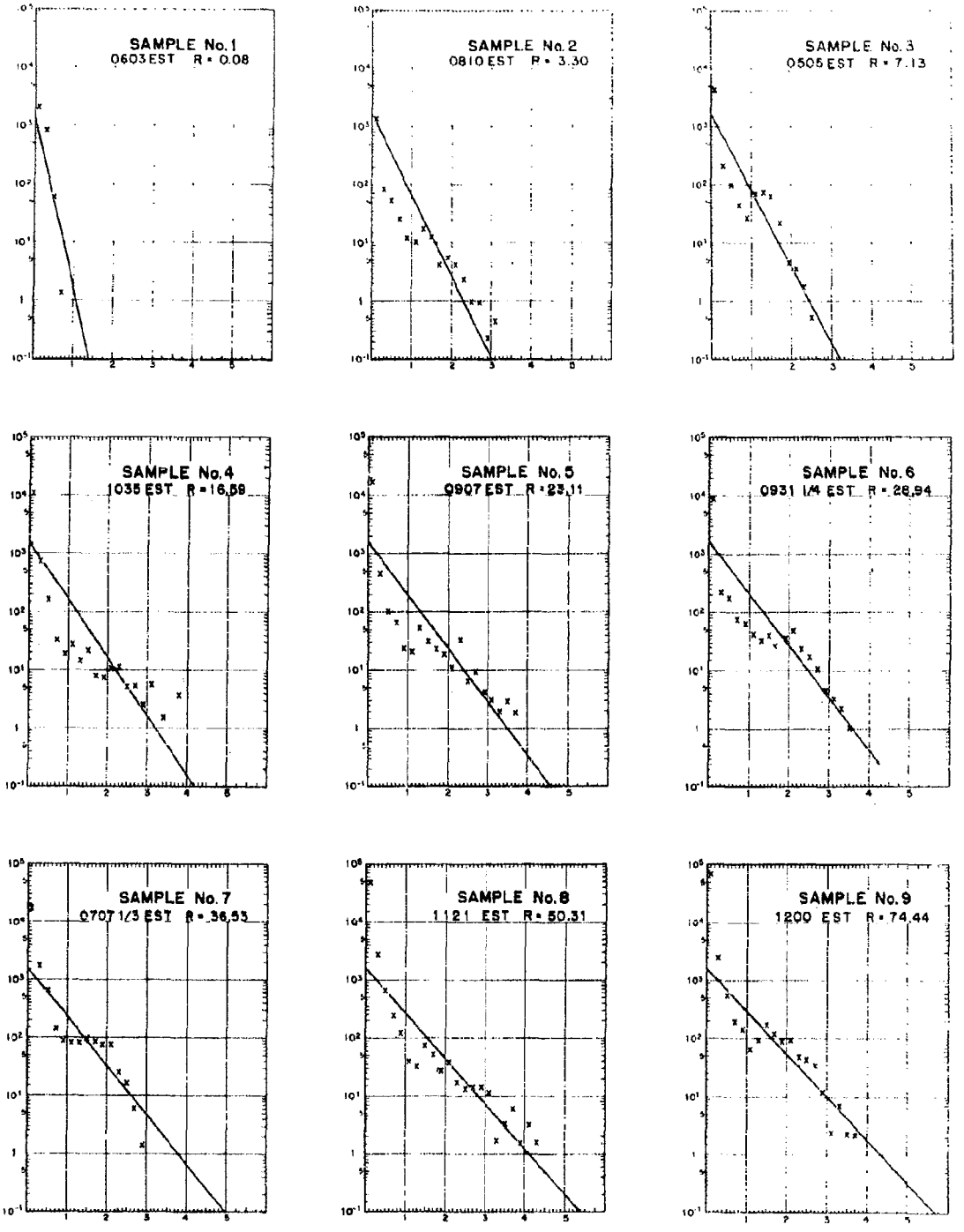

Fig. 6.1. Drop size distributions of raindrop samples collected on 11 Sept. 1954. Rainfall rate, R, is in mm hr. Ordinates represent the numbers of drops per cubic meter per 0.2 mm size range; abscissae are diameters in mm. Solid sloping lines are based on the relation of Marshall and Palmer for the indicated rainfall intensities. The "hump" described in the text is seen to be characteristic of all the samples except 1, 4, and 8. Note also the relatively large numbers of the smallest drops.

constant of about seven seconds. The tipping bucket instrument with special 19" diameter circular collector is otherwise the standard Friez gage.

Differences among the rainfall rate measurements listed in Table 5 may be attributed in part to large percentage errors in the exposure time of the filter paper during high wind and heavy rain; the time lags of the gages are also of importance during rapidly fluctuating rainfall rates. In view of the other possible sources of error as discussed by Middleton (1941), it is gratifying that the agreement is as good as indicated in the table.

Figure 6.1 presents the N_D vs. D curves for each of the nine distributions, where N_D is the number of drops per unit volume per 0.2 mm range of diameter and D is the diameter. Drop size distribution parameters, with the exception of those derived from Sample #1, are plotted in Fig. 6.2. In both Figs. 6.1 and 6.2 are plotted standard curves based on Marshall and Palmer's (hereafter M-P) relation (Marshall and Palmer, 1948) $N_D = N_0 e^{-\lambda D}$, where N_0 is 0.08 cm^{-4} for any intensity of rainfall and $\lambda = 41 R^{-0.21}$, where R is in mm hr^{-1}, λ is in cm^{-1} and D is in cm. For further reference, Fig. 2 of M-P's paper is reproduced here as Fig. 6.3.

Proceeding first to a discussion of Sample #1, it is seen in Fig. 6.1 that there are more small drops and fewer large drops than are given by the M-P curve for the same precipitation intensity. When this sample is portrayed on a plot of N_D vs. D/D_0 or the equivalent N_D vs. λD^*, all points fall above this M-P curve. It has been found by Donaldson (1955) that this is typical of drizzle samples. Quantitative data concerning drop size distribution in Hawaiian rains have been presented by Blanchard (1952). Comparison between Sample #1 and five of Blanchard's samples ranging in intensity from 0.061 to 0.12 mm/hr (of these, four were taken within a dissipating orographic cloud and one well within an active orographic cloud) shows that D_0 of the Edna sample is considerably larger than all the others. This difference may be attributed in the main to the larger depth of cloud present when Sample #1 was taken. The TPQ-6 radar record for this time (Fig. 3.7) shows a solid echo to 5000 ft. and some scattered return to 10,000 ft. The Hawaiian clouds are limited by a temperature inversion characteristic of the trade wind system and which is at a modal elevation of 6,000 ft. The Edna drizzle and Blanchard's cases are both evidently derived from coalescence processes taking place entirely below the melting level; but the greater D_0 of Sample #1 is made possible by the great depth of cloud through which the accretion process can operate, the rain intensities being approximately equal.

---

* Atlas (1953) has shown that $D_0 = 3.75/\lambda$ in a Marshall-Palmer distribution.

The N_D vs. D curves corresponding to the other drop samples (Fig. 6.1) are generally quite similar in shape to the empirical curves of M-P (Fig. 6.3). The relatively small differences between the M-P theoretical distribution and Edna samples vary from curve to curve, but in general, may be summarized as follows: At diameters of 0.1 and 0.2 mm there are more drops in the Edna samples; between 0.5 and 1.5 mm there are fewer in the Edna samples; above 2 mm there are more drops; above 3 mm there are sometimes more and sometimes less. It should be noted that the 0.1 mm drops were counted by neither M-P nor Laws and Parsons (1948) whose experimental curves are also given in Fig. 6.3. It may also be noted that at diameters less than 1.5 mm both the Edna samples and the observations of Fig. 6.3 contain fewer drops than given by the distribution function. This deficit is striking in the Edna samples and gives rise to a hump in the individual curves between 1 and 2 mm. This also appears in some dozen other drop samples of rain heavier than 10 mm/hr, which were taken at random from the authors' files. It is probable that the hump is characteristic of other rains too, since such a feature is suggested by the observational curves of Fig. 6.3 which are based on the averages of many samples.

Turning now to the drop distribution parameters of Fig. 6.2, it may be seen that the Z-R relation is such that evaluation of rainfall intensity from radar reflectivity, using the theoretical curve $Z = 296\ R^{1.47}$ (derived from the analytical M-P distribution function) is in these cases always accurate to well within a factor of 2.* However, it is also true that most of the sample Z's are less than those computed from the M-P curve. As noted by Marshall and Palmer, the usual deficit of drops about 1 mm in size should make the observed values of $M = \frac{\pi}{6}\sum ND^3$, and to a lesser extent that of $Z = \sum ND^6$, smaller than those derived from the equations. Some of the deficit may also arise from the integration to infinite drop size involved in determination of the Z-R relation from the distribution function. This procedure gives too much weight to large drops which do not occur in nature, owing to their aerodynamic instability. The conspicuous departure of theoretical Z's from the Z's computed in the case of Samples #6 and #8 is undoubtedly most closely tied to the deficit of largest drops in these samples (Fig. 6.1) relative to the number to be expected in the theoretical distribution for the same rain intensity.

Conclusions regarding the variation of rain water content in space M with rain intensity R, as shown in Fig. 6.2, are similar in part to those with regard to Z. However, since larger drops fall faster and are more spread out in space, M tends to be larger at any given rainfall rate

---

* The empirical and more commonly used curve, $Z = 200\ R^{1.6}$ (Marshall et al 1955) is also plotted on Fig. 6.2. The locus is nearly the same as that of the curve based on the distribution function, at least in the region of interest.

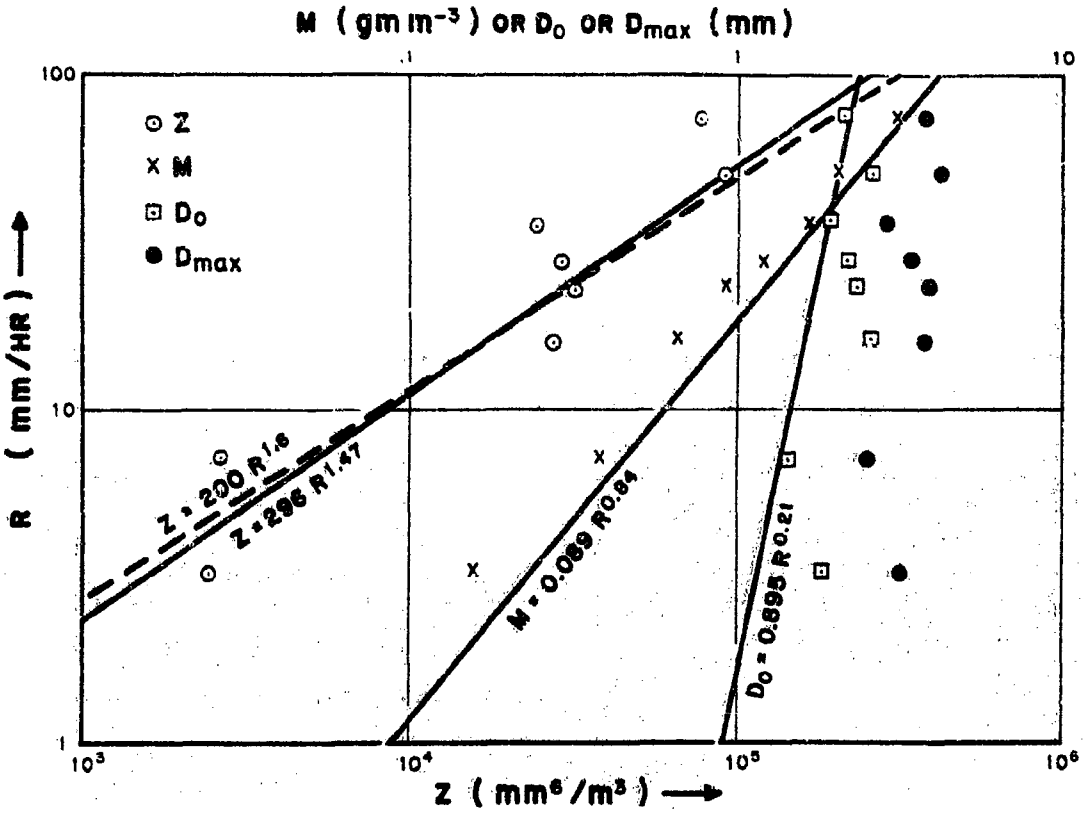

Fig. 6.2. Raindrop size distribution parameters derived from the samples of Fig. 6.1. (except for sample No. 1). The sloping solid lines are based on the relation of Marshall and Palmer, while the dashed Z curve is a commonly used empirical relation.

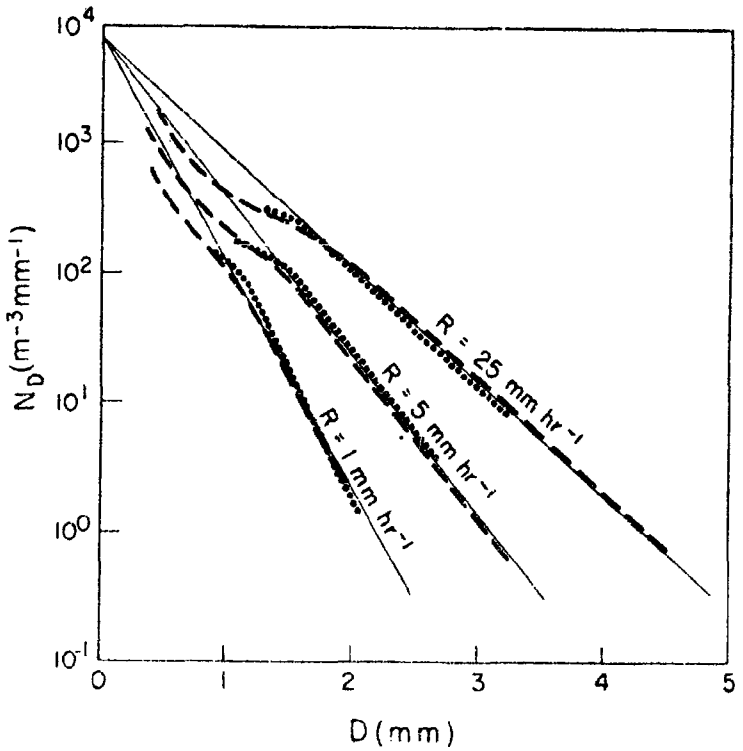

Fig. 6.3. Reproduction of Fig. 2 of Marshall and Palmers' paper "The Distribution of Raindrops with Size". The distribution function (solid straig lines) is compared with results of Law and Parsons (broken lines) and Ottawa observations (dotted lines).

when the drops comprising that rain are smaller. Thus, the samples which show relatively small Z, owing to scarcity of largest drops, evidence relatively large M, owing to the relative abundance of slow falling smaller drops.

The most striking feature of the Edna samples is the relatively large D_0 of five of the eight cases. Also, there is little correlation between D_0 and R for samples #4 to #8; rather, the D_0 values tend to cluster between 2 and 2.6 mm. The relatively very large D_0 of Sample #2 may be a transient feature, due to sorting of various sizes by wind shear (Atlas and Plank, 1953). However, the clustering of D_0 values in the other samples and their relatively high values suggest the importance of other factors for the determination of this parameter. We shall offer an explanation for this behavior below.

The data, though sparse, vary systematically from standard curves and therefore provide a reasonable subject for study. It is of additional interest to consider the special factors in this case which are associated with the observations as a whole, for these might be the cause of particular departures from the standard. During Edna, the melting level was near 14,000 feet. The M-P observations taken at Ottawa in summer are assuredly associated on the average with a lower melting level. Laws and Parsons state that their observations were made during 1938 and 1939 at Washington, D. C. While it is evident that some of their data were gathered in summer thunderstorms, there were presumably some winter observations associated with a relatively low melting level. We come thus to the conclusion that the Edna observations are associated with a significantly higher melting level than was the case, on the average, with the other observations cited here. This may be important because in Edna's rains, the drops could more readily grow by accretion of cloud and aggregation with each other to sizes limited by their aerodynamic stability. The M-P and Laws and Parsons data probably bear a stronger imprint of growth in the ice phase and of the breakup of wet snow aggregates into a relatively large number of small droplets during melting. This may explain why their average D_0's are less for equal rain intensities.

It may be argued further that in more usual widespread tropical rains, D_0 should be even larger for a given rain intensity than is suggested by these samples; for with light surface winds the absence of intense small scale turbulence in the low levels would reduce the probability of drop breakup. Indeed, the turbulence found at the lower levels during high winds may be responsible for the clustering of the D_0's, as noted above. In this regard it is probably significant that the largest drop recorded in Edna is only 4.3 mm in diameter; in other cases drops up to at least 6 mm have been reported. Numerous observations in tropical-type rains are necessary if these arguments are to be firmly supported or denied.

It is of further interest that in all the Edna rain samples, large numbers of very small drops are observed. In the heaviest rain, however, substantial general updrafts must exist which would tend to hold the smallest drops aloft. Therefore, we shall attempt to show in what follows that the numerous small drops most likely originate below that level at which the general updraft would prevent their fall.

In order to gain a quantitative notion of the factors at work here, consider a rainfall which arises as the sum of contributions by condensation at levels from the surface to 200 mb. A linear distribution of divergence with pressure, zero at 600 mb, serves to fix the distribution of vertical velocity and also determines the amount of the contribution of each layer. The individual change of pressure at pressure P is given by:

$$\left(\frac{dp}{dt}\right)_P = -\int_{P_s}^{P} \left(\frac{\partial u}{\partial x} + \frac{\partial v}{\partial y}\right) dp, \qquad (2)$$

where P_s is surface pressure and u and v are the winds in the x (eastward) and y (northward) directions, respectively. The precipitation rate is given by:

$$-\frac{1}{g}\int_{P_s}^{P} \frac{dq_s}{dt}\, dp = \frac{1}{g}\int_{P_s}^{P}\left[\int_{P_s}^{P}\left(\frac{\partial u}{\partial x} + \frac{\partial v}{\partial y}\right) dp\right]\left(\frac{\partial q_s}{\partial p}\right)dp \qquad (3)$$

where g is the acceleration of gravity and q_s is the saturation specific humidity. The terms have been tabulated with the aid of the skew T-log P diagram, and evaluated numerically under the assumption that the atmosphere is saturated and has a temperature at every level given by the moist adiabat which intersects 1000 mb at 18°C. Figure 6.4 portrays the results for divergence at 1000 mb of -10^{-4} sec^{-1}. It is only necessary to multiply the indicated updrafts and precipitation contributions by a factor x/6.8, where 6.8 mm hr^{-1} is the precipitation corresponding to values of Fig. 6.4 and x is the precipitation rate for which information is desired.*

---

* Rough computations of low level convergence, using the reported surface winds, have indicated reasonable agreement (within a factor of 2) between that which actually occurred and that which is assumed above to be necessary in order to provide the rainfall amounts observed.

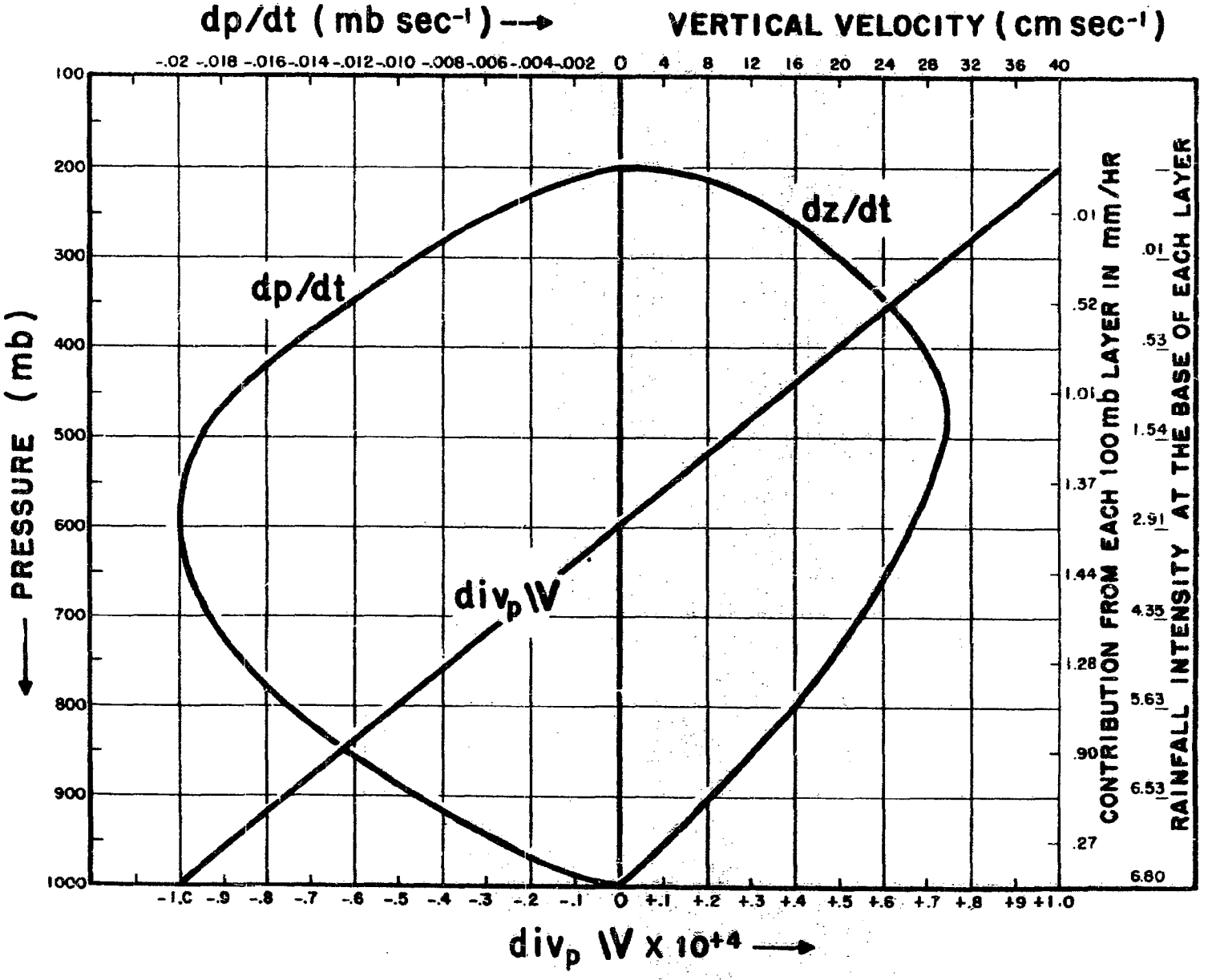

Fig. 6.4. Vertical distribution of individual pressure change, vertical velocity, and condensation rate for a simple distribution of divergence, a moist adiabatic saturated atmosphere, and a 1000 mb temperature of +18°C. The indicated rainfalls would occur if there were no storage of cloud water.

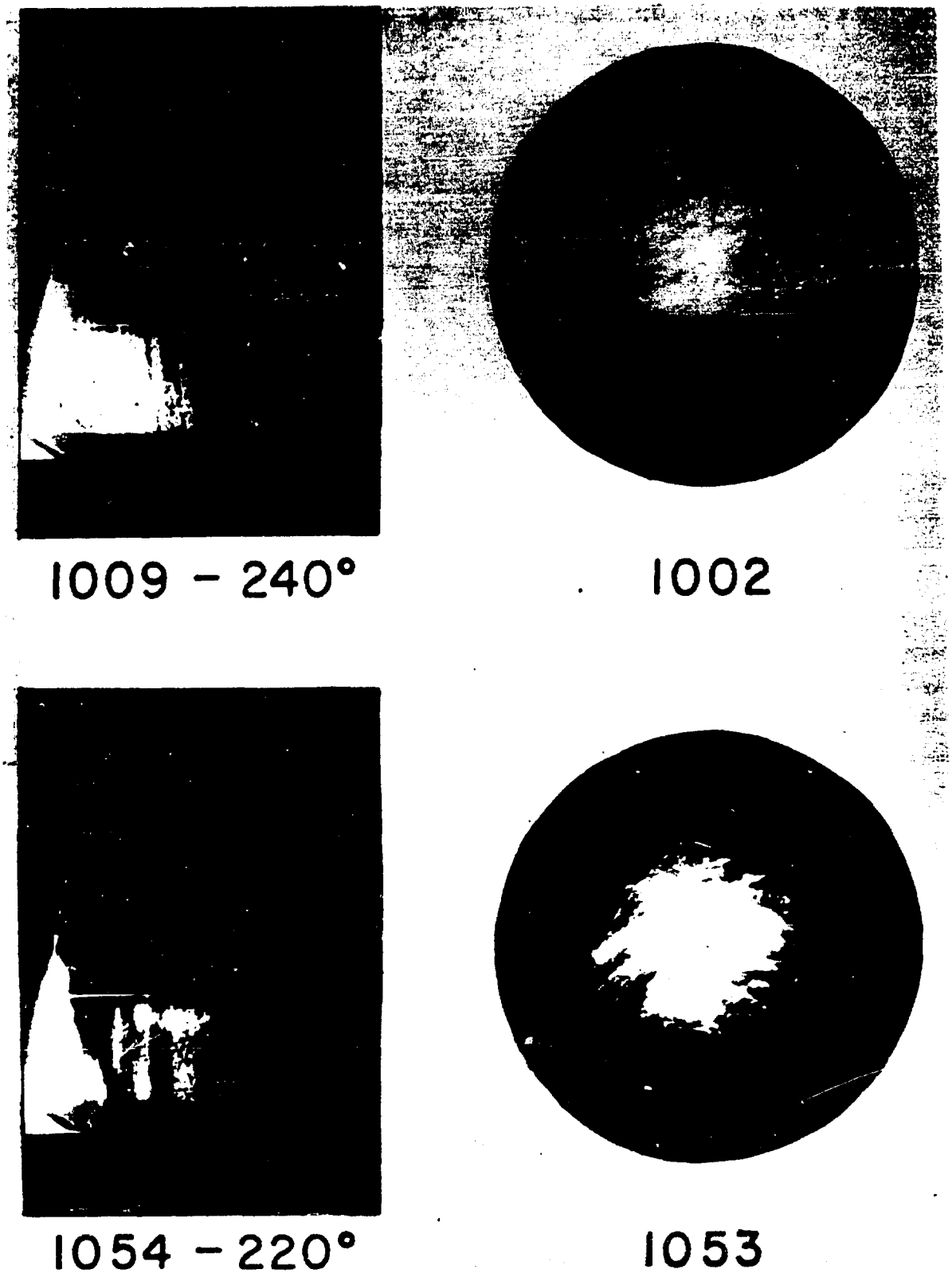

Fig. 6.5. RHI (FPS-6) and PPI (FPS-3) pictures taken at So. Truro on 11 Sept 1954. Numbers beneath the figures refer to EST and the azimuth toward which the RHI antenna was directed. The top RHI picture demonstrates the transition from snow to rain at the melting level, but rapid low level growth in this case tends to cancel the decrease of echo intensity usually noted below the melting level. The lower RHI portrays a bright band of more typical appearance. The nearly constant echo intensity between the ground and bright band layers is to be expected with only slight growth in the low levels of particles falling from above.

It is found that in rainfall of 25 mm/hour the updrafts at 3000 feet are about 30 cm/sec, the same as the fall velocity of 0.1 mm drops. While turbulence can bring drops which are created aloft to the ground, we would not expect large numbers of small drops in every sample if this were the only factor operating. Therefore, we are led to believe that in this general heavy rain the smallest drops are continuously created in the lowest levels (and indeed at every level) just as drizzle is created in low lying clouds, and partly as a product of drop breakup near the ground. Of course, in between the intense rain bands the small drops may fall through weak updrafts. This appears to have been the case in Sample #1 of Table 5.

It should be noted that the above arguments do not explain the origin of the distributions observed.* They do demonstrate the likely importance of several processes long cited as part and parcel of lighter rains, and the probable role of certain processes in producing distributions slightly different from those previously observed. For now we must regard the basic shape of the drop size distribution as due to factors which are quantitatively unknown; the reasonably good fit given by the application of the M-P relation to torrential rains is a fortunate coincidence.

The radar observations themselves also provide a key to the rainfall mechanisms. Figure 6.5 illustrates two rather different RHI presentations with corresponding PPI pictures. These RHI's were taken with much reduced gain** so as to show details near and below the melting level.

The precipitation rates represented by these photographs are unknown. However, it appears that at 1009, snow from aloft, melting as it passes below 14,000 feet, gives a sudden rise of reflectivity at that level. Just below the melting level appreciable growth of raindrops must occur, for there is not the usual sharp decrease of reflectivity characteristic of a conventional bright band.*** It can be seen also that the echo intensity continues to increase downward to the ground; this must be due almost entirely to accretion of cloud drops by rain and collision of raindrops with each other. The persistence of such a feature indicates that this region of growth must be one in which the cloud water continues to be resupplied by fairly intense updrafts.

---

* For a recent interesting approach to this problem see Hitschfeld (1955).

** The gain of the radar at the time these pictures were taken was reduced, but not precisely calibrated. Thus, the two pictures may have been taken with somewhat different receiver gain.

*** This explanation for the absence of a conventional bright band has been proposed by Atlas (1955b).

At 1054, on the other hand, the conventional bright band appears quite strongly at the same ranges at which it is absent in the 1009 picture. (Thus the absence of a bright band in the previous picture can be due only in small part to beam width averaging.) Below the bright band the echo brightness is about constant with height. In this case, there is good evidence of little or no growth of the raindrops below the melting level. This, in turn, indicates the absence of significant cloudiness and updraft. In both cases, of course, the particles originate as snow well above the melting level. It appears, therefore, that those bands evidencing continued growth through and below the melting level correspond to bands of convergence and updraft; other precipitation areas, viz. those displaying the conventional bright band structure and no low level growth, correspond to intervening regions of little or no low level updraft. The former type of band is generally the intense, well defined one on the PPI scope and is commonly associated with the heavier rain intensities; while the latter type is weaker, more diffuse, and usually corresponds to the lighter rainfalls. This correspondence between PPI and RHI characteristics is actually demonstrated better by Figs. 4.5 and 4.6 than by Fig. 6.5.

While we have associated the bands showing strong low level growth with the heavier rainfall rates, there is some question regarding the true physical character of the most intense rainfall. We are not certain, for example, that the heaviest rainfall evidenced any discontinuity of radar reflectivity at the melting level, since the heaviest rains occurred to the northwest of South Truro, while the RHI observations were made primarily to the southwest. Indeed, it is difficult to conceive how general rains of the order of 50 mm/hr in intensity could demonstrate such a feature. Previous computations indicate that a steady rainfall of 25 mm/hr at the ground would require an updraft velocity of approximately 80 cm/sec at 14,000 ft, the approximate height of the melting level. Thus, greater rainfall rates would be associated with updraft velocities which would prevent the fall of ordinary snowflakes into the melting zone. One would assume than that the particles would form graupel or hail, which could fall through such intense updrafts. In the case of graupel, however, the small and gradual increase in echo intensity upon melting to rain does not appear to be adequate to explain the rise observed (qualitatively) at the melting level in the pictures studied here.* On the other hand, fast falling wet hail would display practically no discontinuity in reflectivity at the melting level. If such hail were present, we would expect to see vertical echo columns extending through the melting zone in the manner of ordinary thunderstorms. In only a few cases (e.g. Fig. 4.6, 1038 EST) can such an echo structure be discerned, and then not with certainty. Therefore, although it is felt that the most intense rainfall probably originates as graupel or

---

* The change in reflectivity associated with the transition from graupel to rain has been treated by Atlas (1955a).

hail, this cannot be supported by the present observations.

The effects of strong updrafts, which are of common occurrence in active thunderstorms (where the bright band does not appear), are evident in the photographs of Edna's eye (see Fig. 8.5). At 40° azimuth, the melting level is readily distinguished as the flat top of the echo mass between 8 and 18 miles range. At 20 to 40 miles, however, the bright band is faint or absent, since solid particles present in the very intense updraft of the wall cloud have very high reflectivities and remain water coated as they are carried aloft. In the 50° picture, the disappearance of the bright band as the core of the wall cloud is approached is apparent. (Other pictures of the wall cloud, however, show faint evidence of a discontinuity in otherwise bright echo.) With the high vertical velocities implied by sustained rainfall rates of 2 and 3 inches per hour, a significant amount of snow must be literally tossed out of the cloud tops and dispersed in the divergent wind field necessarily present aloft. This too is indicated in the eye pictures by the echo layer aloft similar to the anvil cloud of a thunderstorm, which is connected to the wall cloud in a small column and spread out in a fan-like fashion above the eye; it is also suggested by the apparent greater width of the rain bands farther from the radar site (Section 4).

In summary, we note the following: Drop distributions collected during Hurricane Edna roughly approximate the distributions given by the function of Marshall and Palmer. Departures from this standard are associated with a hump in the curves between the approximate limits of 0.5 and 1.5 mm diameter. The smallest drops are more plentiful than normal; drops between 0.5 and 1.5 mm are less plentiful than expected and drops greater than 2 mm are generally in excess. Departures from the standard such as these are not believed to be uncommon; but they largely disappear in the averaging of many observations because the hump is not the same in location or intensity for different individual curves. The hump appears to be a noteworthy feature of the individual observations, which requires explanation.

Departures from standard of the Edna samples are manifested collectively as an unusual abundance of drops larger than 2 mm and, as a consequence, rather large median drop sizes. This is attributed to the relative importance of accretion and aggregation in the Edna rain. The agreement between the Edna and M-P drop size distributions is sufficiently good to permit the use of the M-P reflectivity-rainfall relationship $Z = 200R^{1.6}$ to estimate hurricane rain intensities from radar measurements within a factor of 2.

The rainfall at various times and places in Hurricane Edna seems to have been generated by practically every known precipitation mechanism. Based on the information of this and preceding sections, these may be summarized as follows:

(1) Well in advance of the eye (at about 450 miles) precipitation is initiated entirely in the form of water in discrete convective cells oriented in bands (see Section 3). These cells grow and penetrate the 0°C level at 14,000 ft and then develop into cumulonimbus at about the time that they penetrate the base of an overlying ice crystal deck at 20,000 ft. Whether these cells would develop into cumulonimbus on their own is not known; however, it seems reasonable that the combination of high water content in convective cells and the presence of plentiful ice crystals in the upper deck would cause a rapid release of heat as the crystals grow at the expense of the water. This would provide a sudden acceleration to the cloud top and permit its growth to cumulonimbus proportions. Subsequently, the cells merge and are transformed into a more diffuse and continuous band with remnants of convective activity at the eastern extremity.

(2) From roughly 250 to 450 miles in advance of the eye, the precipitation appears to break out as diffuse bands initiated from the snow aloft, as well as in the form of bands of discrete warm showers. Occasionally, this occurs simultaneously, resulting in the superposition of convective and diffuse bands on the PPI scope.

(3) Within roughly 250 miles of the eye the precipitation becomes generally continuous and intense, with only small breaks between bands of heaviest intensity. The lighter precipitation in this region appears to form from the snow aloft, demonstrating a more or less conventional bright band pattern on the RHI. The presence of the bright band suggests that these regions are in between the bands of intense low level convergence where the snow can fall, melt, and accelerate without significant low level growth. The heavier precipitation, however, corresponds to regions in which the echo intensity increases suddenly at the melting level (in a downward direction) and continues to increase downward in the low levels. This suggests that these heavy rain bands are areas in which low level convergence and vertical motion are causing the development of dense cloud which permits the rapid growth of the rain and the melting snow by accretion. There is doubt, however, about the nature of the very heaviest precipitation, since the required vertical velocities indicate the need for a graupel or hail process which is not clearly evidenced by the radar records.

7. Edna's Path: An Analysis of the Position Reports

During Edna's approach to land, its eye was tracked by reference to the standard synoptic maps based on weather reports from land stations and from ships, by reference to ground based radar PPI presentations and by a reconnaissance aircraft from Bermuda. The reconnaissance aircraft was guided into the eye on the basis of information given by the airborne radar and the aircraft pressure and radar altimeters, as well as by visual data on the curvature of rain and cloud bands and the distribution of precipitation. The geographical position of the aircraft

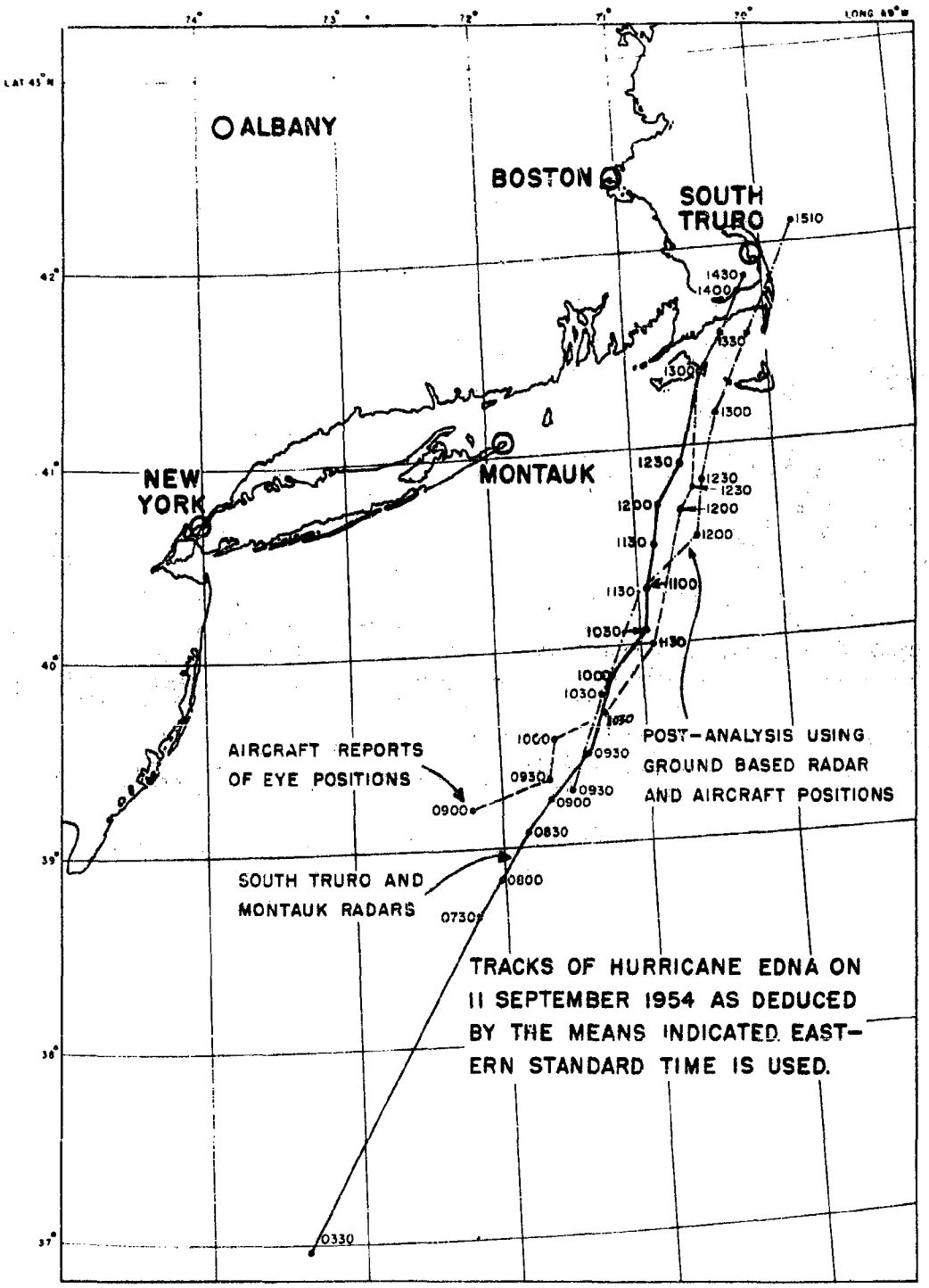

Fig. 7.1. Tracks of Hurricane Edna as deduced with different aids. That labelled "Aircraft Reports of Eye Positions" is based on the reconnaissance reports. That labelled "South Truro and Montauk Radars" details the eye positions as determined operationally from the PPI scopes of the radar sites during the approach of the storm. The Post Analysis is based on conventional synoptic data as well as studies of the radar records of the hurricane rain area and aircraft positions, and of the original observers' logs.

and eye then was determined by Loran, other standard navigation techniques, or by reports of ground radar when the aircraft was within range.

For obvious reasons, it is appropriate to investigate eye locations as reported and charted during Edna by observers aboard the plane and on land. This will enable at least a partial determination of the relative effectiveness and accuracy of various methods, and may suggest the means whereby more accurate tracking may be realized in the future.

The earliest eye position to be considered in detail here is that given by Navy aircraft 4U93 at 0330 EST, 11 September 1954. This report, the last to be sent by this aircraft prior to its departure from the storm for Jacksonville, places the eye by airborne radar at 36°59'N X 73°24'W, with an estimated uncertainty of 5 miles. The proximity of the aircraft to the coastline at this time indicates that relatively high confidence may be placed in the position report, navigation being a somewhat more certain procedure with land based aids. This position checks within a couple of miles of that interpolated for the same time from locations recorded with the aid of ground based radar at Cape Charles, Virginia. Because of this agreement, this point is used as "anchor" for the remainder of the track northeastward and over Cape Cod.

Aircraft 3459 (WB 29) left Bermuda early on the morning of 11 September and proceeded northwestward to Seal intersection at 39°50'N and 69°40'W. It arrived there at 1230Z, circled briefly before obtaining final clearance, and then departed westward for the storm center. The plane maneuvered into the storm area while simultaneous observations were being made at land based radar stations. The radar reports also serve as a check on the aircraft positions, as determined by Loran or other navigational procedures.

In Table 6, below, is a list of eye positions determined by the means indicated. The positions given by ground radar are aircraft locations at times when reports from the aircraft stated that it was in the eye. These have been determined from the radar pictures, as well as from the original logs kept by personnel of the Lincoln Laboratory and the Air Defense Command Radar Station at Montauk Point.

Two possible hurricane paths, based on the positions listed in Table 6, are illustrated in Fig. 7.1. A third path labeled "South Truro and Montauk Radars" is based on eye positions determined by Atlas at South Truro and by ADC personnel at Montauk Point solely from the radar patterns shown on the PPI scopes as the storm approached. These positions are generally to the north of the others. Track 2 positions up to #9 are based on examination of the aircraft tracks logged by Project Lincoln and Montauk Point personnel, as well as from inspection of radar photographs which show the aircraft. The tracks recorded by the Montauk and Lincoln sites differ somewhat and for various possible reasons. First, the usual tolerance in azimuth for a radar is about 1°, and the

Table 6. List of eye positions of Edna and the means by which they were determined.

		TRACK 1		TRACK 2	
No.	Time (Z)	Transmitted Aircraft Position	How Determined	Other Aircraft Position	How Determined
1	1400	39°12'x 72°13'	Loran		
2	1430	39°20'x 71°41'	Loran	39°17'x 71°34'	Montauk radar
3	1500	39°32'x 71°38'	Loran		
4	1530	39°39'x 71°18'	Loran	39°46'x 71°18'	Montauk radar
5	1600				
6	1630	40°00'x 70°55'	Loran	40°18'x 70°59'	Montauk and Lincoln
7	1700	40°40'x 70°40'	Loran	40°34'x 70°33'	Montauk radar
8	1730	40°48'x 70°33'	Montauk radar	40°50'x 70°29'	Montauk and Lincoln
9	1800	41°15'x 70°30'	Montauk radar	41°10'x 70°23'	Montauk and Lincoln
10	1830	Martha's Vine-yard	Visually from aircraft		
11	1830-1900			Martha's Vine-yard	Ground observation
12	1930			Chatham 69°59'x 41°43'	W.E. Fishback
13	1944			S. Truro	Ground observation
14	2010			42°06'x 69°45'	S. Truro radar

range error is usually less than a mile at any range. A reading 1° incorrect in azimuth corresponds to a 2 mile error at a range of 100 miles and proportionally more or less at greater or smaller ranges. An elementary statistical treatment shows that the probable difference in reading of two radars is then about 3 miles if a target is 100 miles from both of them. Secondly, there may be an important contribution to error by nonsynchronous clocks. A one minute difference between clocks at the two stations results in a 4 mile difference of readings for a target which moves at a constant heading at a 4 mile per minute rate. This source of error is not of overwhelming importance in hurricane reconnaissance when the aircraft is in radio contact with a single radar station. The aircraft position and that of the hurricane eye may be determined by radar when notice is received that the aircraft is in the eye; the error of time in this case leads at worst to a small mistake in a velocity computation when the fix is referred later to others which are correct in time. For the purposes of this paper, however, the error is of possible importance because the path of the storm is being reconstructed from the records kept of a fast moving airplane which flew a complicated course and was in the hurricane eye at only certain reported times.

Another important source of error may be misreading or uncertainty on the part of the ground radar observers. Such errors tend to magnify the average differences between reports from two stations.

In view of all these considerations, it may be considered good performance that Lincoln and Montauk radars indicate agreement within eight miles whenever reports synchronous in time are available. Unfortunately, there are only four such pairs of observations, as shown in Table 7.

Table 7. Comparison of Lincoln and Montauk recordings of aircraft positions when the reports are at the same time (taken from copies of the original logs).

Reported time (Z)	Lincoln Position	Montauk Position	Distance from Montauk to Lincoln Position
1704	EL 2129*	EL 2831	7 miles WSW
1840	EM 3921	EM 3218	7 1/2 miles ENE
1853	EM 2526	EM 2327	2 miles SE
1923	EM 5635	EM 5230	5 1/2 miles NE

* Georef coordinates

In spite of these differences up to 7 1/2 miles, it is believed that the eye positions given in Track 2 of Fig. 7.1 are correct within four miles, plus whatever error may be ascribed to the aircraft personnel as they identified their location in the eye center at the given times. The reason for this is that examination of the tracks reveals all the locations where the plane orbited in the eye, and there are enough separate fixes within these small areas to make an uncertainty of four miles appear reasonable. Furthermore, Lincoln and Montauk photographs, which indicate the aircraft positions, have been available to the authors and these have been carefully checked. They have to some extent filled in gaps in the logs and have provided a cross check on many of the points recorded there.

These considerations lead to the conclusion that the prominent differences between the combined ground radar track and the Loran track are due primarily to Loran errors. The differences do not depend on the aircraft observer's ability to place himself in the eye accurately, since both tracks are based on positions when he believed the aircraft to be in the eye. Positions 1, 3 and 6 of the Loran track appear especially unreasonable, although position 6 is the only one of the group for which a definite radar fix is available. The differences between Loran and radar fixes of the aircraft up to 18 miles are of great interest because of the generally accepted high accuracy of both of these procedures.

The diameter of Edna's eye was reported by aircraft to be 15 miles at position 1. Furthermore, the eye had been doubled for a time (see Section 9) and the isobars were irregularly shaped when the eye was over Cape Cod. In view of this, it is remarkable that smooth curves enclosing all the variations of the various tracks (except position 1 of the Loran track) have a maximum separation of only 14 miles. It may be concluded that such oscillations of the point of lowest pressure, if they exist at all, are smaller than the dimensions of the eye itself. Of course, we should be surprised if the point of lowest pressure, or any other singular point, doesn't bob and weave a bit when it is part and parcel of such a complicated mechanism.

North of position 8, Captain Taylor, the weather officer, fixed the aircraft position and that of the eye by visual contact with surface features. Many of the eye positions reported by aircraft at these later times are incorrect by tens of miles. The extensive area of light and moderate winds was very great at this time and made location of a precise calm center difficult, especially because outlying islands in the Cape Cod area and the Cape itself lend protection to the adjoining waters. Further, the marked eccentricity of the pressure field near the eye and the relatively slack gradient on its western side (see Section 9) made it easy to mistake a trough for the true minimum in the pressure field. Fatigue of personnel aboard the plane was, no doubt, also of importance. However, the most important factor leading to misplacement of

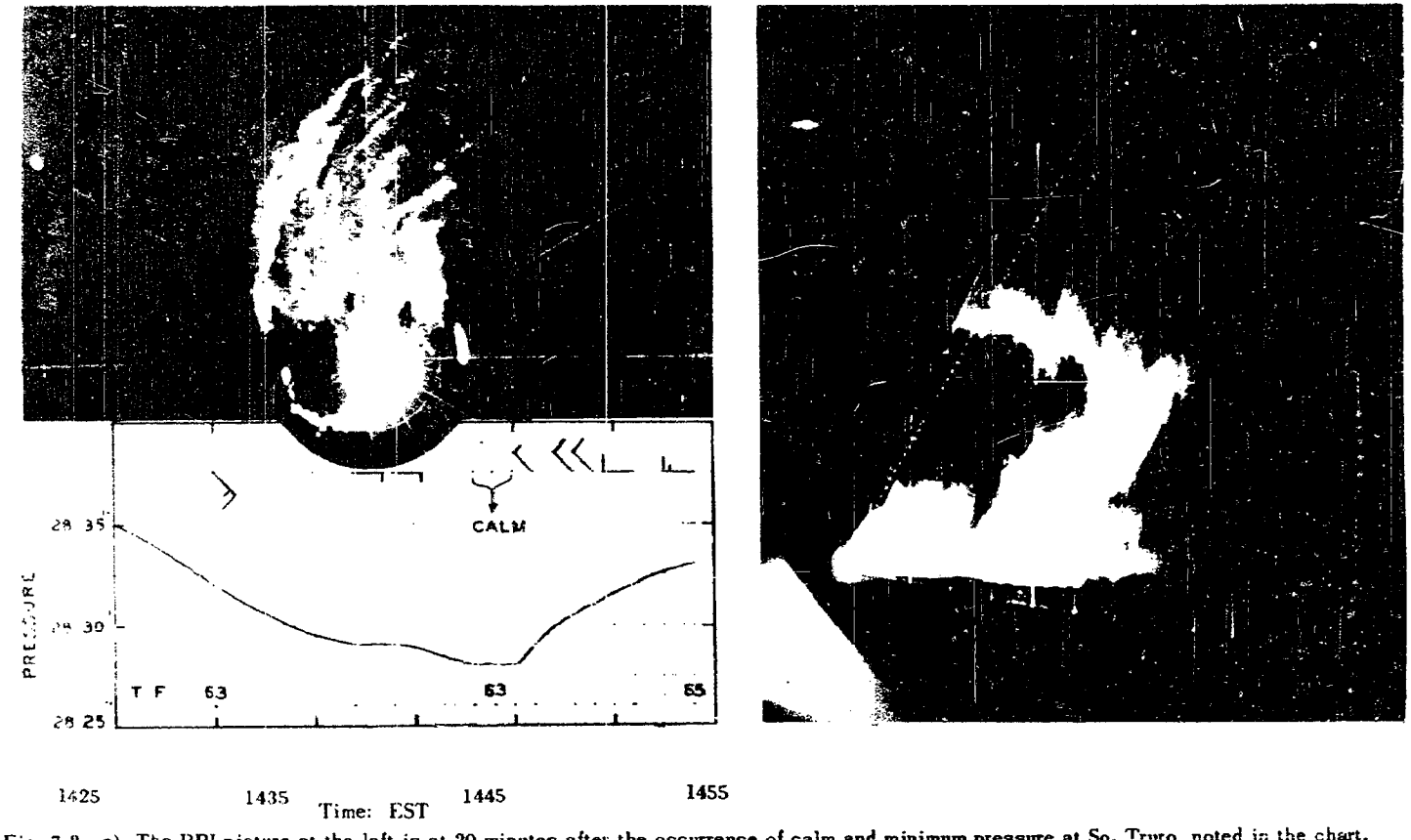

Fig. 7.2. a) The PPI picture at the left is at 20 minutes after the occurrence of calm and minimum pressure at So. Truro, noted in the chart. b) The RHI picture, looking toward 40°, shows the eye as a "V" in the return at about 17 nautical miles. The "V" is believed to be a good indication of the eye location; the layer aloft may not always be present.

the eye after 1800Z was a relatively rapid change of the cloud and precipitation structure which started at about this time. As the eye passed over the Cape, a line of heavy cloud extended southward on the western side of its center. Seen from its western side it looked like the wall cloud, and due to its very heavy appearance, Captain Taylor notes that there was no wish to attempt a penetration. This is shown best in Fig. 7.2a, where the cloud line is visible as a brilliant band just east of northern Cape Cod. When the eye was reported from the aircraft as a "gigantic eye over Provincetown," its center was actually to the east of the cloud line shown in the picture. In Fig. 7.2, the eye is at 40°, 15 miles range. Further confusion was caused at this time by the rain bands' termination along a nearly east west line. The ends of the rain bands were believed to be wall cloud on the north side of the eye. These errors might not have been made had the plane's radar been operative at this time, although the low powered 3 cm APQ-13 aboard the aircraft would be subject to severe attenuation and pattern distortion. The reader may at this point wish to review all of the recco reports as received from the aircraft. These and corrections to them made with the assistance of Captain Taylor, appear in the Appendix.

We come now to consider the eye positions determined by Atlas at the South Truro site.* Actually, it was not the eye that was tracked but the southern side of the most southerly band. This band, as seen on the radar scope and which often resembled the silhouette of a soaring bird at a distance (e.g. see Fig. 8.2), was evidently as much as 20 miles north of the point of lowest pressure at times. Atlas himself believed the point he was tracking to be 5 or 10 miles northeast of the supposed true eye. From Martha's Vineyard on, he attempted to fix on a feature which he believed to be the north rim of the eye. At great ranges the radar sees the upper reaches of the band. The eye of the hurricane was reported by the aircraft to slope northeast and this is confirmed by radar photographs (Fig. 7.2). A slope of the wall cloud in this sense would increase the difference between the band location as seen on radar and the position of the surface eye when the eye is southwest of the radar observer. (At a range of 100 miles, the base of a horizontally directed beam is at an elevation of 5,000 feet above ground level; the upper half power point of a 3° beam is 19,000 feet above the ground at this range.) Figure 7.2 shows that the wall cloud northeast of the eye slopes about 15 miles toward the northeast between the surface and 30,000 feet. Such a slope may result in 5 to 10 mile errors in determining range to the eye from a great distance.

Further difficulties were experienced as the eye and its attendant

---

* The first five positions of Track 3 were made by the Montauk ADC station. It appears likely that both Atlas and the Montauk observer tracked the same feature, as judged by the continuity of the path. Unfortunately, there were no radar fixes of the hurricane eye from Montauk after 1440Z

heavy rains came near because of the way the radar was used. The gain of the radar receiver was reduced so that details of the eye structure would not be obscured in glare associated with general scope saturation. Because Sensitivity Time Control (STC) was not used, this operation resulted in the disappearance of outer rain bands and a loss of information of value in determining the general storm layout. At the same time, decreased range to the eye resulted in increased echo intensity which caused an apparent change in the eye's appearance. Some ground clutter at close ranges was also confusing. Use of Moving Target Indicator (MTI) cancelled ground return, but led also to poorer resolution of detailed features of the precipitation.

Further, after the eye crossed the passage between Nantucket and Martha's Vineyard, the first rain band west of the eye became so intense and extended so far to the south (Fig. 7.2) that Atlas confused this feature with the apex of the actual wall cloud which he had previously been tracking. Since he believed the apex to be northeast of the actual eye, his reported positions were then some 10-20 miles to the WSW of the actual eye. This error explains the sudden decrease in speed of the storm as reported by Atlas. It is a striking coincidence that the same feature of the storm observed visually from the aircraft caused Captain Taylor to make an almost identical mistake. Somewhat better radar positions might have been obtained when the eye was within about 50 miles of the radar site if more extensive use had been made of the RHI radars (FPS-4 or FPS-6) to check the locations indicated on the PPI scope (see Section 8 for a description of the recommended technique). Radar position #13 was determined in the post analysis from the 3 cm RHI records taken at South Truro, as well as synoptic reports. Incidentally, it should be noted that the differences of eye positions noted here are comparable to those observed by Bunting et al (1951) in their study which utilizes aircraft and PPI radar reports.

The above considerations notwithstanding, it may be concluded that the location of the eye by radar was accurate within limits comparable to the dimensions of the eye itself. This appears adequate for most storm advisory work. Improved estimates might have been obtained if allowance had been made for a typical eye radius within which there is no radar echo; unfortunately, this depends somewhat on the radar. Although it is highly desirable to fix the eye absolutely, it is more important to obtain an accurate measure of its speed and direction. This can be done by the consistent tracking of an outstanding feature of the wall echo band as described in Section 8.

It should also be borne in mind that the data of this section does not lead to unalterable conclusions concerning the best tracking methods, since no one of the reconstructed paths is considered entirely correct. Even the post analysis suffers because of radar errors, nonsynchronous clocks, incomplete and insufficient synoptic data and because the aircraft may not have been in the center of the eye when it was thought to be by those aboard.

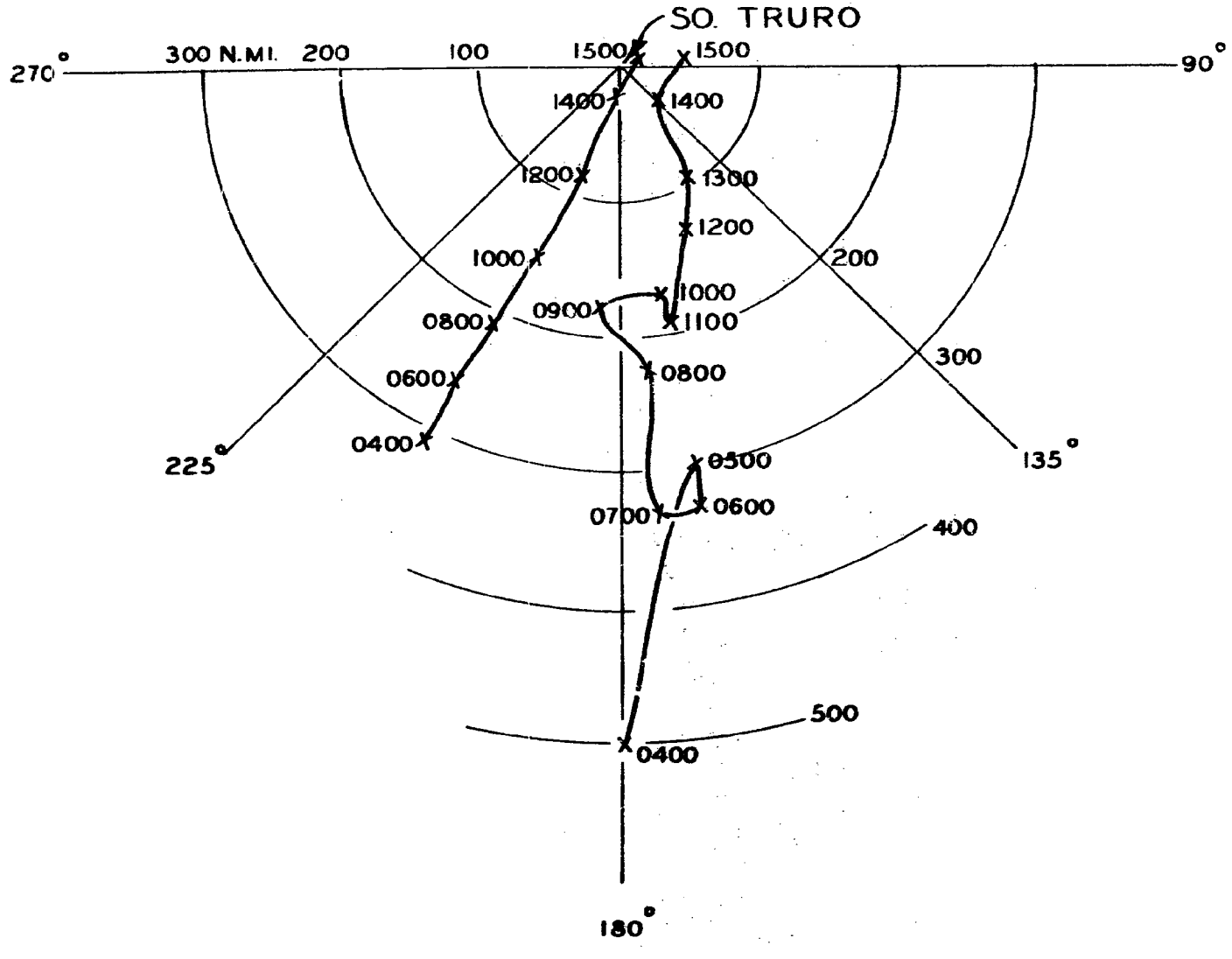

Fig. 8.1. The nearly straight path is approximately that of the eye of Hurricane Edna relative to So. Truro, 11 Sept. 1954. The irregular track marks the location of the subjectively determined average of the centers of curvature of major bands near So. Truro, at the indicated EST's.

8. Identification of the Hurricane Eye as Displayed on the Radar Scope

The eye of a hurricane as displayed on the radar scope is perhaps the most important single feature to recognize and follow. Since the hurricane is a constantly changing entity, there is probably no one aspect of the radar presentation which will invariably serve to mark the eye. However, a combination of one or more characteristics of the precipitation pattern will generally permit the observer to pinpoint the eye with a relatively high degree of accuracy. Some of these features and other helpful guides will be summarized in this section. Although most of the material presented here pertains specifically to "Edna," the proposed identification criteria should apply well to other hurricanes in temperate latitudes. The features of low latitude storms are based primarily on photographic records taken by one of the authors (Atlas) during the Florida hurricane of 15-16 September 1945. For a detailed study of the latter storm, see H. Wexler (1949).

The eye of a hurricane appears on the radar PPI scope approximately at the center of spiralling of the bands. Sometimes it is at the center of curvature of the bands, especially of those near the eye, but more often it is "offcenter" as a consequence of the tendency for the downwind ends of the bands to lie closer to the eye and to spiral in toward it continuously.

The centers of curvature of the bands of Edna are only rough guides to the eye positions, as is shown by Fig. 8.1 below. The individual positions given in the figure are based on the radii of curvature of the most prominent bands near South Truro, or the average of several such radii when no one band appears outstanding. Generally, the inner bands give a somewhat better indication of the eye position than the outer ones, although it is clear from the photographs that the radius of curvature of bands in any one region relative to the eye is itself subject to change. This is illustrated by Figs. 8.3 and 8.4.

In the subtropics, the eye is often completely surrounded by precipitation. Figure 8.2 illustrating the eye positions of the 1945 hurricane, shows rain bands completely encircling the eye. As this hurricane moves northward over the Florida peninsula, it is seen that the radii of curvature of the inner bands increase and this tendency has been correlated with the weakening of the hurricane circulation.

In temperate latitudes, precipitation is mainly confined to the northern semicircle of the storm (Dunn, 1951); this is the case with Edna. In these circumstances, the eye is to be found south of the band of smallest radius of curvature, the cusps of which point generally south; usually this is also the southernmost band.

The eye positions of Edna are indicated by arrows in Figs. 8.3 and 8.4, some of which also point to the reconnaissance aircraft. These eye

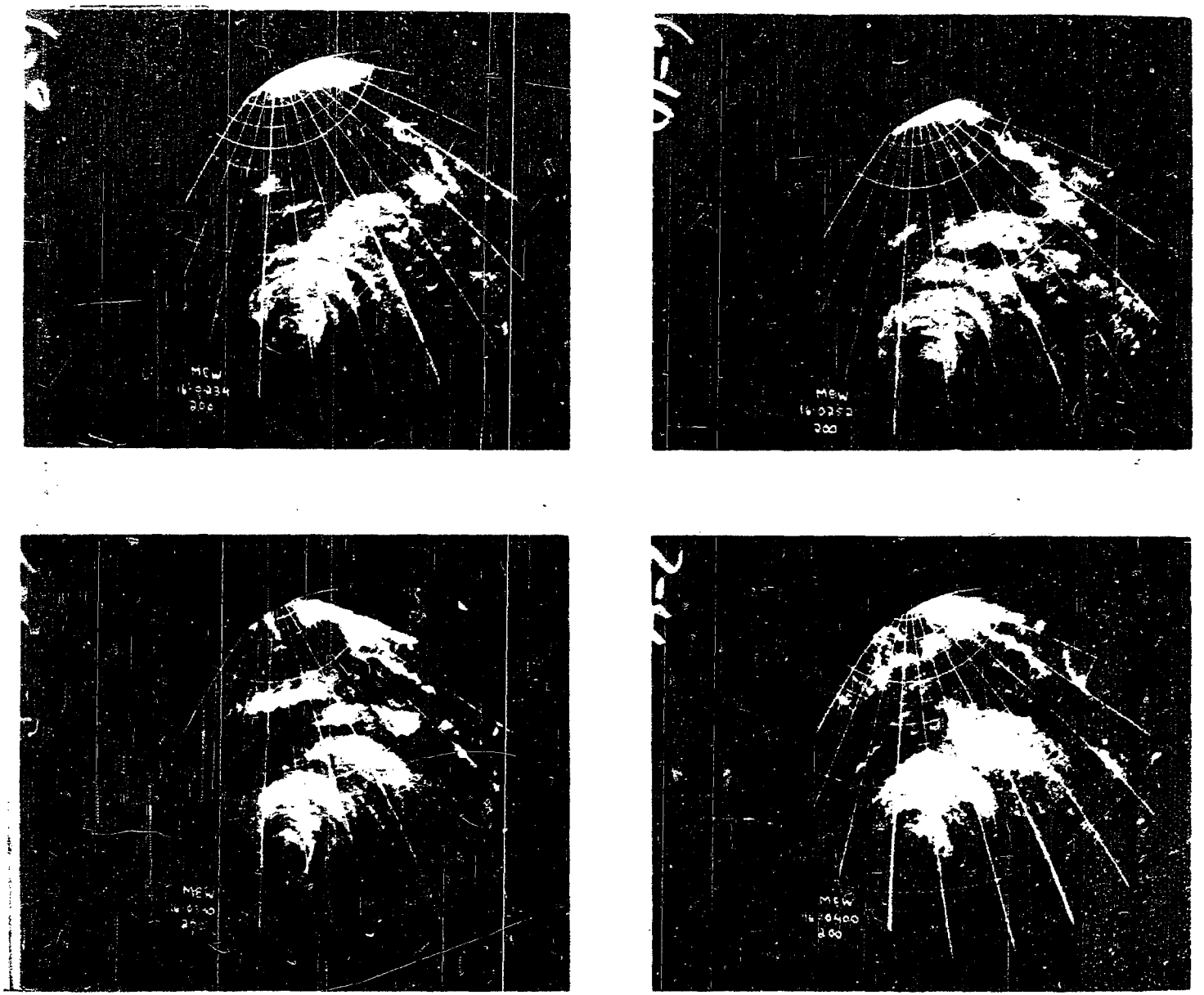

Fig. 8.2. Hurricane of 16 Sept. 1945, as seen from Orla Vista, Florida. Note rain bands completely encircling the eye at 0234 and 0252 EST; this feature is common in slow moving hurricanes, and in low latitudes. Range marks are spaced 10 na. mi. Radar is 10 cm. AN/CPS-1.

positions have been determined by cross checking of aircraft, radar and synoptic reports. Discussions with Captain Wallace Taylor, observer on the WB 29, have proved of great value in these determinations which are discussed at greater length in Section 7. Another method of eye identification is based on the fact that discrete radar weather elements near the eye move around it in the same sense as the surface winds. Thus the center of spiralling of the bands as observed at a single instant is, as far as can be determined from time-lapse pictures, identical with the center of rotation of small precipitation echoes. In practice, it may prove rather difficult to locate the eye on the basis of this information because of the short lifetimes of the discrete echo elements near it. In most cases, these elements do not persist long enough to allow reliable velocity determinations.* In addition, precipitation near the eye is not especially cellular. Such cells as do exist are small and it is difficult to find discrete elements to track. It is necessary that a narrow beamed radar such as the FPS-3 be used for determining the eye location by this means. Otherwise, the small elements near the eye are not resolved and the larger forms of which they are parts are seen to move with the storm as a whole, rather than with the horizontal winds.

The comment above may be amplified further with regard to proper tracking of the eye. It may be more convenient to pick out a fairly stable appearing feature (such as the apex of the "spread eagle" noted in Fig. 8.3) which is near the eye and follow its motion. This, in fact, was the method used by Atlas in tracking Edna from the South Truro site. This method is advantageous in that a definite feature is followed, rather than a large hole in the echo mass. However, it should be remembered that the positions of a feature such as the spread-eagle may be as much as 20 miles distant from the eye, although it moves with the eye's velocity. Of course, in a mature storm such as Edna, with an eye area of light or moderate winds perhaps 30 miles in diameter, it is at least as important for forecast purposes to assess accurately the velocity of the storm as a whole as to determine the exact eye position at every moment.

In tracking, one must take care not to become transfixed while a particular feature slowly transforms. The eye area is subject to important changes of appearance over periods of an hour or so, and constant reference must be had to the total picture in order to avoid improper tracking. Changes of eye structure in Edna were, in fact, partly responsible for errors by Atlas and by the crew of the WB 29. (See Section 7.)

---

* Our qualitative finding is that discrete cells and masses are most persistent in the outskirts of the storm and of very short duration (a few minutes) near the eye. McIntyre (1955) reports on echo lifetimes in Hurricanes Carol and Edna, 1954, and finds similarly that the most persistent cells are farthest from the eye.

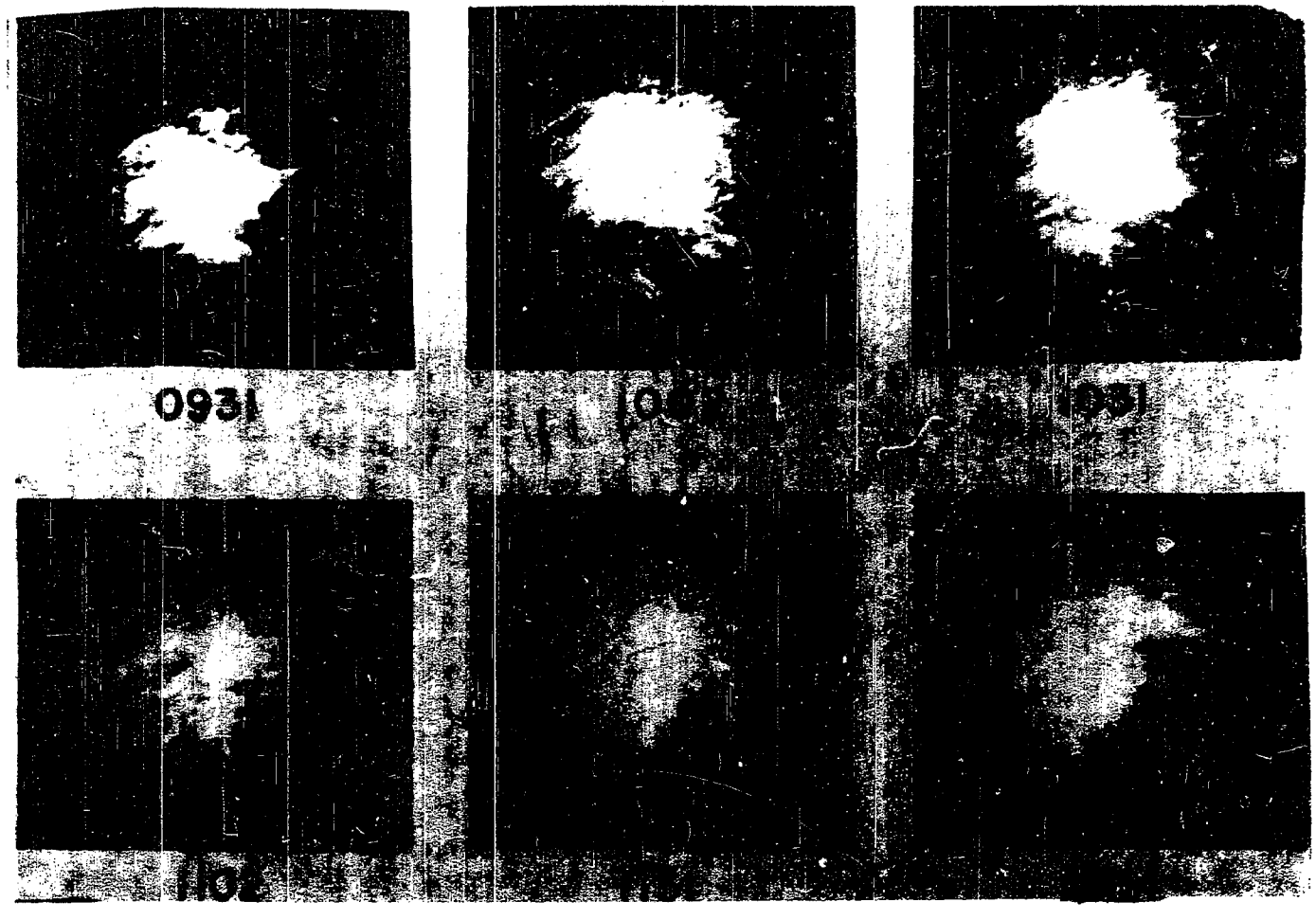

Fig. 8.3. Positions of the eye of Edna, 11 Sept. 1954. At 0931 the eye is out of range of the FPS-3 presentation. Note the comparatively convective nature of the eastern ends of the bands. At 1031, 1102, and 1131, the rain area immediately north of the eye has the appearence of a "spread eagle".

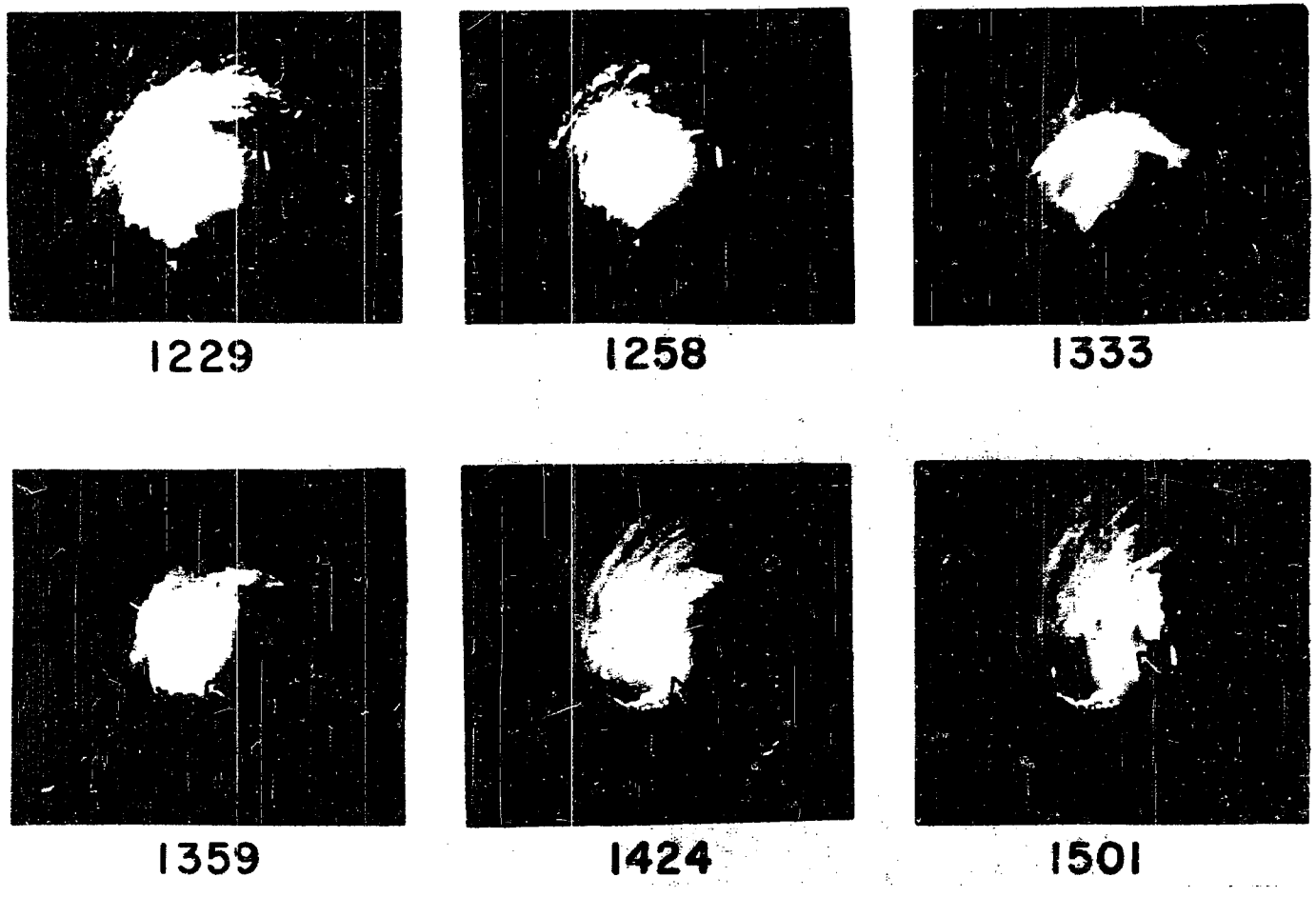

Fig. 8.4. Positions of the eye of Edna, 11 Sept. 1954. Radar echoes from Cape Cod terrain are visible at 1258 and in the subsequent pictures. Note the squall line-like appearance of the eastern ends of the bands. Winds of hurricane force are entering the line head on. The elongation of the bands in the last pictures is well correlated with elongation of the surface isobars.

Another method of eye identification is suggested by the post analysis. Figures 8.5 and 8.6 illustrate RHI photos taken at 10° increments of azimuth when the eye was within 20 miles of the radar. (The picture at 40° is shown again with its associated PPI photo in Fig. 7.2.) The eye is associated with the "V" in the radar echo in the pictures at 40°, 50°, 60° and 70°. It is apparent that the most intense convection occurred at the time of these pictures to the north-northeast of the eye, while in its immediate vicinity general precipitation occurs from west through north. The area south of an east-west line through the eye is practically devoid of rain. Thus, when the eye is suspected to be within about 50 miles, RHI search in the area of its presumed location may reveal a structure similar to that revealed here. The relatively great vertical extent of the wall cloud or side of the eye in the direction of its movement and the trailing cirrostratus canopy overhead may be frequent features of hurricanes in temperate latitudes.*

Of course, if radio contact between a reconnaissance aircraft and the radar site is established, one of the most effective means of tracking the eye is to fix the location of the aircraft when its crew declares that it is in the eye. Such a fix should, in most cases, be correct within the limits of radar accuracy, usually better than one mile. By cross checking the interpretations of radar observer and aircraft crew, errors on the part of both can be minimized, although one may question whether this technique would have rendered an improvement in the tracking of Edna** in the immediate vicinity of Cape Cod.

We now turn to consideration of tracking procedures which can be used when the eye region is so far distant that it does not appear on the PPI scope. These may be especially important when tracking a storm far at sea from coastal or island sites; in these cases, the usual synoptic weather reports may not give sufficient indication of a storm's path. The pictures presented in this section and elsewhere in this report demonstrate that the band direction at South Truro is, in its most general sense, unchanging with time as the eye approaches. A series of photographs taken at Pope Air Force Base (Fig. 8.7) demonstrates the changing band direction near the station as Edna moves northward along a path far to the east of the station. (This figure also illustrates again the convective nature of the outermost bands.) Thus, in analogy with similar statements regarding surface wind direction, the following simple rules apply:

(1) If the large scale band direction through the station is

---

* Potter (1952) presents a time cross section of a hurricane passage at Halifax, based on visual observations, which is quite similar to the photograph of Fig. 9.5 at 40°.

** As described in Section 7, aircraft and radar observers were misled in tracking Edna by the same feature of the storm.

unchanging with time, the hurricane is approaching directly.

(2) If the large scale band direction through the station rotates in a clockwise sense with time, a northward moving hurricane is passing west of the station.

(3) If the bands rotate in an anticlockwise sense with time, the hurricane is passing east of the station.

With regard to application of the above, Fig. 8.8 illustrates the development of a rather confusing situation. At 0800 the band direction through South Truro would probably be placed at 260°-80° by most observers. However, an area oriented along 300°-120° intensifies and moves over the station. At 0845, some observers might give the direction of this bright region as the "large scale band direction." The dilemma can be resolved somewhat by noting that this sequence is of a rapidly developing nature. Later pictures, as suggested by that at 0901E, show that it gradually loses its identity. The intense oddly shaped echoes SE of the station at 0901 are shown by RHI to be strongly convective in nature, while most of the precipitation south and west of the station shows the bright band. These convective echoes gradually attain more stable characteristics and take on the general appearance of the rest of the pattern.

It is probably improper to relate the above comments to hurricanes in general, but they give notice to beware the drawing of sweeping inferences from rapid developments. Care should be taken, especially when the eye is at great ranges, to follow the broad evolution of the PPI pattern rather than be influenced by small scale or transient developments. Reference to synoptic reports should result in increased value of both radar and synoptic observations. It should also be remembered that neither radar nor synoptic analysis is infallible (the latter especially over oceans where data is sparse and often inaccurate) and that the principles suggested here are very probably not valid in all cases.

Figure 8.9 shows a complicated and confusing situation. The various orientations of the banded structures to the south may well lead to different interpretations as to the eye positions. The surest aid here is again an acquaintance with earlier radar and synoptic developments. Incidentally, this "crossed bands" structure is even more prominent in the limited radar records of Hurricane Carol, 1954. The authors have not observed such in pictures of low latitude hurricanes, but this is not to suggest a definite geographic restriction to its occurrence.

In identification of the eye, phenomena of which the radar observer should be especially aware are "false radar eyes." One such case is

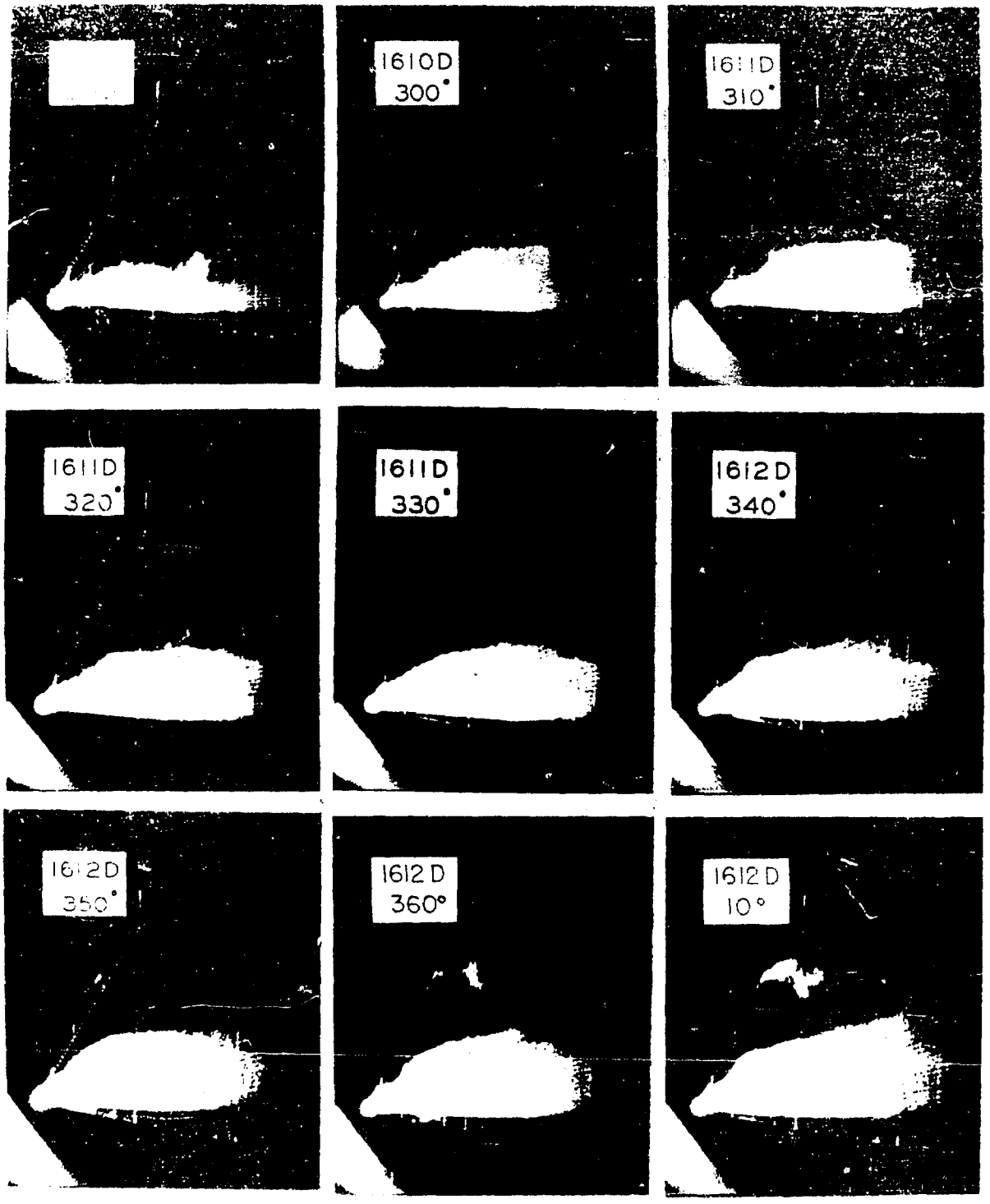

Fig. 8.5. [illegible] taken at 10° increments on 11 Sept. 1954 when the eye of Hurricane Edna was about 15 nautical miles [illegible] the radar site. Range marks are 5 nautical miles and indicated times are [illegible]. The flat top of the echo [illegible] 300°, 310° and 320° is presumably associated with the melting level. At 290° the presence of [illegible] may be indicative of rain which is advected by strong northerly winds west of the eye, southwest [illegible] precipitating area. In the last pictures note the presence of [illegible] bright band.

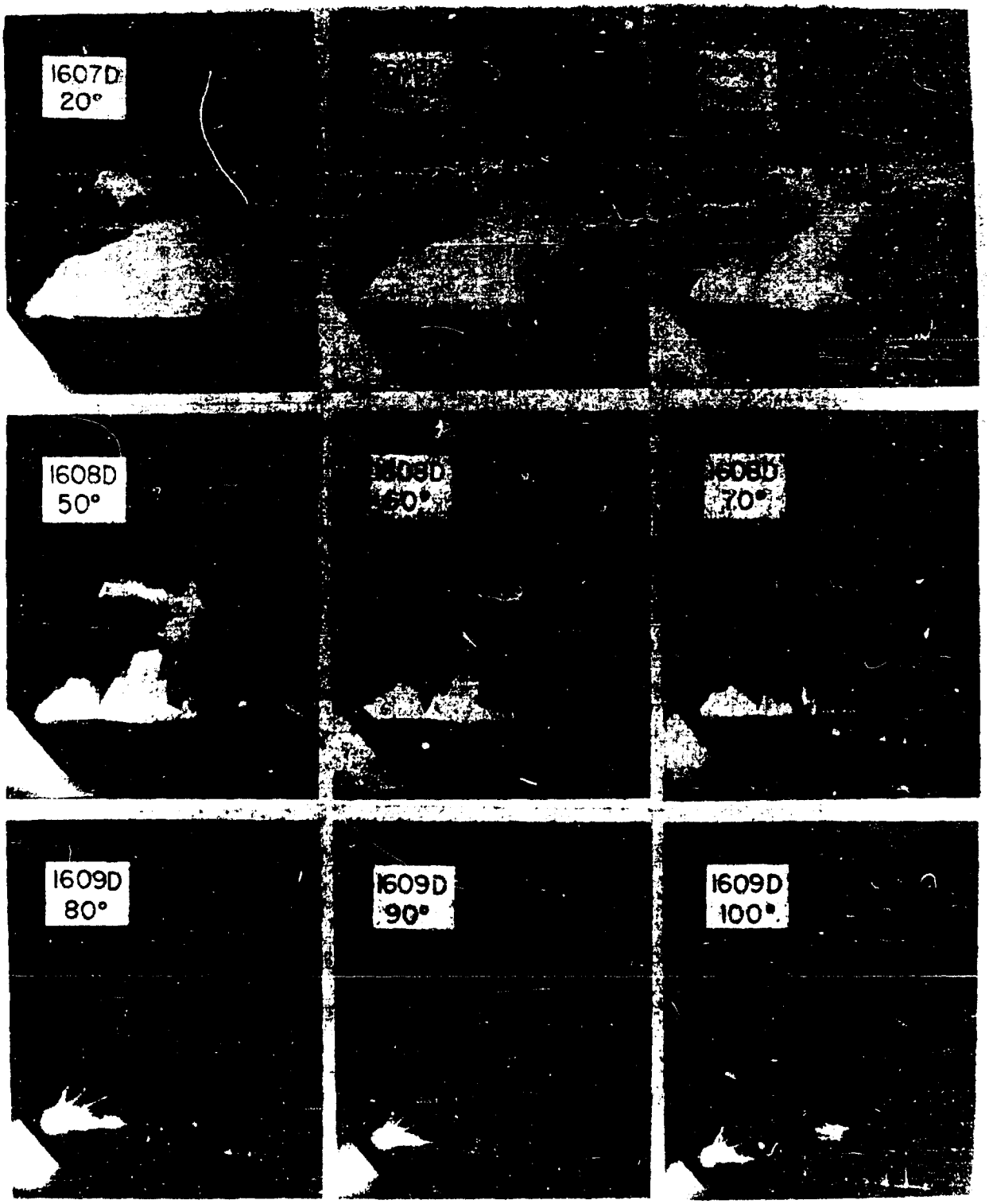

Fig. 8.6. FPS-4 RHI photos taken at 10° azimuthal increments on 11 Sept. 1954, when the eye of Hurricane Edna was about 15 nautical miles northeast of the radar site at So. Truro. Range marks are at intervals of 5 nautical miles and indicated times are EDST. The great echo mass at 40° is indicative of convection north-northeast of the eye, which appears as a "V" in that picture and also at 50°, 60° and 70°. The upper lever visible in the upper 6 pictures is indicative of high level divergence. Note that the eye is open to the south.

1435 EST.
EYE AT 118°
278 STATUTE MILES

1540 EST.
EYE AT 114°
273 STATUTE MILES

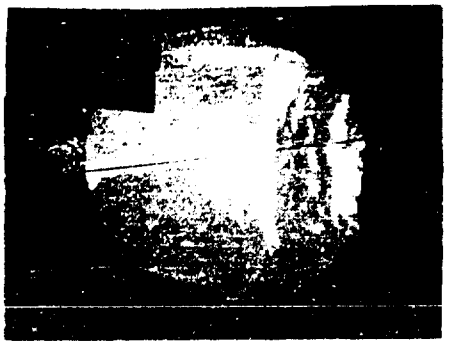

1645 EST.
EYE AT 111°
268 STATUTE MILES

Fig. 8.7. These radarscope photographs of Hurricane Edna 10 Sept. 1954, are from the CPS-9 (3 cm) installation at Pope AFB, North Carolina. North is toward the top of each picture and the range of each is 200 statute miles. Note the cellular nature of the outermost bands and their slight counter-clockwise rotation during the period between top and bottom pictures. The rotation results from the northward progress of the whole spiralling system.

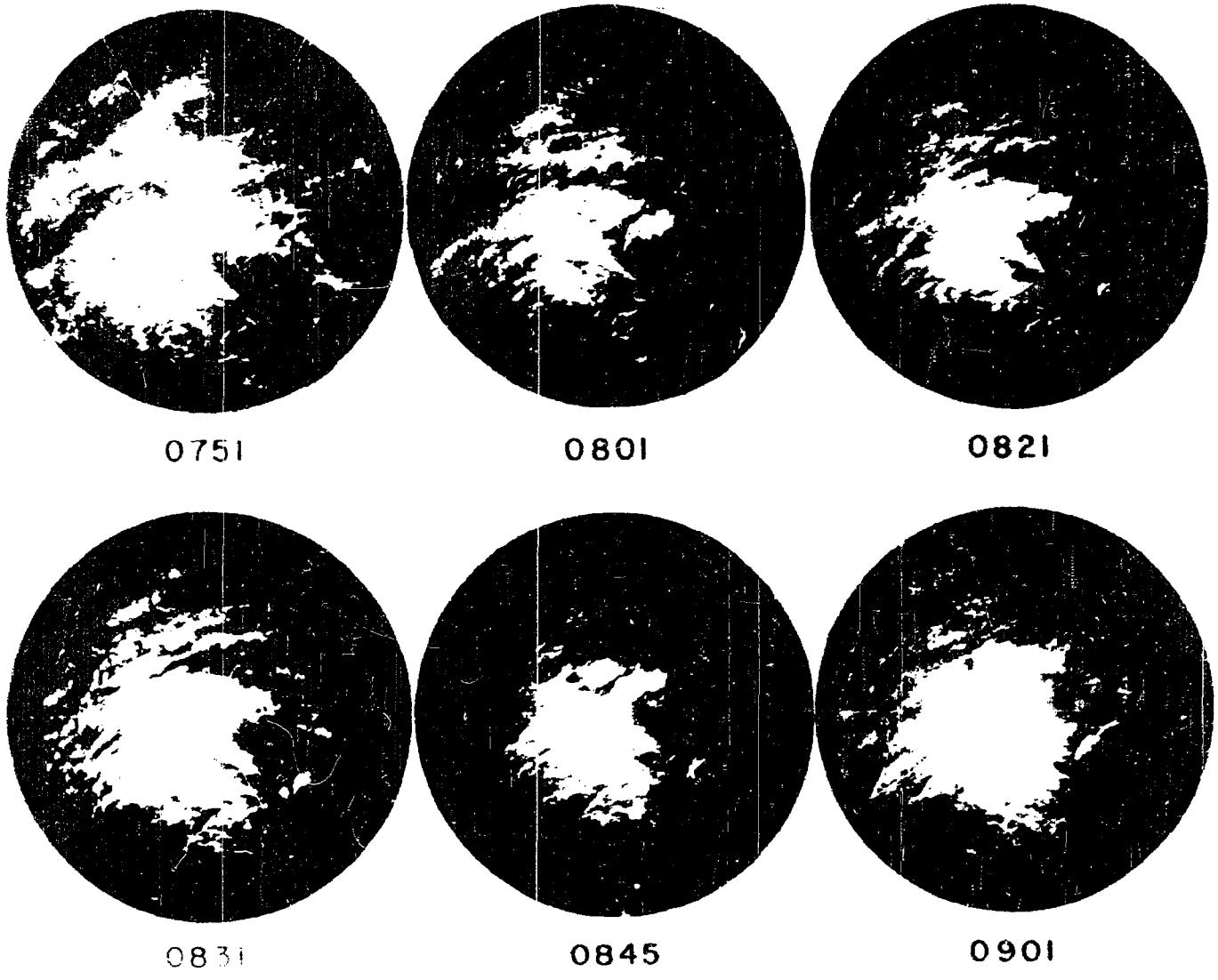

Fig. 8.8. Varied band directions as observed by FPS-3 radar during Hurricane Edna, 11 Sept. 1954. Times indicated are EST. The eye of the storm decreases in range from 210 to 180 na. miles during this sequence of pictures and is near 205° azimuth. Maximum range shown

shown in Fig. 8.10.* Simpson (1955) has suggested that these form in connection with relatively small scale motions in association with individual rain bands. When the observer is familiar with the evolution of the PPI pattern, errors of eye location due to improper identification of a "false eye" may be avoided, since these are transient features lasting perhaps fifteen minutes to an hour. Further aid to proper identification may be sought in the large scale spiralling pattern of the band which is not about the false eye, except perhaps in its immediate vicinity, and in the motions of individual elements which likewise tend to be around the true eye.

9. Miscellaneous Synoptic Aspects of Hurricane Edna

Six hourly surface charts and twelve hourly 500 mb charts of Hurricane Edna are illustrated in Figs. 9.1 and 9.2. It may be seen that Edna was affected by a trough in the westerlies and that its motion was in good agreement with the large scale flow at 500 mb. The motion of Edna has been studied in detail by Malkin and Holzworth (1954) who found excellent agreement between its movement and space averages of the pressure weighted mean wind between 1000 and 200 mb.

For comparison, Fig. 9.3 shows the 500 mb pattern just prior to the northward acceleration of "Carol" and "Hazel," 1954. Carol entered New England after crossing Long Island; Hazel went inland near Myrtle beach, South Carolina. The basic similarity of the various cases is obvious.

The regular expansion of the surface circulation of Edna is evident in Fig. 9.1. This type of change has been noted by many authors as characteristic of the transition from youth to maturity. The distribution of precipitation relative to the eye of Edna is shown by Fig. 9.4. The heaviest rain is seen to be in the northwest quadrant of the storm. This distribution is also indicated by Fig. 9.5b which shows the total amounts associated with the storm and the relationship of this pattern to the path. Figure 9.5a shows the total precipitation and path of Carol. The hourly precipitation data shows that little or no rain fell after the eye of Carol passed north of any given New England point and that the maximum intensity of rainfall was nearest the eye. Thus Carol, like Edna, had rain mainly confined to the forward semicircle, but unlike the latter, had rain distributed more or less evenly in NE and NW quadrants.

It is likely that the rainfall distribution in these northward

---

* This picture is one of many taken with "Moving Target Indication." MTI effects a disappearance from the radar scope of fixed targets, such as hills and buildings, and a weakening of other echoes. Comparison of nearly simultaneous MTI and normal pictures of Edna reveal only a tendency for the weaker precipitation echoes to disappear with MTI.

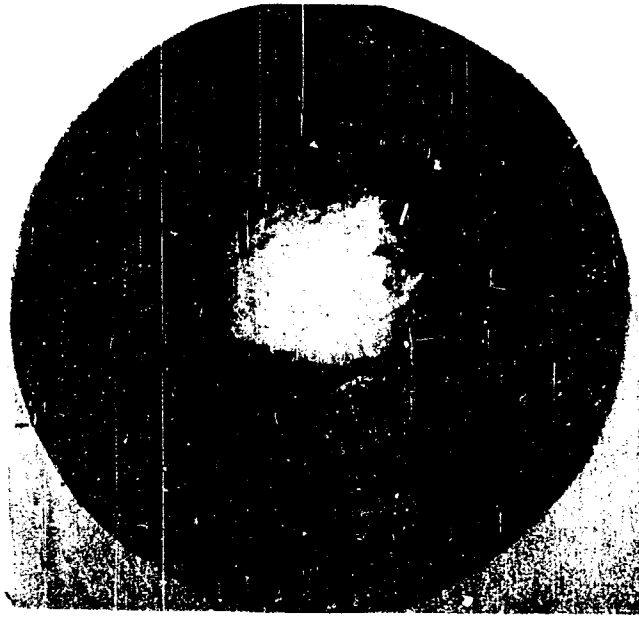

Fig. 8.9. This photo, taken at 1016 EST, 11 Sept. 1954, illustrates the crossed bands which appear occasionally in the record of Hurricane Edna. At high gain, additional curved bands are seen toward 200° at this time, and demonstrate that the eye lies in that direction. At times, however, the crossed bands may lead to ambiguous indication.

Fig. 8.10. This photograph taken from So. Truro at 1215 EST, 11 Sept. 1954, with Moving Target Indication, shows a "false eye" of Edna at 220°, 50 miles. The true eye is near 200°, 90 miles. The recco aircraft is seen adjacent to the true eye position.

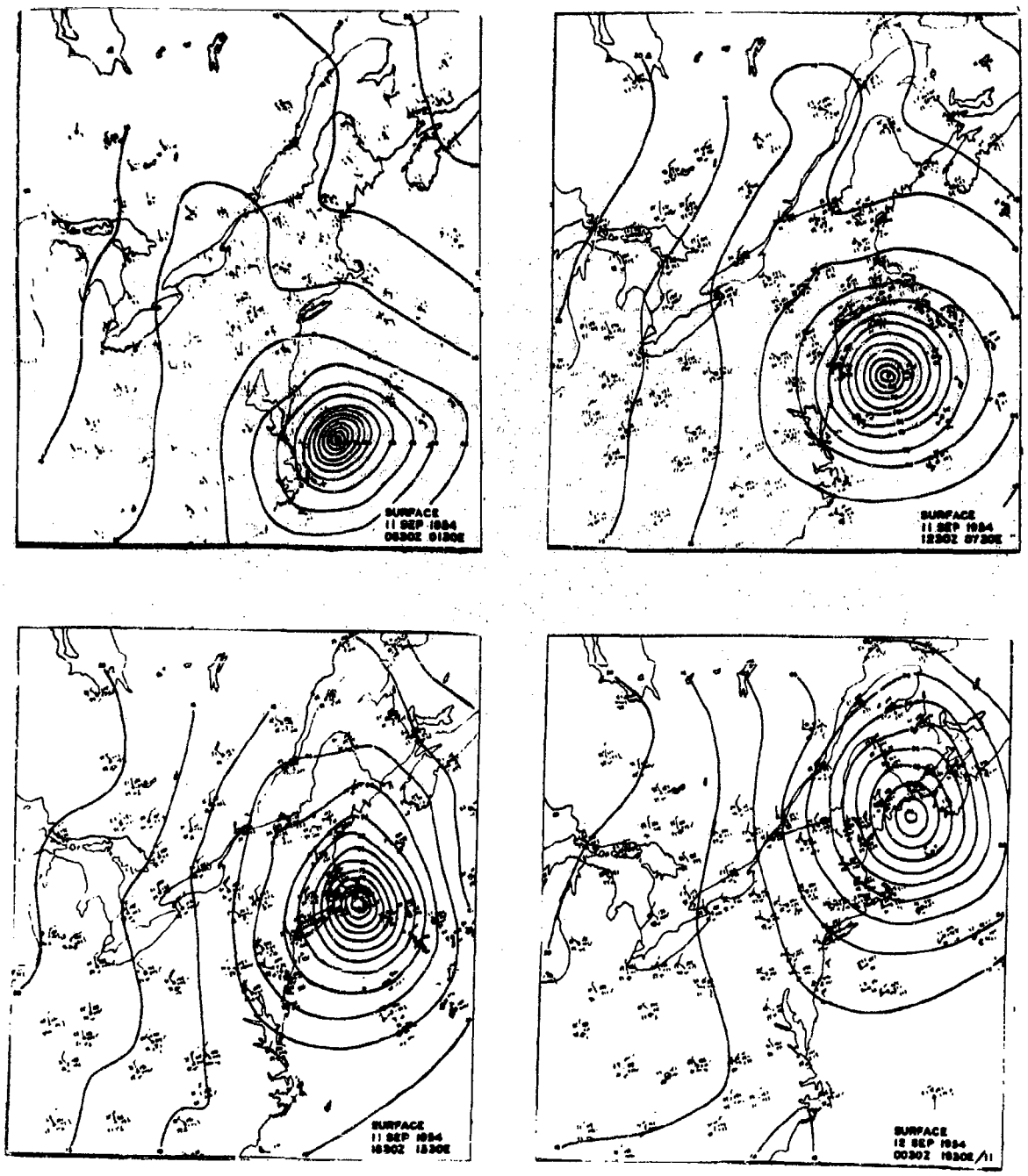

Fig. 9.1. Six hourly surface charts of Hurricane Edna, 1954. Note the progressive enlargement of the circulation. North-south elongation is evident at 1830Z, 11 Sept. and 0030Z, 12 Sept.

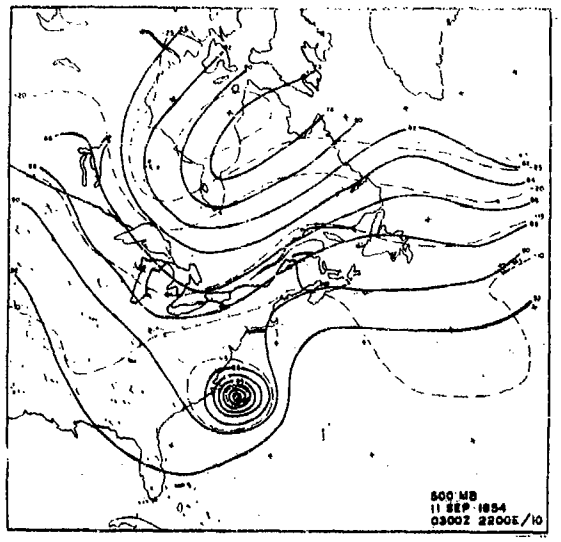

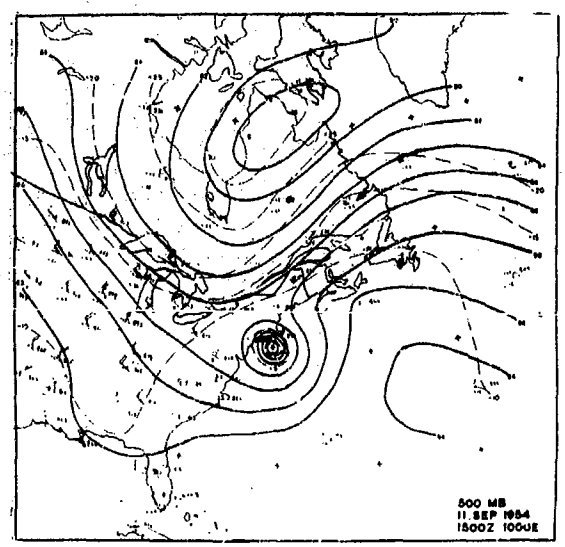

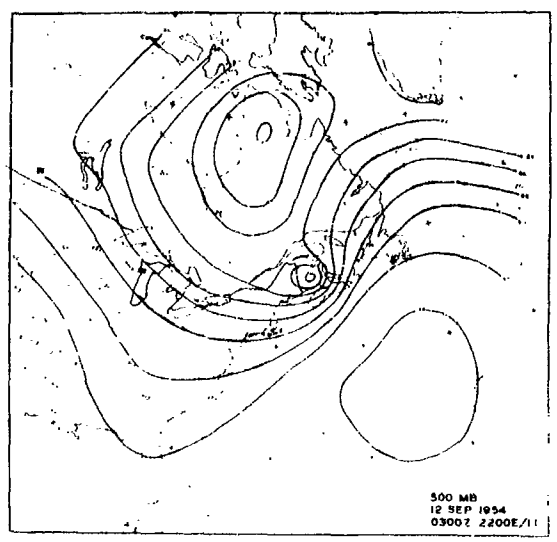

Fig. 9.2. Twelve hourly 500 mb charts showing Hurricane Edna, 1954. The low pressure center east of Hudson Bay remains about stationary as Edna moves northeastward.

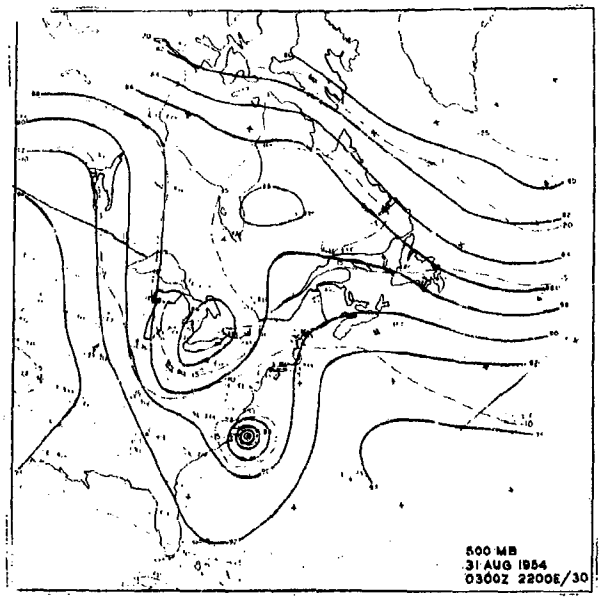

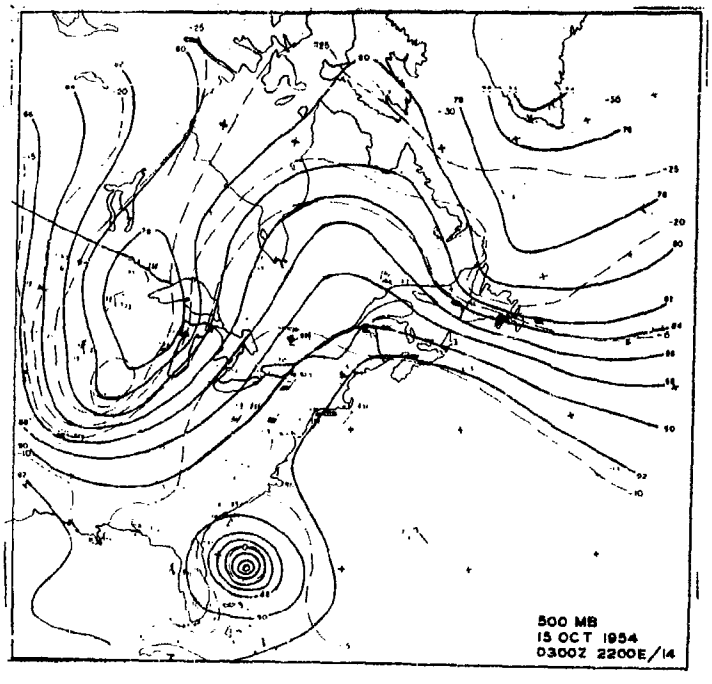

Fig. 9.3. These charts depict conditions during the northward motion of Hurricanes Carol (above) and Hazel (below), 1954.

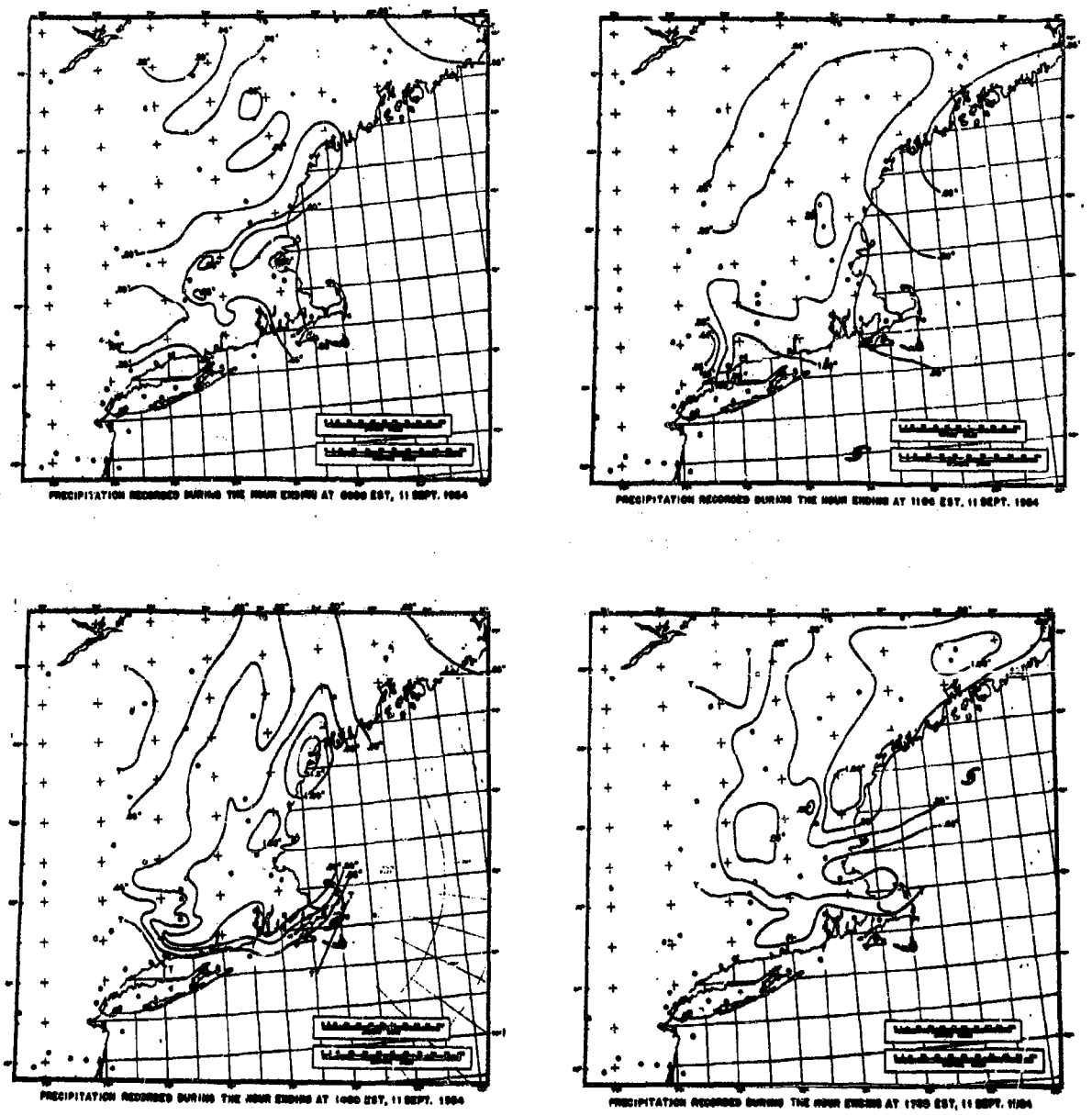

Fig. 9.4. Distribution of precipitation relative to the eye of Edna, indicated by the cyclone symbol in all but the first picture. Rainfall is most intense and widespread in the northwest quadrant, with maximum hourly amounts occuring about 90 miles from the eye.

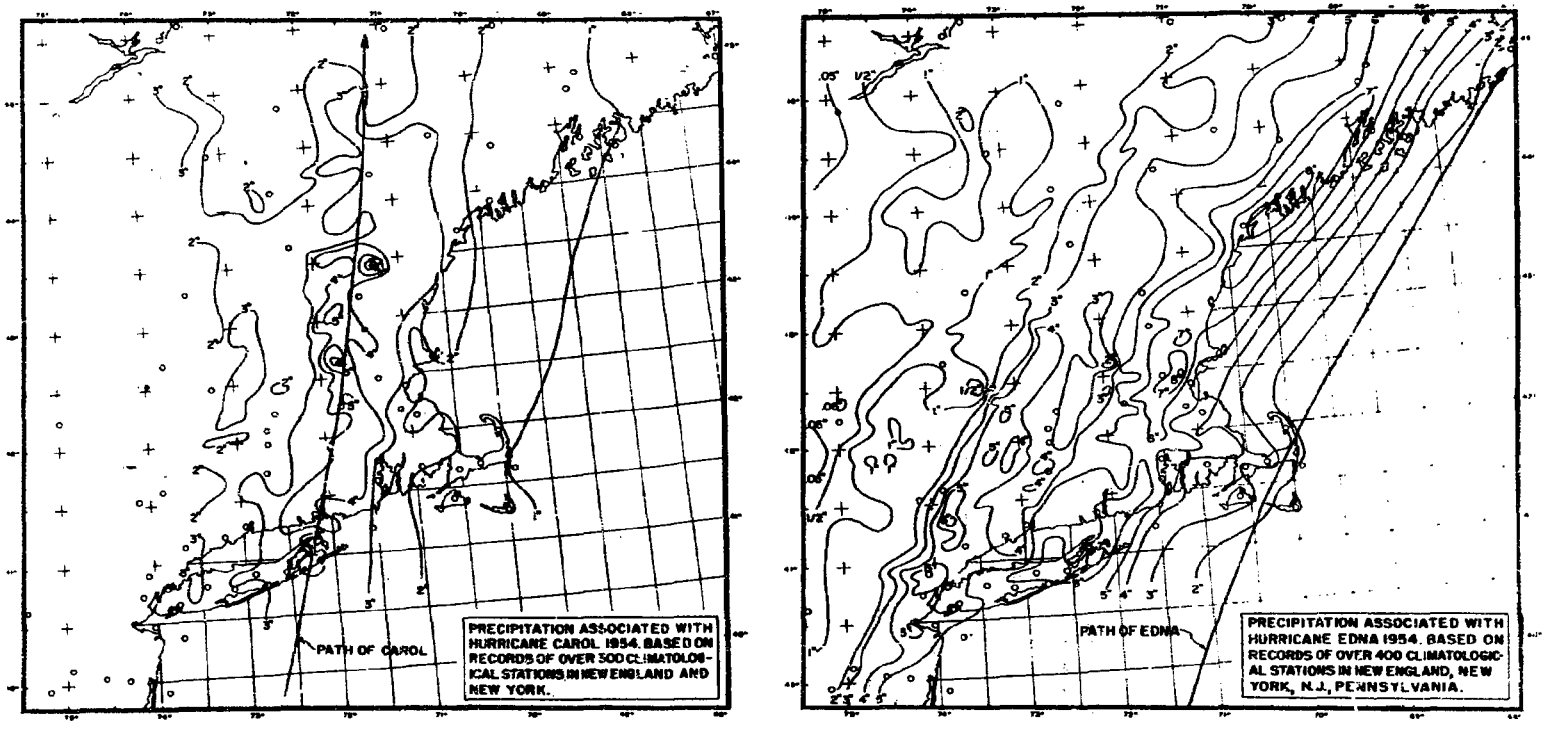

Fig. 9.5. Precipitation amounts associated with Hurricane Carol and Edna, 1954, shown in their relation to the paths of the storms. During Carol, maximum hourly amounts occurred immediately preceding passage of the eye; precipitation is about evenly distributed on both sides of the path. In Edna the occurrence of maximum hourly precipitation rates almost 100 miles NW of the eye and the NNE motion of the storm resulted in the highly skewed distribution shown.

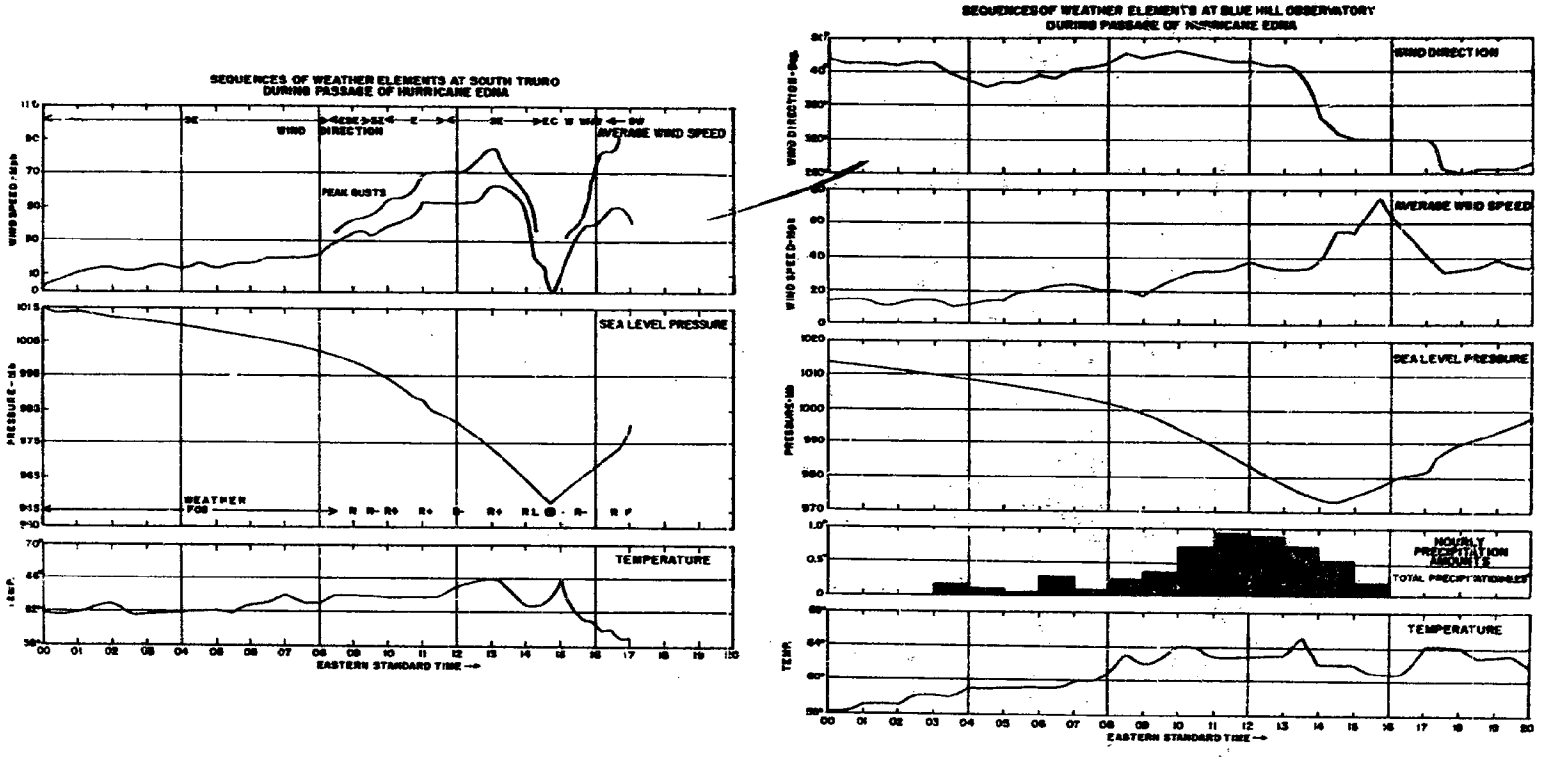

Fig. 9.6. So. Truro and Blue Hill meteorograms of Hurricane Edna, 1954. At So. Truro, the eye is overhead at 1444 EST, 11 Sept; calm wind and steady barometer of 28.26 in. are reported for 3 minutes. The temperature variations at about the time of eye passage at So. Truro can be linked closely to variations of wind velocity and sunshine. At Blue Hill, almost all the rain falls prior to the time of minimum pressure (as is also the case elsewhere); of particular interest is the wind shift completed at the time of minimum and the subsequent increase of wind speed while the pressure rises. The end of the wind burst is marked by a pressure jump and a sudden shift of direction amounting to 40°.

moving storms bears an important relationship to the temperature field. Northeast storms of New England generally are accompanied by precipitation maxima in the region of strong low level thermal gradient. The differences between the precipitation patterns of Carol and Edna may therefore be attributed in part to the greater air mass contrast in Edna. Hurricane Hazel, 1954, which is associated with an intense polar trough, is also characterized by maximum precipitation to the west; in Hazel there is also an important orographic contribution in the region of maximum rain. The 1938 and 1944 New England hurricanes also produced more rain on their western sides, but only the former appears to have been associated with strong air mass contrast (Brooks and Chapman, 1945, and Pierce, 1939). Recent cases which evidence complex relationships between the positions of surface low centers and precipitation distributions are Hurricanes Connie and Diane, 1955, illustrated and discussed in Weatherwise (Sumner and O'Connell, 1955).

One of the interesting features of Hurricane Edna is the great and rapid increase of northwest wind which occurs after the time of lowest pressure at stations west of the eye path. The maximum velocity of the northwest wind considerably exceeds that of the winds which precede the time of lowest pressure. The Blue Hill meteorogram, Fig. 9.6, graphically illustrates this phenomenon. The anomalous northwest gale appears first at southernmost stations, such as Block Island, and progresses northward at the speed of the hurricane eye, appearing at least as far north as Brunswick, Maine, though somewhat weakened. Efforts to relate this feature, which commences with some characteristics of a burst or squall line, to pressure jump or trough lines, using the extensive original data and hourly maps available, have not been at all conclusive. It does appear, however, that some reasonable interpretation of the relationship between the observed wind and pressure fields is possible on the basis of available data. The hourly weather maps show that 100 miles to the northwest of the eye the wind speeds are much less than gradient. A typical observation shows a wind of 15 miles per hour blowing across the isobars toward lower pressure at an angle of 45°, where the gradient wind is 90 miles per hour (see Fig. 9.7). Some limited trajectory analysis indicates that the hurricane winds from the northwest are initially a part of such a weak subgradient flow. It is also seen from the maps that as the air parcels northwest of the eye travel toward lower pressure, they are acted on by progressively greater pressure gradients. Under these conditions, the parcels accelerate rapidly; elementary computations have indicated that the equations of motion explain the observed accelerations approximately.* Therefore, it is felt that the unusual northwest wind can be described largely in terms of observable differences between the pressure and pressure change fields of Edna and those of other hurricanes.

---

* A geostrophic departure of 100 mph indicates an acceleration of about 40 mph per hour in these latitudes.

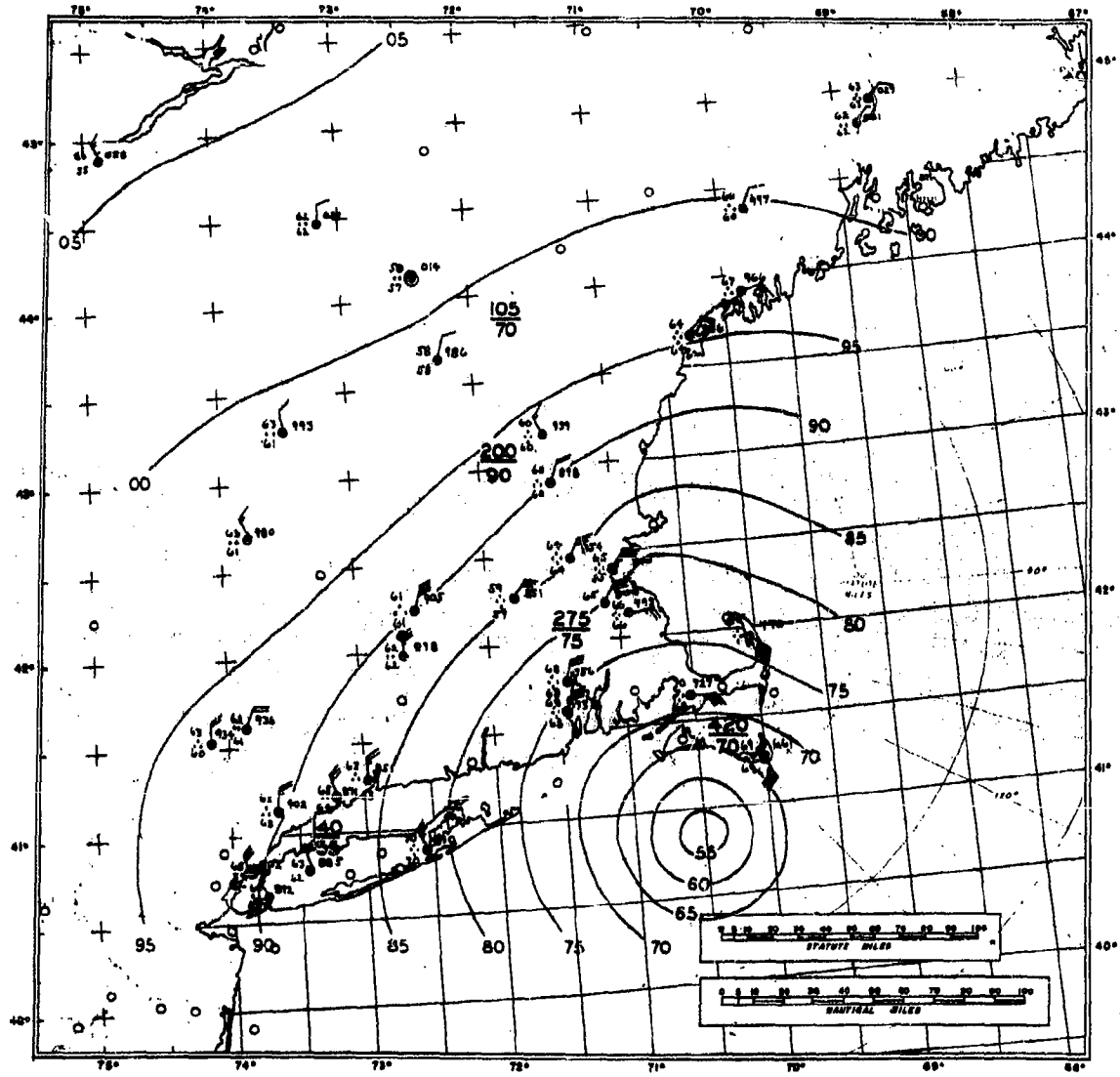

Fig. 9.7. Synoptic map of Hurricane Edna based on observations made at airways stations at 1230 EST, 11 Sept. 1954. The numbers in large type, placed one over the other in the form of a fraction, refer to the geostrophic and gradient winds respectively, at the locations where the numbers are indicated. All wind speeds are in statute miles per hour. Note that winds a considerable distance to the north and northwest of the eye are very much less than those given by the gradient and geostrophic approximations. The accelerations associated with this unbalance of wind and pressure, are believed to have given rise to unusual northwest gales observed at stations west of the eye path after the times of lowest pressure had passed. These northwest winds exceeded in strength those which occurred during falling pressure at the same stations.

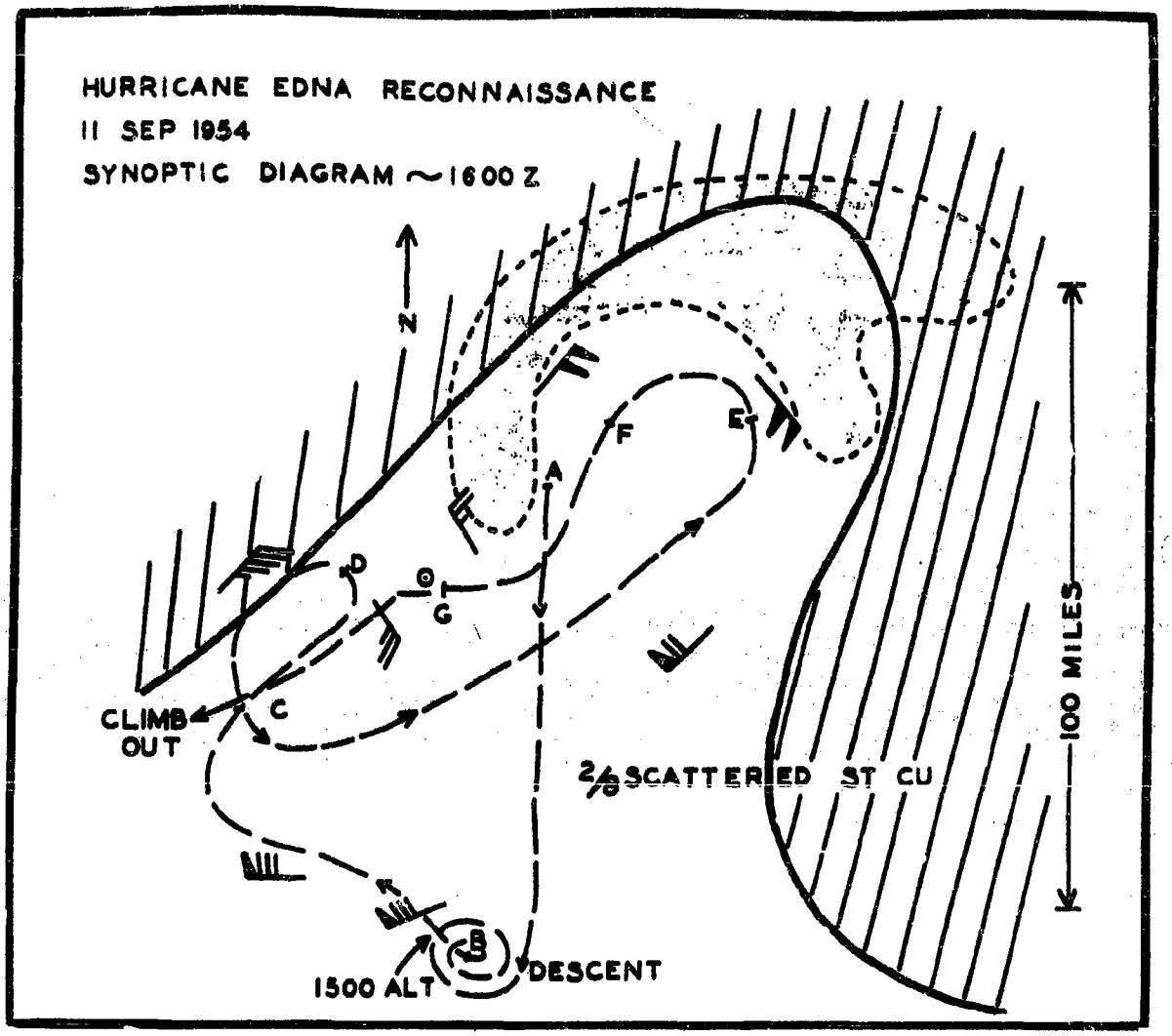

Fig. 9.8. Double eye of hurricane Edna as drawn from memory by Capt. Wallace Taylor, observer aboard WB29 which performed reconnaissance of Edna's eye. Except for minor oscillations, all the radar photographs taken from the plane presented approximately the shaded configuration. A thin cirrus layer existed in the hatched area. All winds shown are observed surface winds. The dashed line is the flight path, of approximately 45 minutes duration. At 700 mb, a minimum at point A was regularly reported at the eye position. Minima in the surface pressure field existed near A and also near point C. The centers of the two apparently closed wind circulations maintained their relative positions until they merged near Martha's Vineyard. Swells of 40 to 50 feet appeared to be radiating outward from both eyes.

The northwesterly wind burst was of great importance at the time that it occurred. Radio broadcasts made shortly after the lowest pressure had passed Boston indicated that the worst of the wind was over; whereas in truth, the worst had not yet begun. Further studies should be particularly oriented so as to exploit the possibility of forecasting an occurrence of this nature from hourly maps an hour or two in advance. It is probable that surface friction and vertical transport of momentum will also have to be considered if satisfactory interpretation of the many details of the surface weather elements is to be obtained. Unfortunately, little theoretical work has appeared on the low level winds in a moving circular pressure field since the classical work of Shaw (1931).

Another noteworthy phenomenon peculiar to Edna is its double eye. This feature was first reported by the reconnaissance aircraft at 1000E, 11 September. A diagram drawn from memory by Captain Wallace Taylor, weather observer on the plane, is included as Fig. 9.8. It is noted that only the northern eye is bounded by precipitation; therefore, the radar data give no indication of the double structure. According to Captain Taylor, the eye was still elongated as it passed Martha's Vineyard and this is borne out by the hourly synoptic charts (not extensively reproduced here; some indication of the elongation is given by Fig. 4.10, 1433 EST). The report by the aircraft of a double eye over Provincetown is in error, as explained in Section 7 and in the Appendix. It appears that Edna's double eye is a transient feature of the storm. (Captain Taylor has also informed the authors of his experience in a Pacific typhoon which possessed a double eye.)

It is of interest that Martha's Vineyard and Nantucket experience minimum sea level pressures within 0.10 inch of each other. (The exact difference and its sign are unknown because of uncertainties concerning the Martha's Vineyard reading.) The center, in fact, passed between Nantucket and Martha's Vineyard. Nantucket's wind at the time of minimum pressure (953.9 mb) was from the south, with gusts over 80 miles per hour. Martha's Vineyard, at time of minimum, appears to have experienced a northerly or northwesterly wind which was not more than 25 mph. (The wind at the exact time of lowest pressure is unknown.) This nonsymmetry of the wind distribution is reflected also by reports from other stations near the eye. Immediately adjacent to the eye, winds were much stronger to the east than to the west. This may reflect in part the relative displacement of the centers of lowest pressure and the centers of rotation, as discussed by Shaw.

A sounding made in the eye of Edna at 1030 EST by personnel of the WB 29 is presented in Fig. 9.9. This shows that Edna has a warm core structure apparently common to all tropical hurricanes, and deduced previously for the eye region of this storm from the velocity measurements discussed in Section 5. The temperature of +16°C at 700 mb is 5° higher than may be realized by moist adiabatic ascent from the surface. The high mixing ratio reported at 700 mb in the eye is higher than the highest that can be attained by ordinary processes in the saturated air

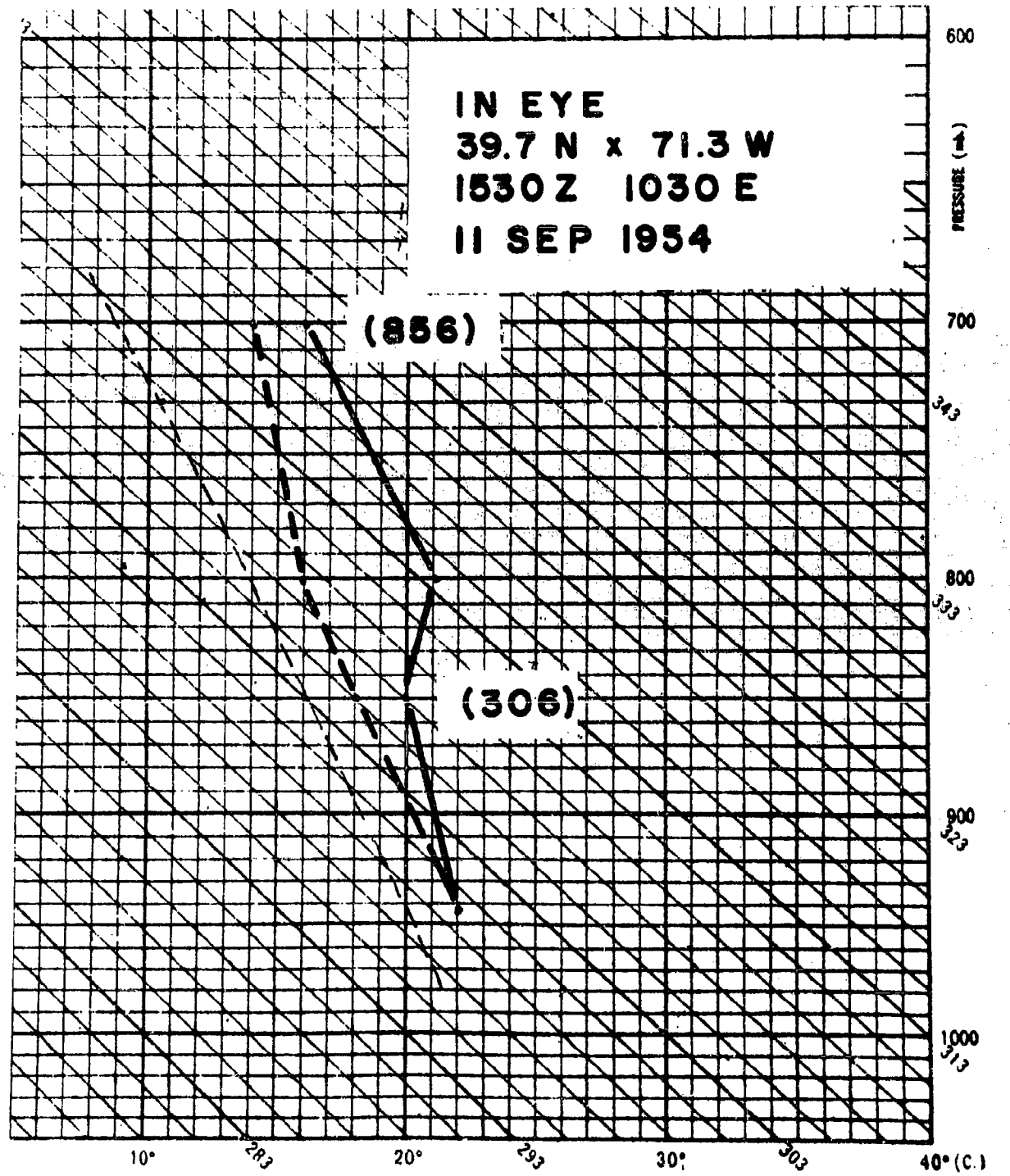

Fig. 9.9. Eye sounding of Hurricane Edna made by crew of WB29 aircraft. Heights of the 850 and 700 mb levels are indicated in parentheses. The heavy solid line is the curve of temperature, the dashed line is that of dewpoint. Sloping solid lines are dry adiabats and the light dashed line is a moist adiabat.

outside; and it is therefore probable that this report is erroneous.

Finally, certain other experiences of the reconnaissance aircraft crew bear reporting. Turbulence was observed in most of the rain area and was greatest in the heaviest clouds and precipitation. Severe turbulence was experienced near the eye, especially just to its north. However, there was little or no turbulence in the light wind area of the eye.

At about 2030Z the aircraft flew from Cape Cod SSE to the distressed Nantucket Lightship. Captain Taylor reports that the cloud tops were at only 7,000 feet, but that severe turbulence and heavy rain was experienced within them. The authors of the present paper have computed that the vertical velocities necessary to give condensation equivalent to precipitation of 10 mm/hr in such a thin layer would be accompanied by low level convergence of about 1.5×10^{-3} sec^{-1}. It is of interest in this connection to note the strong convergence in the southeast quadrant of the hurricane which is indicated by the ship reports at 1830Z (see Fig. 9.1). However, the chart neither verifies nor disproves the magnitude given above. Captain Taylor further reports that the tops of these clouds were smooth, with no cumuliform buildups. Such a relatively low cloud top may have been produced by continuous advection of dry air above 7,000 feet. The presence of strong shear implied by such a process may also help to explain severe turbulence in clear air immediately above similar clouds, as was observed later at a point some 100 miles SSW of the eye.

10. Summary of Highlights

First evidence on radar of Hurricane Edna, as observed from South Truro, Massachusetts, is an RHI echo which corresponds to a dense upper ice crystal deck (see picture 1, Fig. 10.1). These crystals are carried ahead of the main rain area nearer the eye by the high level winds and their continued existence far in advance of the main precipitation also implies some lifting in this vicinity. As the storm approaches, the upper echo layer thickens and its base slopes downward toward the precipitation area, as shown in pictures 2-5. This structure is similar to that in advance of a typical cyclone of temperate latitudes. The outflowing echo layers are generally separated by blank spaces in the pictures from the rain bands from which they appear to emanate. This is attributed to a local compensating downdraft region ahead of the main rain band which results in partial evaporation of the icy crystals and a weakened radar return.

At about 450 miles in advance of the eye, the development of low level convergence in convectively unstable air results in the formation of lines of convective showers which are oriented along the surface isobars. Their initial formation takes place entirely below the melting level (13,700 feet) and they move in good agreement with the winds between 3,000 and 9,000 feet (Fig. 10.2, top). Many of these later grow

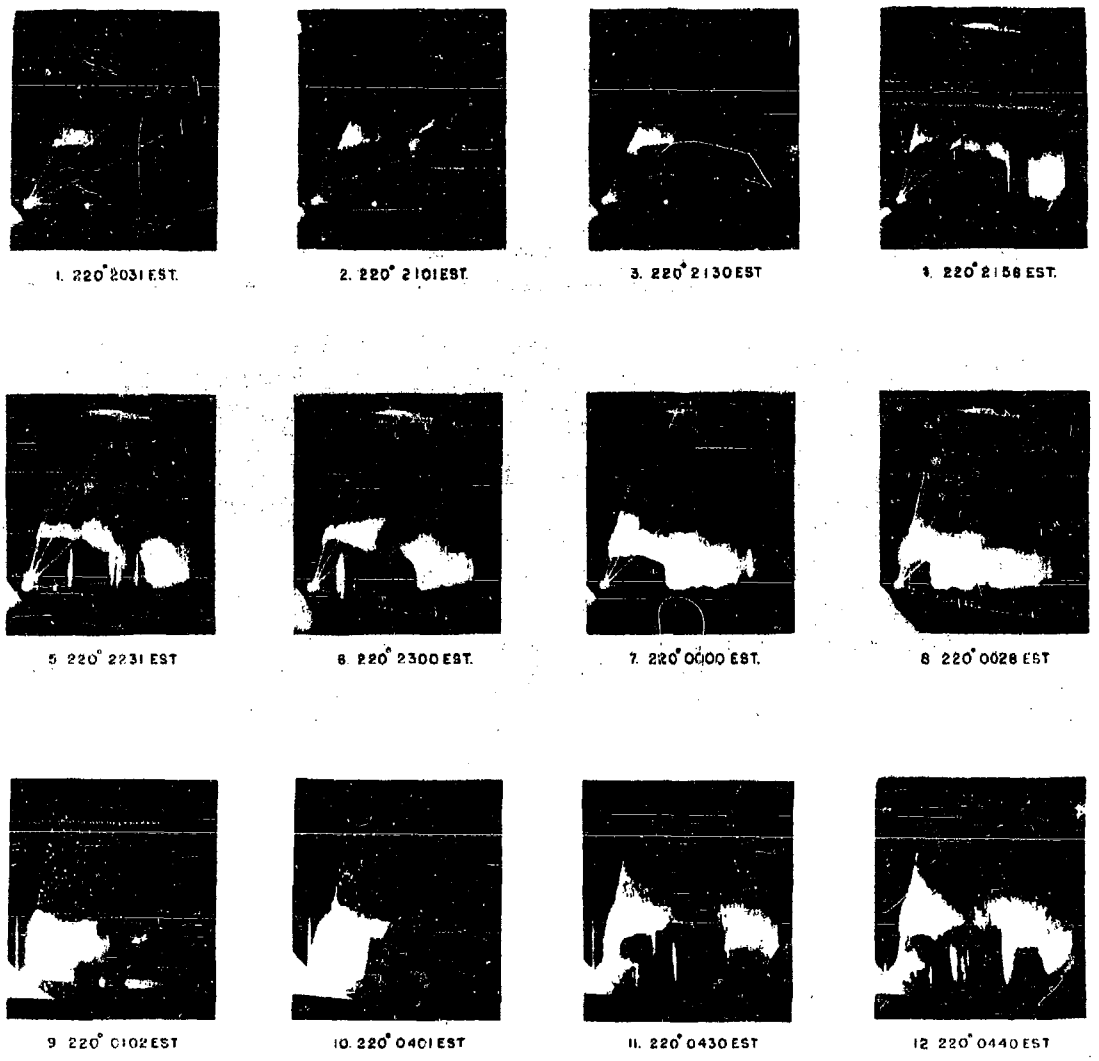

Fig. 10.1. Sequence of RHI pictures looking toward the eye of Edna as the storm approaches. Pictures 1-3, FPS-4 radar, 5 nautical mile markers; Pictures 4-8, FPS-4 radar, 10 nautical mile markers; Pictures 9-12, FPS-6 radar, 10 nautical mile markers. Note the open space between the forward edge of the rain band and the upper cloud in advance of it in pictures 4, 5, 6, 11, and 12. Picture 7 with the gap at close range demonstrates that the gap of pictures 4, 5, and 6 is filled with relatively small particles.

to cumulonimbus proportions; ultimately the lines of showers merge and decay to stratiform type precipitation. On the RHI scope the appearance of the warm showers is as illustrated by pictures 5, 6, and 11-14 of Figs. 10 1 and 10.3; they are discussed in considerable detail in Sections 3 and 4 of this report. Subsequent bands are composed more and more of rain characteristic of a stable air mass, although occasional convective elements occur even into the immediate eye region. The upwind (eastern) ends of the rain bands are more cellular in structure and this is believed due to the initial development of precipitation in convectively unstable air. The precipitation becomes more uniform downwind under the action of continued low level convergence.

While practically all of the hurricane is banded and is associated with a banded structure of low level convergence and rising motion, the mechanism giving rise to the bandedness is still unknown. At times, the upper cloud layers are affected by passage through a region or band of intensified vertical motion. In these cases, the echoes develop and fall downward as the particles grow by condensation; this is discussed in Section 4 and is illustrated by pictures 13-16 of Fig. 10.3. The main rain bands tend to be wider in their upper parts than near the surface, which is consistent with a pattern of high level divergence. They are most widely separated in the outskirts of the hurricane and tend to merge near the eye as indicated by Fig. 11.2. They are approximately parallel to the surface winds and isobars, especially at the upwind ends of the bands (except for intense convective echoes in the eastern semicircle of the storm). Downwind, both bands and winds tend to spiral toward the eye, the winds more strongly. The result of this in Edna is that the bands are oriented about halfway between the directions of surface winds and isobars. No consistent relationship between the bands and the upper winds or vertical wind shear has been discovered in this study.

It is suggested that precipitation growth and echo intensification in low level clouds is responsible for some of the finer structures, such as the cross-band striations which are observed in Fig. 4.13, and the smaller filamentary structures comprising most of the major bands. These finer features are also reflected in the rapid fluctuations of the surface rain intensity. However, the major banded structures extend through great depths of the troposphere, sometimes with and sometimes without low level growth.

The motion of the showers in the northern outskirts of the storm is about 40° to the left of the direction of the storm motion and nearly perpendicular to the bands; the upper ice crystal or snow masses in this area appear faintly on the FPS-3 PPI scope and are seen to move at a rapid rate from the same direction as the storm (SSW). Within 50 miles of the eye, the motion of discrete precipitation echoes (presumably of the low level convective type) is in nearly the same direction as the surface winds, and hence nearly along the bands. (Sections 4, 5 and 8.)

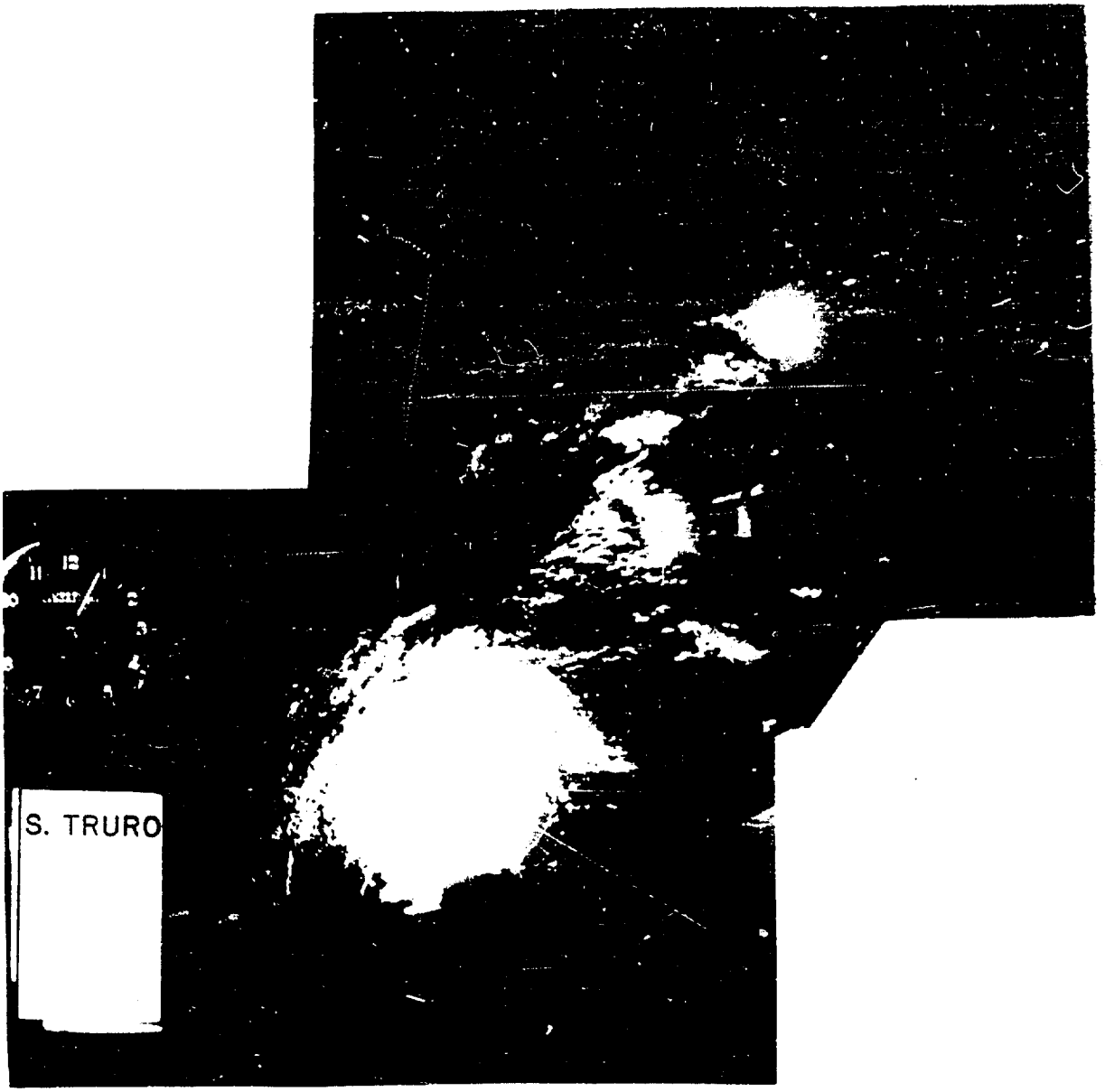

Fig. 10.2. Composite PPI display of Hurricane Edna, constructed by piecing together three FPS-3 pictures taken at So. Truro about 6 hours apart, on 11 Sept. 1954. Note the regular appearance where the pictures join, which suggests that the hurricane is in an approximately steady state. First convective bands may be seen in the upper right; in the center there is evidence of convective elements and stratiform type precipitation superimposed. The relatively close spacing and uniformity of the large scale bands near the eye is evident in the lower left of this figure.

The speed profile of discrete precipitation echoes is similar in shape to that of the surface winds, showing the decrease of speed near the eye which is characteristic of mature hurricanes. Comparison of radar and surface wind speeds indicates that the winds in the lowest 7,000 feet increase in speed with increasing height outside the ring of maximum surface winds. Within the ring of maximum surface winds the wind speed decreases with height. This pattern of vertical wind shear is consistent with recent observations of Simpson. Further study of the relationships between echo and surface wind velocities should make possible the accurate determination of hurricane intensities by radar. The wide scatter of individual echo velocity observations noted in the present study can be reduced by simultaneous use of narrow beam RHI and PPI radars (Section 5).

The eye of the hurricane may be identified on the PPI scope by the spiralling of the bands and by the rotation about it of discrete weather echoes, as noted above. On the RHI scope Edna's eye appears as an open "V" in the radar echo which leans toward the northeast; a cirrostratus shield over the eye at 35,000 feet is connected to the northeastern portion of the wall cloud by a thin column. (This spreading canopy over the eye is indicative of high level divergence.) "False" radar eyes also appear in Hurricane Edna; they are identified as spurious by their relatively short lifetimes and by the absence of rotation or spiralling about them of large scale features (Sections 7 and 8). A double eye, identified by distinct centers of circulation and pressure, is reported by reliable aircraft reconnaissance to have existed in Edna for an hour or more prior to the time the central region of the storm passed the islands south of Cape Cod. However, the centers have not been observed separately on the radar because the southernmost one was divorced from precipitation (Section 9).

A feature of the major homogeneous precipitation bands is the radar "bright band" at the melting level; this implies that snow or ice crystals are descending through the melting level from aloft. Differences in the detailed appearance of the bright band are associated with variations of middle and low level growth. Where there is little or no mid-level cloudiness and updraft, and hence only slight growth of precipitation particles, a sharply defined bright band appears and the radar echo intensity is about constant in the layer which extends to the ground from below the bright band. On the other hand, the appearance of generally increasing echo intensity from the melting level downward is attributed to major growth of the melting snow and rainfall by accretion of cloud. This characterizes the bands of moderately heavy precipitation which must correspond, therefore, to areas of major convergence and lifting. The very heaviest precipitation (requiring intense updrafts) must be associated with a graupel or hail process for which there is no strong evidence in the radar data, except in the region of the main wall cloud. (The greatest rains in Hurricane Edna occurred along a line passing about 75 miles west of the main radar site at South Truro.)

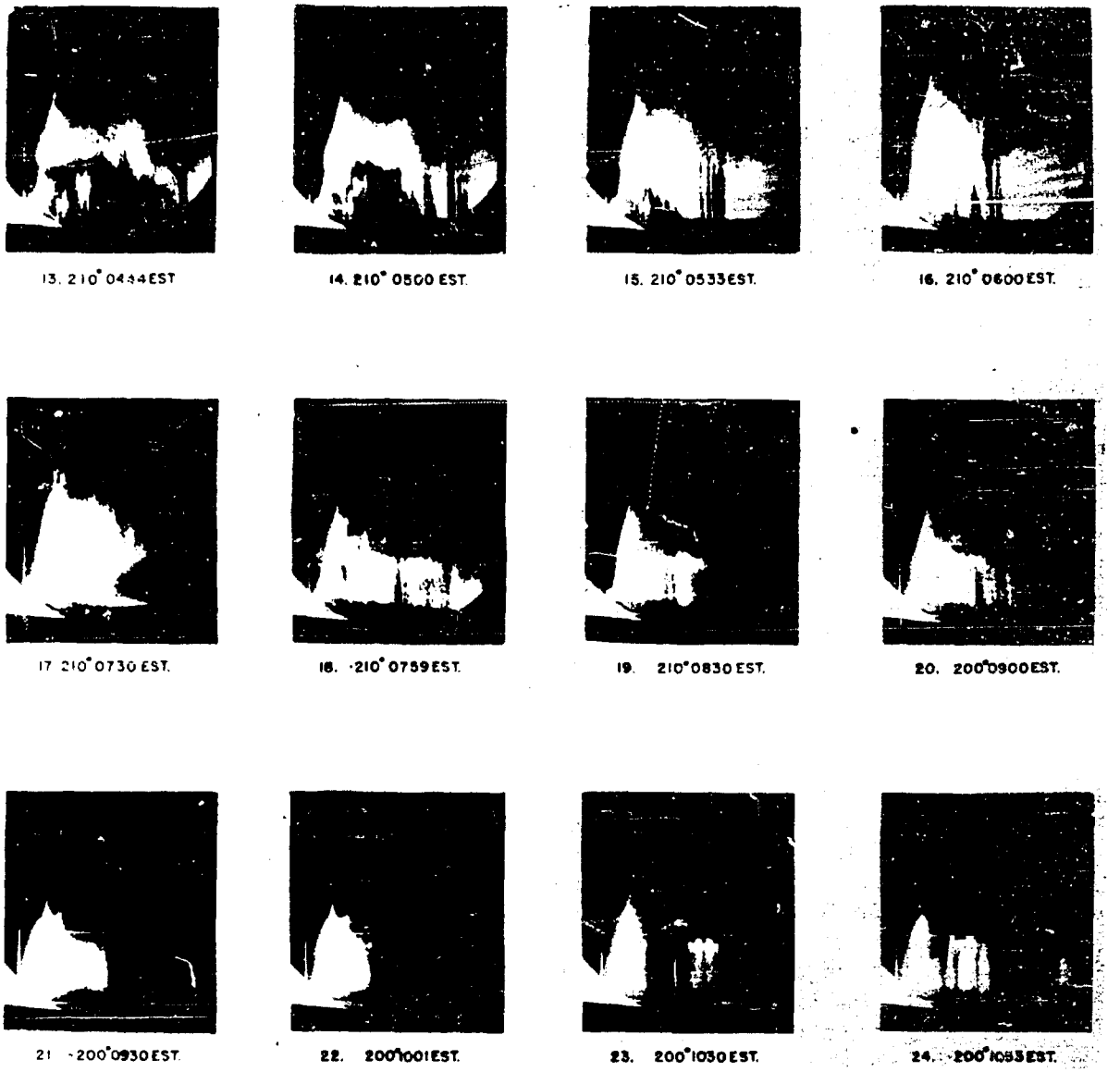

Fig. 10.3. Photographs of the FPS-6 scope at So. Truro during the approach of Hurricane Edna. Pictures 13, 14, and 15 demonstrate the occurrence of low level convective showers and descent of an upper ice crystal layer in a region of low level convergence and rising air motion. Pictures 19 and 23, at low gain, illustrate the conventional bright band at 13,500 feet. The pictures numbered 18-24 at low gain fail to show snow above the melting level except at very close ranges.

Characteristics of the drop size distributions of hurricane rains (examined by the filter paper technique) ranging in intensity from 3 to 75 mm/hr, are in good agreement with those to be expected on the basis of Marshall and Palmer's empirical relation. The median drop diameters are somewhat larger than usual, however, and are attributed to the unusually important role of aggregation in this hurricane rain. The empirical relation $Z = 200R^{1.6}$, where Z is the radar reflectivity factor (summation of the 6th powers of the drop diameters) and R is the rainfall rate, has been tested, using the filter paper samples of Edna rain. The value of R determined by the application of this equation is always well within a factor of 2 of the observed value, thus suggesting the possible use of long wave radar to monitor the intensity of hurricane rains (Section 6).

The path of Edna is found to be much more regular than originally reported; oscillations of the path are of smaller amplitude than the eye diameter. Analysis of position reports from various sources indicates that when an aircraft is within radar range, errors of position may be reduced to a minimum if reports are based on cooperative estimates of both aircraft and radar observers (Sections 7 and 8).

Land stations west of Edna's eye experienced highest winds during the storm after the times of lowest pressure. Analysis of trajectories and pressure gradients, based on analyzed hourly weather maps, indicates that the air associated with these northwest gales can be traced to an origin in a field of gross unbalance between winds and pressure. At a distance of 100 to 200 statute miles northwest of the eye over land, wind speeds are typically only 15 percent of their gradient values and accelerations implied by the equations of motion in this case appear adequate to explain the observed increase in wind speed (Section 9).

ACKNOWLEDGMENTS

No study of this kind is possible without the labors of many. The authors wish to thank Mr. William MacDonald and Dr. Alex Nedzel of Lincoln Laboratory, Massachusetts Institute of Technology, for arranging the use of the South Truro facilities during Hurricane Edna. Without the around-the-clock work of technicians at this radar site, the record which is the main subject of this study would never have been obtained. These men include Graham Armstrong, of Air Force Cambridge Research Center, and Richard Petersen, Herman Gibsen, Eugene Heath, James Johns, Arwin Brown, William Gaughan and Alfred Kennedy, of Lincoln Laboratory. Special thanks go to Asa Wing and Lincoln Carteledge, who supervised the technicians at the site. Acknowledgment to Lincoln Laboratory is also made for use of a time lapse radar movie obtained at Hanscom Field, Massachusetts.

Credit is due Major John Connolly and his team, of the Air Force Cambridge Research Center, who made many special radiosonde ascents and the record of the TPQ-6 radar during adverse weather conditions. For especially valuable information the authors are indebted to Captain Wallace Taylor, observer aboard the WB 29 which probed the storm as it approached Cape Cod.

Thanks also go to the Air Defense Command which made available to the authors a valuable PPI time lapse movie obtained at Montauk Point, New York.

For processing hundreds of photographs with great care, thanks are due to John Moore, Clifford Rodberg and Ray McAnn of the AFCRC photo laboratory. Albert Chmela, Leo Simon, Dave Snow and Hal Gould contributed greatly by their painstaking preparation of illustrations for which captions were prepared and which were mounted and sized by Theresa Gillis. Ralph Donaldson, of AFCRC, and Dr. Fred Sanders, of MIT, have aided the work by their enlightening discussions with the authors and by constructive criticisms. Edith Miller has prepared the copy for printing and by her typing of early drafts has facilitated the author's final editing.

APPENDIX A

List of Aircraft Reconnaissance Reports, Corrections and Comments

Corrections were made possible through the assistance of Captain Wallace Taylor, observer aboard the aircraft.

Plain Language Portions As Received	Plain Language Portions As Corrected
Duck Edna 1 (1130Z). Position 36°17'N 67°15'W; surface wind 170° 030 knots; flight wind 195° 057 knots; squalls lines curves to NW	Duck Edna 1. Position 36°17'N 67°15'W; surface wind 170° 030 knots; flight wind 195° 057 knots; squall line curves to NW

There was just one small cloud line which curved into the northwest from the aircraft position, thus

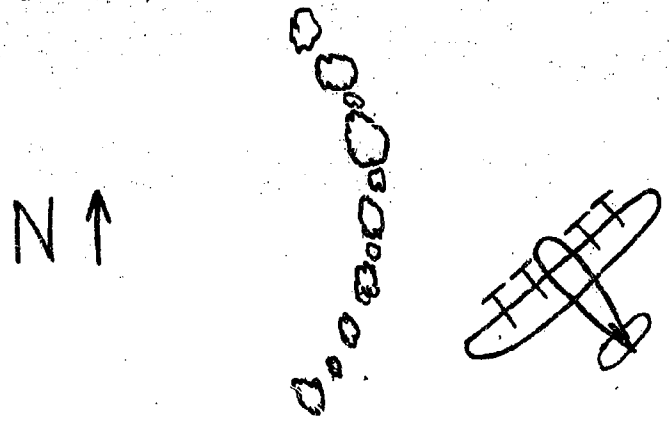

Duck Edna 2 (1200Z). Radar returns all quadrants; position 36°06'N 68°20'W; surface wind 170° 050 knots; flight wind 190° 060 knots; proceeding to seal intersection.	Duck Edna 2. Radar returns all quadrants; position 36°06'N 68°20'W; surface wind 170° 050 knots; flight wind 190° 066 knots; proceeding to seal intersection.

The only change here involves the flight level wind.

Plain Language Portions As Received	Plain Language Portions As Corrected
Duck Edna 3 (1230Z). Position 39°50'N, 69°40'W; surface wind 920°, 065 knots; flight wind 170°, 076 knots; circling Seal intersection due to ATC clearance.	Duck Edna 3 (1230Z). Position 39°50'N, 69°40'W; surface wind 120°, 065 knots; flight wind 170°, 076 knots; circling Seal intersection due to ATC clearance.

The direction of the surface wind is 120° rather than 920°. The plane was not authorized to fly directly into the storm, but had to wait at Seal intersection for final clearance.

Duck Edna 4 (1300Z). Position 39°47'N, 71°07'W; surface wind unknown; flight wind unknown.	No change.

Duck Edna 5 (1330Z). Position 38°32'N, 71°18'W; surface unknown; flight wind unknown; penetration eye.	Duck Edna 5 (1330Z). Position 38°32'N, 71°18'W; surface wind unknown; flight wind unknown; penetrating eye.

"Penetration eye" should read "penetrating eye." This means that the plane is on a course for the eye, not actually entering it.

DUCK EDNA SIX IN EYE (1400Z). Double eye forming; swells to 60 feet; blue sky over Seal; position 39°12'N, 72°13'W; surface wind diffuse 40 knots; will remain in eye due to proximity of coastline; eye position to follow every 30 minutes.	Duck Edna 6 in eye (1400Z). Double eye forming; swells to 60 feet; blue sky overhead; position 39°12'N, 72°13'W; surface wind diffuse 40 knots; will remain in eye due to proximity of coastline; eye position to follow every 30 minutes.

The plane was in the eye region and blue sky was overhead, not over Seal. The eye was open to the south and it was difficult to find a minimum in the pressure field. The analysis of "D" values gathered during reconnaissance of the eye indicated an elongation of the pressure pattern in a northeast-southwest direction. Finally, two minima at 700 mb were located. The lesser minimum was about 30 miles SW of the major minimum, which latter was reported as the eye location.

Plain Language Portions As Received	Plain Language Portions As Corrected
Duck A 3459 Edna recco six, eye centered 39°12'N, 72°13'W 1400Z; Loran position accurate within 5 miles; maximum winds 120 knots north quadrant; eye poorly defined, 15 miles diameter; radar coverage feasible; remarks: eye horseshoe shaped, open to south, surface in eye very diffuse 40 knots.	No change.

As indicated by Fig. 8.1 and the discussion of Section 8, this Loran fix was probably not as accurate as indicated. The sea surface in the eye was confused, with swells moving in different directions. The wave and spray formations were of about the same magnitude as those formed under the influence of a 40 knot wind. In this case, however, it was not possible to determine wind direction from the appearance of the sea, hence the phrase "surface wind diffuse 40 knots."

Edna seven in eye (1430Z). Eye changing shape continuously. Position 39°20'N, 71°41'W.	No change.

The reference to changing shape pertains mainly to the pressure pattern immediately about the eye. The steepest gradient shifted from the north side in a clockwise direction to the west side during the half hour period centered on this observation.

Duck Edna eight in eye (1500Z). Surface wind 20 miles sou: of center 270° 120 knots; position 39°32'N, 71°38'W.	No change.

Duck A 3459 Edna nine in eye (1530Z). Descending to 1500'. Next ob 1630Z; position 39°39'N, 71°18'W.	No change.

Plain Language Portions As Received	Plain Language Portions As Corrected
Duck A 3459 Edna in eye (1630Z). Subcon press 1600Z 947 mbs; eye center pressure slopes upward northwest; position 40°00'N, 70°55'W, 700 mb level drop wing. Second surface eye 40 miles southwest of ob position.	Duck A 3459 Edna in eye (1630Z). Surface pressure at 1600Z, 947 mbs; eye center slopes upward toward northeast; position 40°00'N, 70°55'W, 700 mb level dropping, second surface eye 40 miles southwest of ob position.

Several transmission errors in this one. The northeast tilt of the eye was also determined by 3 cm radar at South Truro (see Fig. 9.5). The decrease of height of the 700 mb surface was noted in order to confirm the coded portions of the messages; it was believed that the movement of the storm into higher latitudes would normally be accompanied by rising 700 mb central heights.

Duck A 3459 Edna eleven in eye (1730Z). Loran temporarily inoperative; Fax by defense radar net; position 40°48'N, 70°33'W; eye position at 1700Z, 40°40'N, 704W	Duck A 3459 Edna eleven in eye; Loran temporarily inoperative; Fix by defense radar net; position 40°48'N, 70°33'W; eye position at 1700Z, 40°40'N, 70°40'W.

The 1700Z fix was by Loran; the 1730Z and 1800Z fixes were by ground radar at Montauk Point. The longitude of the 1700Z fix was garbled in the message.

Duck A 3459 Edna twelve in eye (1800Z); eye opening more to south; position 41°15'N, 70°30'W.	No change.

The wall cloud to the south, already much smaller than that to the north, underwent further dissipation.

Duck A 3459 Edna thirteen (1850Z) in eye over land; eye over Martha's Vineyard at 1850Z.	No change.

Post analysis indicates that the point of lowest pressure did not pass over Martha's Vineyard, but over the ocean between Mar+ha's Vineyard and Nantucket. At this time the eye was extremely asymmetrical, with the minimum pressure located east of the mid-point of a representative outer isobar. The gradient over Martha's Vineyard was quite light and the center of the area of light winds and comparatively unruffled ocean may well have passed over the island. At this time there was no white water visible from the plane north of the line connecting Martha's Vineyard and Nantucket to Massachusetts' south shore. An additional confusing feature at this time was a band of heavy cloud which had swung southward (relative to the storm) until it bordered the point of minimum pressure on the west. This heavy cloud appeared to the aircraft to be the wall cloud east of the eye center. The bands terminated along a nearly east-west line at this time - this line of termination was thought to be wall cloud to the north. Analysis indicates that the eye was not truly double at this time or as the eye crossed Cape Cod.

Plain Language Portions As Received	Plain Language Portions As Corrected
Duck Edna south eye centered 41°29'N, 70°10'W, 1930Z; visual position accurate within zero miles; north eye centered at 1935Z in middle of Cape Cod Bay; eyes well defined 40 miles diameter; radar coverage feasible.	No change.

Here the double eye was erroneously reported. Due to the wide flat pressure pattern, "D" values were not closely checked, and fatigue of personnel aboard the aircraft greatly reduced efficiency. The reported positions were based largely on visual attempts to place the eyes or eye. The distribution of cloud lines in the eye made this difficult, as noted above. The cloud line over the Cape extended at least to 20,000'.

Duck A 3459 Edna recco eye centered 2010Z, visual position. Maximum winds unknown, wall clouds dissipated east through south to west; double eyes now forming gigantic eye roughly centered over Provincetown. Eye poorly defined.	No change.

The cloud line referred to previously was now much less ominous, and no longer appeared to be a wall cloud. Thus the wall cloud was reported to be dissipating, although such probably existed to the northeast, out of site behind the weakening cloud line.

Plain Language Portions As Received	Plain Language Portions As Corrected
Duck Edna departing storm to distressed surface vessel 75 miles southeast of eye. Do you desire 2200Z fix on eye? Reply immediately.	No change.
Duck A 3459 Edna 15 southeast of eye; position 40°37'N, 69°18'W 2045Z; surface wind 270°, 100 knots; sea phenomenal; overcast 300 feet.	No change.
Duck Edna relieved on station of distressed vessel by Coast Guard aircraft; this message terminates weather reconnaissance of Hurricane Edna; Loran inoperative; position uncertain; proceeding to a suitable east coast field; insufficient fuel to attempt Kindley; last message.	No change.

APPENDIX B

Horizontal Temperature Gradients as the Melting Level
(Note added in proof)

Determination of horizontal temperature gradient by radar is dependent on knowledge of the lapse rate and on measurements of the height of the bright band, which corresponds to the layer about 1500 feet below the 0°C isotherm, and in which snow melts to rain (Austin and Bemis, 1950). The quantitative relationship between the height variations of an isotherm (assumed continuous) and the horizontal temperature gradient is given by $\partial T/\partial x = -(\partial H/\partial x)_T(\partial T/\partial H)$, where $(\partial H/\partial x)_T$ is the slope of the isotherm and $\partial T/\partial H$ the lapse rate. An estimate of the quantity $(\partial H/\partial x)_T$ near the +2°C isotherm may be obtained from measurements of the height of the bright bands at different distances from the eye of the storm. Although numerous RHI photographs were made during Hurricane Edna, little thought was given to this problem at that time, and the data are therefore not all that is now desired. The table below lists measurements which are probably uncertain by 500 feet.

Height of Bright Band in Edna

Distance NNE of Eye (nautical miles)*	Ht. of Center of Bright Band (feet)	Radar Used
325-170	12,700	FPS-4 and FPS-6
160	13,500	FPS-6
125	14,000	FPS-6
20	16,000-16,500	FPS-4
In Eye	16,000-17,000	FPS-4

* No bright band data are available between 125 and 20 nautical miles of the eye.

Following the Jordans'(1954) as well as the radiosonde data of this report, we adopt a value of $\partial T/\partial H = -1.6$°C per thousand feet. The difference of some 4000 feet of the bright band height from a distance 170 miles ahead of the eye to the eye region is thus indicative of a horizontal temperature variation at about 15,000 feet of 6 or 7°C. It may be noted that Figs. 4.7, 4.8, and 9.9 indicate a 6°C temperature change over a similar distance at the 10,000 foot level; earlier soundings (Figs. 3.2,

3.8, and 4.3) indicate smaller irregular changes. These results are generally very similar to the Jordans' mean thermal structures (1952 and 1954) and the cross section of Simpson for the 1946 Tampa storm.

Since the temperature at which naturally falling snow melts is somewhat a function of particle size, updraft, and lapse rate, the precise correlation of bright band and temperature is a formidable task. However, the utilization of more precise relationships between bright band height and temperature than attempted here, coupled with accurate measurements, could be applied to such small scale phenomena as the individual rain bands as well as to the total hurricane.

REFERENCES

Abdullah, A. J., 1954: A proposed mechanism for the development of the eye of a hurricane. J. Meteor., vol. 11, no. 3, pp. 189-195.

Atlas, D., 1953: Optical extinction by rainfall. J. Meteor., vol. 10, pp. 486-488.

Atlas, D., 1955: The radar measurement of precipitation growth. Doctoral dissertation, Mass. Inst. of Tech.

Atlas, D., 1955: Radar measurements of precipitation growth. Proceedings of Conference on the Physics of Cloud and Precipitation Particles, Woods Hole, Mass., Amer. Geophys. Union, in press.

Austin, P. M. and A. C. Bemis, 1950: A quantitative study of the "Bright Band" in radar precipitation echoes. J. Meteor., vol. 7, no. 2, pp. 145-151.

Blanchard, D., 1952: Raindrop size distribution and associated phenomena in Hawaiian rains. Tech. Rpt. No. 4, Woods Hole Ocean. Inst., Woods Hole, Mass.

Brooks, C. F. and C. Chapman, 1945: New England hurricane of September 1944, in the Report of the Smithsonian Institution, pp. 235-246.

Bunting, D. C., R. C. Gentry, M. H. Latour and G. Norton, 1951: Florida hurricanes of 1950. Engineering Progress at the Univ. of Fla., vol. 5, no. 7.

Donaldson, R. J., Jr., 1955: Drop size distribution, liquid water content, optical transmission and radar reflectivity in fog and drizzle. Paper presented at 5th Weather Radar Conference, Fort Monmouth, N. J.

Dunn, G. E., 1951: Tropical cyclones. Pp 887-901 in Compendium of Meteorology. American Meteorological Society, Boston, Mass.

Hatakeyama, H., I. Imai and Y. Masuda, 1955: On some radar observations of Typhoon Lorna. Proceedings of the UNESCO Symposium on Typhoons, Nov. 1954, Japanese National Commission for UNESCO, pp. 121-128.

Hitschfeld, W., 1955: Size distribution of precipitating particles and effects of growth and shear sorting. Proceedings of Conference on the Physics of Cloud and Precipitation Particles, Woods Hole, Mass.

Jordan, C. L., 1952: On the low level structure of the typhoon eye. J. Meteor., vol. 9, no. 4, pp. 285-290.

Jordan, C. L. and E. S. Jordan, 1954: On the mean thermal structure of tropical cyclones. J. Meteor., vol. 11, no. 6, pp. 440-448.

Jordan, E. S., 1952: An observational study of the upper wind circulation around tropical storms. J. Meteor., vol. 9, no. 5, pp. 340-346.

Kuettner, J., 1955: The origin of cloudstreets in trade winds and tropical cyclones. Paper presented at 141st National Meeting of AMS at Honolulu, Hawaii.

Laws, J. O. and D. A. Parsons, 1943: The relation of raindrop size to intensity. Trans. Amer. Geophys. Union 24, part II, pp. 452-460.

Ligda, M. G. H., 1955: Analysis of motion of small precipitation areas and bands in the hurricane, August 23-28, 1949. Tech. Note No. 3, Dept. of Meteor., Mass. Inst. of Tech.

Malkin, W. and G. C. Holzworth, 1954: Hurricane Edna, 1954. Monthly Weather Review, vol. 82, no. 9, pp. 267-279.

Marshall, J. S., 1953: Precipitation trajectories and patterns. J. Meteor., vol. 10, no. 1, pp. 25-29.

Marshall, J. S. and W. McK. Palmer, 1948: The distribution of raindrops with size. J. Meteor., vol. 5, pp. 165-166.

Marshall, J. S., W. Hitschfeld and K. L. S. Gunn, 1955: Advances in radar weather. In Advances in Geophysics, ed. by H. E. Landsberg, Academic Press, N. Y.

McIntyre, H. D., 1955: Radar study of Hurricanes"Carol" and "Edna," 1954. S. M. Thesis, Dept. of Meteorology, Mass. Inst. of Tech.

Middleton, W. E. K., 1941: Meteorological Instruments. The University of Toronto Press, Toronto.

Pierce, C. H., 1939: The meteorological history of the New England hurricane of September 21, 1938. Monthly Weather Review, vol. 67, no. 8, pp. 237-285.

Potter, J., 1952: Note on the structure of a hurricane in its late mature stage. Bull. Amer. Meteor. Soc., vol. 33, no. 3, pp. 122-123.

Rossman, C. G., 1949: The Hudson Design-Jardi type recording rain intensity gauge and rainfall totalizer. Bull. Amer. Meteor. Soc., vol. 30, pp. 97-103.

Shaw, N., 1931: Manual of Meteorology, vol. IV (Meteorological Calculus. Pressure and Wind). University Press, Cambridge.

Simpson, R. H., 1947: A note on the movement and structure of the Florida hurricane of October 1946. Monthly Weather Review, vol. 75, no. 4, pp. 53-58.

Simpson, R. H., 1953: Exploring eye of Typhoon Marge. Bull. Amer. Meteor. Soc., vol. 33, no. 7, pp. 286-298.

Simpson, R. H., 1954: Structure of an immature hurricane. Bull. Amer. Meteor. Soc., vol. 35, no. 8, pp. 335-350.

Simpson, R. H. and L. G. Starrett, 1955: Further studies of hurricane structure by aircraft reconnaissance. Bull. Amer. Meteor. Soc., vol. 36, no. 9, pp. 459-468.

Sumner, H. C. and T. J. O'Connell, 1955: Hurricane rains cause devastating floods. Weatherwise, vol. 8, no. 5, pp. 124-126.

Wexler, H., 1947: Structure of hurricanes as determined by radar. Ann. N. Y. Acad. Sci., vol. 48, art. 8, pp. 821-844.

GEOPHYSICAL RESEARCH PAPERS

No. 1. Isotropic and Non-Isotropic Turbulence in the Atmospheric Surface Layer, Heinz Lettau, Geophysics Research Directorate, December 1949.

No. 2. Effective Radiation Temperatures of the Ozonosphere over New Mexico, Adel, Geophysics R-D, December 1949.

No. 3. Diffraction Effects in the Propagation of Compressional Waves in the Atmosphere, Norman A. Haskell, Geophysics Research Directorate, March 1950.

No. 4. Evaluation of Results of Joint Air Force-Weather Bureau Cloud Seeding Trials Conducted During Winter and Spring 1949, Charles E. Anderson, Geophysics Research Directorate, May 1950.

No. 5. Investigation of Stratosphere Winds and Temperatures From Acoustical Propagation Studies, Albert P. Crary, Geophysics Research Directorate, June 1950.

No. 6. Air-Coupled Flexural Waves in Floating Ice, F. Press, M. Ewing, A. P. Crary, S. Katz, and J. Oliver, Geophysics Research Directorate, November 1950.

No. 7. Proceedings of the Conference on Ionospheric Research (June 1949), edited by Bradford B. Underhill and Ralph J. Donaldson. Jr , Geophysics Research Directorate, December 1950.

No. 8. Proceedings of the Colloquium on Mesospheric Physics, edited by N. C. Gerson, Geophysics Research Directorate, July 1951.

No. 9. The Dispersion of Surface Waves on Multi-Layered Media, Norman A. Haskell, Geophysics Research Directorate, August 1951.

No. 10. The Measurement of Stratospheric Density Distribution with the Searchlight Technique, L. Elterman, Geophysics Research Directorate, December 1951.

No. 11. Proceedings of the Conference on Ionospheric Physics (July 1950) Part A, edited by N. C. Gerson and Ralph J. Donaldson, Jr., Geophysics Research Directorate, April 1952.

No. 12. Proceedings of the Conference on Ionospheric Physics (July 1950) Part B, edited by Ludwig Katz and N. C. Gerson, Geophysics Research Directorate, April 1952.

No. 13. Proceedings of the Colloquium on Microwave Meteorology, Aerosols and Cloud Physics, edited by Ralph J. Donaldson, Jr., Geophysics Research Directorate, May 1952.

No. 14. Atmospheric Flow Patterns and Their Representation by Spherical-Surface Harmonics, B. Haurwitz and Richard A. Craig, Geophysics Research Directorate, July 1952.

No. 15. Back-Scattering of Electromagnetic Waves From Spheres and Spherical Shells, A. L. Aden, Geophysics Research Directorate, July 1952.

No. 16. Notes on the Theory of Large-Scale Disturbances in Atmospheric Flow With Applications to Numerical Weather Prediction, Philip Duncan Thompson, Major, U. S. Air Force, Geophysics Research Directorate, July 1952.

GEOPHYSICAL RESEARCH PAPERS (Continued)

No. 17. The Observed Mean Field of Motion of the Atmosphere, Yale Mintz and Gordon Dean, Geophysics Research Directorate, August 1952.

No. 18. The Distribution of Radiational Temperature Change in the Northern Hemisphere During March, Julius London, Geophysics Research Directorate, December 1952.

No. 19. International Symposium on Atmospheric Turbulence in the Boundary Layer, Massachusetts Institute of Technology, 4-8 June 1951, edited by E. W. Hewson, Geophysics Research Directorate, December 1952.

No. 20. On the Phenomenon of the Colored Sun, Especially the "Blue" Sun of September 1950, Rudolf Penndorf, Geophysics Research Directorate, April 1953.

No. 21. Absorption Coefficients of Several Atmospheric Gases, K. Watanabe, Murray Zelikoff and Edward C. Y. Inn, Geophysics Research Directorate, June 1953.

No. 22. Asymptotic Approximation for the Elastic Normal Modes in a Stratified Solid Medium, Norman A. Haskell, Geophysics Research Directorate, August 1953.

No. 23. Forecasting Relationships Between Upper Level Flow and Surface Meteorological Processes, J. J. George, R. O. Roche, H. B. Visscher, R. J. Shafer, P. W. Funke, W. R. Biggers and R. M. Whiting, Geophysics Research Directorate, August 1953.

No. 24. Contributions to the Study of Planetary Atmospheric Circulations, edited by Robert M. White, Geophysics Research Directorate, November 1953.

No. 25. The Vertical Distribution of Mie Particles in the Troposphere, R. Penndorf, Geophysics Research Directorate, March 1954.

No. 26. Study of Atmospheric Ions in a Nonequilibrium System, C. G. Stergis, Geophysics Research Directorate, April 1954.

No. 27. Investigation of Microbarometric Oscillations in Eastern Massachusetts, E. A. Flauraud, A. H. Mears, F. A. Crowley, Jr., and A. P. Crary, Geophysics Research Directorate, May 1954.

No. 28. The Rotation-Vibration Spectra of Ammonia in the 6- and 10-Micron Regions, R. G. Breene, Jr., Capt., USAF, Geophysics Research Directorate, June 1954.

No. 29. Seasonal Trends of Temperature, Density, and Pressure in the Stratosphere Obtained With the Searchlight Probing Technique, Louis Elterman, July 1954.

No. 30. Proceedings of the Conference on Auroral Physics, edited by N. C. Gerson, Geophysics Research Directorate, July 1954.

No. 31. Fog Modification by Cold-Water Seeding, Vernon G. Plank, Geophysics Research Directorate, August 1954.

GEOPHYSICAL RESEARCH PAPERS (Continued)

No. 32. Adsorption Studies of Heterogeneous Phase Transitions, S. J. Birstein, Geophysics Research Directorate, December 1954.

No. 33. The Latitudinal and Seasonal Variations of the Absorption of Solar Radiation by Ozone, J. Pressman, Geophysics Research Directorate, December 1954.

No. 34. Synoptic Analysis of Convection in a Rotating Cylinder, D. Fultz and J. Corn, Geophysics Research Directorate, January 1955.

No. 35. Balance Requirements of the General Circulation, V. P. Starr and R. M. White, Geophysics Research Directorate, December 1954.

No. 36. The Mean Molecular Weight of the Upper Atmosphere, Warren E. Thompson, Geophysics Research Directorate, May 1955.

No. 37. Proceedings on the Conference on Interfacial Phenomena and Nucleation.
I. Conference on Nucleation.
II. Conference on Nucleation and Surface Tension.
III. Conference on Adsorption.
Edited by H. Reiss, Geophysics Research Directorate, July 1955.

No. 38. The Stability of a Simple Baroclinic Flow With Horizontal Shear, Leon S. Pocinki, Geophysics Research Directorate, July 1955.

No. 39. The Chemistry and Vertical Distribution of the Oxides of Nitrogen in the Atmosphere, L. Miller, Geophysics Research Directorate, April 1955.

No. 40. Near Infrared Transmission Through Synthetic Atmospheres, J. N. Howard, Geophysics Research Directorate, November 1955.

No. 41. The Shift and Shape of Spectral Lines, R. G. Breene, Geophysics Research Directorate, October 1955.

No. 42. Proceedings on the Conference on Atmospheric Electricity, R. Holzer, W. Smith, Geophysics Research Directorate, December 1955.

No. 43. Methods and Results of Upper Atmospheric Research, J. Kaplan, G. Schilling, H. Kallman, Geophysics Research Directorate, November 1955.

No. 44. Luminous and Spectral Reflectance as Well as Colors of Natural Objects, R. Penndorf, Geophysics Research Directorate, February 1956.

No. 45. New Tables of Mie Scattering Functions for Spherical Particles, R. Penndorf, B. Goldberg, Geophysics Research Directorate, March 1956.

No. 46. Results of Numerical Forecasting With the Barotropic and Thermotropic Models, W. Gates, L. S. Pocinki, C. F. Jenkins, Geophysics Research Directorate, April 1956.

GEOPHYSICAL RESEARCH PAPERS (Continued)

No. 47. A Meteorological Analysis of Clear Air Turbulence (A Report on the U. S. Synoptic High-Altitude Gust Program), H. Lake, Geophysics Research Directorate, February 1956.

No. 48. A Review of Charge Transfer Processes in Gases, S. N. Ghosh, W. F. Sheridan, J. A. Dillon, Jr., and H. D. Edwards, Geophysics Research Directorate, July 1955.

No. 49. Theory of Motion of a Thin Metallic Cylinder Carrying a High Current, C. W. Duba, Geophysics Research Directorate, October 1955.